

Manuscript Number: PALAE07687R3

Title: Is *Cyprideis agrigentina* Decima a good palaeosalinometer for the Messinian Salinity Crisis?  
Morphometrical and geochemical analyses from the Eraclea Minoa section (Sicily)

Article Type: SI: Papers from 17th ISO

Keywords: Ostracoda; morphometrical analyses; geochemical analyses; palaeoenvironmental reconstruction; post-evaporitic Messinian; Sicily (Italy)

Corresponding Author: Dr. Francesco Grossi, Ph.D.

Corresponding Author's Institution: Roma Tre University

First Author: Francesco Grossi, Ph.D.

Order of Authors: Francesco Grossi, Ph.D.; Elsa Gliozzi, Full Professor; Pedro Anad3n, CSIC researcher; Francesca Castorina, Associate Professor; Mario Voltaggio, CNR researcher

**Abstract:** The living euryhaline species *Cyprideis torosa* (Jones) undergoes morphometric variations in size, nodding and sieve-pore shape linked to the environmental salinity. In particular it is known that salinity values around 8-9 psu represent the osmoregulation threshold and also the turning point between smaller and greater valve dimensions and prevalingly noded against un-noded valves. The variation of the percentage of round-, elongate- and irregular-shaped sieve-pores on the valves has shown an empiric logarithmic correlation with the water salinity from 0 to 100 psu. Due to this ecologically cued polymorphism, *C. torosa* represents an invaluable palaeosalinometer for the Quaternary brackish basins. In this paper we attempt to verify whether the ecophenotypical behaviour of the post-evaporitic Messinian species *Cyprideis agrigentina* Decima was comparable with that of *C. torosa*. To reach this goal, three morphometric characters have been analysed: 1) size variability; 2) nodding and ornamentation; 3) variability of the percentage of the sieve-pore shapes. The palaeoenvironmental interpretation was made using synecological and geochemical approaches [stable isotopes, trace elements, Sr-isotopes and natural radioactivity (NRD)]. For this study, the 250 m-thick Messinian Lago-Mare succession of Eraclea Minoa (Agrigento, Sicily) was chosen for the presence of monotypic assemblages made only by *C. agrigentina* for around 70 m of thickness. The results of the morphometric analyses showed that: 1) size variations are not related to the salinity changes recognized both from synecological and geochemical analyses; 2) no noded specimens have been recovered along the section; 3) the salinities calculated on the basis of the percentage of the sieve-pore shape are not correlated with the salinities inferred from the synecological and geochemical analyses. Thus, in this paper we conclude that *C. agrigentina* cannot be considered a palaeosalinometer for the Messinian Salinity Crisis. There is a correlation of the  $\delta^{13}C$  with the percentages of sieve-pore shapes, linking them to the oxygen availability at the bottom of the basin.

## ANSWERS TO REFEREE COMMENTS

**REFEREE #1 – NEVIO PUGLIESE**

## GENERAL OPINION

Very good paper, well organized and , mainly, original work. Systematics correct. I appreciated the capability to combine different disciplines, mainly micropalaeontology and geochemistry. Thus, I think the work is adequate for the magazine, and worthy of being published with minor corrections. Most of my suggestions are optional. It is not necessary that I revise the text again. My anonymity is not necessary.

## INTRODUCTION

It is very clear; it properly presents the topic of the paper.

The aim of the work is very clear. However, it is included in the introduction. I suggest instead the Authors to better highlight the purpose of the work putting its sentences in a new paragraph. Basically the lines from 98 to 107 should become a new paragraph well separated from the previous text. The lines from 103 to 105 seem not clear. Are they maybe incomplete?

[We have checked the sentence from line 103 to 105 and corrected the English language.](#)

[We have moved the lines from 98 to 107 to a new paragraph as suggested.](#)

## CHAPTER 2

Material and methods: very clear. However, I personally prefer the 0,062 mm-mesh, but I understand that for the purpose of the work the 0.126mm sieve used can be good too.

[To analyze ostracods we generally use two sediment fractions \(0.063 mm 0.125 mm\) as suggested by the referee but in this case, being the work devoted only to the analysis of adult valves of \*C. agrigentina\* \( average sizes around 1 mm in length x....\) we considered that the 0.125 mm mesh was more than enough. We have better specified this in the text.](#)

## CHAPTER 3

It is clear. There is a small mistake in the lines 238 to 240: the authors of the species not in italics: *Livental...Olteanu* become **Livental...Olteanu**.

[All the author names have been written in plain text. Thanks to the referee to have signaled this editing mistake.](#)

## CHAPTER 4

No observations. It is very good. There is a small mistake in line 372: (**DeDeckker...**) becomes (**De Deckker...**).

[We have corrected the misspelled name at line 364.](#)

## CHAPTER 5

I suggest to change a little the order of the paragraphs:

lines **434-439** concern the ornamentation; lines **440-449** concern the sizes; lines **450-464** concern the sieve-pore canals. Thus, following the aims of the introduction (lines **102-103**) I suggest to report the data in this order: sizes, ornamentation, pore canals.

[As suggested, we changed the order of the paragraphs, starting with size followed with ornamentation and pore canals.](#)

## CHAPTER 6

The discussion is well organized and well articulated.

## CHAPTER 7

The conclusions are clear and original, even if apparently negative. The authors well underline the role of *C. agrigentina* as in palaeoenvironmental research, excluding it as marker of palaeosalinity.

## REFERENCES

Lines 734-735: Graham et al. (1982). I do not find it cited in the text.

We have deleted it

## FIGURES

Fig. 2 : I suggest to indicate in the caption the meaning of the numbers 3,4,5,6 reported in the figure

We have better specified in the caption the meaning of numbers in Fig. 2 (now fig 3)

## POSSIBLE OPTIONAL SUGGESTIONS

I suggest to insert a photo of *C. agrigentina*.

Done

## Referee #2 – Julio Rodriguez Lazaro

I have read the ms and in my opinion it is a very good paper, perfectly planned and written, with several sets of data allowing to reach the important conclusions (though they are "negative" for the use of *C. agrigentina* as palaeosalinometer).

Only couple of comments in the text. In particular:

In Fig. 4, are mentioned levels A, B, E, but these haven't been so far described. In Fig. 5 they are included by the first time (and described in paragraph 4.5). Since they are very used through the text, the units A, B, C, D, E must be added to some other figures, in order to easy the reading.

Done. We have changed the order of Fig. 4 and 5 (now fig 5 and 6), mentioned in the paragraphs 4.1-4.4 the intervals and reported the intervals in Fig. 7 (now fig. 8).

Fig. 7 Interval B. The hydrological interpretation with: "High freshwater and detrital inputs. Possible low salinities that slightly increase again around 222-225 m." is in apparent contradiction with the salinity inferred by pores, in the left of figure. After the latter, there is the maximum of salinity in these levels.

Yes, fig. 7 (now 8) is thought to show the contradiction between the salinity inferred by geochemistry and the salinity inferred by sieve pores. To better clarify it, in Fig. 8 we added to "Palaeohydrology" the sentence "inferred from geochemical analyses". The lack of correspondence between the two dataset is widely discussed in chapter "Discussion" and is the core of the paper.

Intervals D, E. There are marked dysoxic levels coincident with the increase of Shannon diversity. In general, the increase of diversity is indicative of some stabilisation of the environment, which is the opposite of indicated. It must be another factor influencing (you mention the oxygen availability, at the end of discussion). (Please correct disoxyc in D, and hydrochemistry in E).

Yes, indeed Shannon-Wiener index and authigenic U curves are negatively correlated. We added a discussion on those results in the paragraph "Discussion" concluding that it is probable that at Eraclea Minoa the causes for the authigenic U accumulation were others than oxygen availability. We have corrected the misspelled words in Fig. 7 (now 8).

In this matter, a "Relatively stable hydrochemical conditions" are indicated in A, but the diversity is very low (monospecific), so some important environmental factor is acting to prevent the "natural trend" of increase of diversity. (oxygen availability, as well?) (have you any proxy for oxygen availability?).

You are right. Some important environmental factor is limiting the colonization by ostracods but....which one? In this paper we have tried to perform different geochemical analyses, but none of them explained us what happened in this close “Lago-Mare” basin after the acme of the Messinian Salinity Crisis. Data show that it was a high suitable environment for *C. agrigentina* alone, but which kind of environment?

Fortunately, the palaeoenvironmental interpretation of the Eraclea Minoa succession wasn't the main aim of this paper, which is focussed to the possible use of *C. agrigentina* as palaeosalinometer. Anyway, in no other Lago-Mare section in which ostracod assemblages were studied there is such a long interval in which *C. agrigentina* is so abundant and alone in the assemblage. But Eraclea Minoa is also the only one section in which diagenetic gypsum cristalized from the groundwater, so....

Concerning the oxygen availability, we hoped that authigenic Uranium could be a good proxy to evaluate it. It seems that in the case of Eraclea Minoa it is not true. Anyway, another good proxy could be, as it has been discussed, the  $\delta^{13}\text{C}$  and, indeed, it seems that the sieve-pore variability in *C. agrigentina* could correlate with it.

#### **COMMENTS BY EDITOR IN CHIEF**

As editor in chief, I will be glad to endorse the guest editor's decision to accept this ms for publication in our journal after one minor change. You have to realize that we have an international readership, therefore Figure 1 is not appropriate. Instead of just showing Italy (without even giving the name of the country), you need to provide a larger view of the Mediterranean, with proper country names (Rome and Florence are not needed on such a map).

We modified fig. 2 as requested.

### Highlights

- We study in a palaeoenvironmental perspective a post-evaporitic ostracod assemblage.
- We perform morphometric and geochemical analyses on *Cyprideis agrigentina* valves.
- *C. agrigentina* sizes and ornamentation are not affected by salinity variations.
- Sieve-pore shapes in *C. agrigentina* seem linked to the bottom oxygen availability.
- *C. agrigentina* is not a palaeosalinometer for the Messinian Salinity Crisis.

1 **Is *Cyprideis agrigentina* Decima a good palaeosalinometer for the Messinian Salinity Crisis?**  
2 **Morphometrical and geochemical analyses from the Eraclea Minoa section (Sicily)**

3  
4 F. Grossi <sup>a,\*</sup>, E. Gliozzi <sup>a,b</sup>, P. Anadón <sup>c</sup>, F. Castorina <sup>d</sup>, M. Voltaggio <sup>b</sup>

5  
6 <sup>a</sup> *Dipartimento di Scienze, Università Roma Tre, Largo S. Leonardo Murialdo, 1, I-00146, Roma, Italy*

7 <sup>b</sup> *IGAG, CNR, Area della Ricerca di Roma RM1, Via Salaria km 29,300, CP 10, I-00016, Monterotondo Stazione,*  
8 *Roma, Italy*

9 <sup>c</sup> *Institut de Ciències de la Terra “Jaume Almera” (CSIC), C. Lluís Solé Sabarís sn, 08028, Barcelona, Spain*

10 <sup>d</sup> *Dipartimento di Scienze della Terra, Università Roma La Sapienza, P.le A. Moro, 5, I-00185, Roma, Italy*

11

12

13

14

15 \* Corresponding author: Present address: Dipartimento di Scienze, Università Roma Tre, Largo S. Leonardo Murialdo,  
16 1, I-00146, Rome, Italy

17 e-mail address: [francesco.grossi@uniroma3.it](mailto:francesco.grossi@uniroma3.it) (F. Grossi)

18

19

20 **ABSTRACT**

21

22 The living euryhaline species *Cyprideis torosa* (Jones) undergoes morphometric variations in size,  
23 nodding and sieve-pore shape linked to the environmental salinity. In particular it is known that  
24 salinity values around 8-9 psu represent the osmoregulation threshold and also the turning point  
25 between smaller and greater valve dimensions and prevalingly noded against un-noded valves. The  
26 variation of the percentage of round-, elongate- and irregular-shaped sieve-pores on the valves has  
27 shown an empiric logarithmic correlation with the water salinity from 0 to 100 psu. Due to this

28 ecologically cued polymorphism, *C. torosa* represents an invaluable palaeosalinometer for the  
29 Quaternary brackish basins.

30 In this paper we attempt to verify whether the ecophenotypical behaviour of the post-evaporitic  
31 Messinian species *Cyprideis agrigentina* Decima was comparable with that of *C. torosa*. To reach  
32 this goal, three morphometric characters have been analysed: 1) size variability; 2) nodding and  
33 ornamentation; 3) variability of the percentage of the sieve-pore shapes. The palaeoenvironmental  
34 interpretation was made using synecological and geochemical approaches [stable isotopes, trace  
35 elements, Sr-isotopes and natural radioactivity (NRD)]. For this study, the 250 m-thick Messinian  
36 Lago-Mare succession of Eraclea Minoa (Agrigento, Sicily) was chosen for the presence of  
37 monotypic assemblages made only by *C. agrigentina* for around 70 m of thickness.

38 The results of the morphometric analyses showed that: 1) size variations are not related to the  
39 salinity changes recognized both from synecological and geochemical analyses; 2) no noded  
40 specimens have been recovered along the section; 3) the salinities calculated on the basis of the  
41 percentage of the sieve-pore shape are not correlated with the salinities inferred from the  
42 synecological and geochemical analyses. Thus, in this paper we conclude that *C. agrigentina* cannot  
43 be considered a palaeosalinometer for the Messinian Salinity Crisis.

44 There is a correlation of the  $\delta^{13}\text{C}$  ~~and NRD data~~ with the percentages of sieve-pore shapes, linking  
45 them to the [behavior of the dissolved inorganic carbon \(DIC\) and to the](#) oxygen availability at the  
46 bottom of the basin.

47  
48 **KEYWORDS**

49 [Ostracoda; morphometrical analyses; geochemical analyses; palaeoenvironmental reconstruction;](#)  
50 [post-evaporitic Messinian; Sicily \(Italy\).](#)

51  
52 **1. Introduction**

53 Since the pioneering studies by Schäfer (1953), Sandberg (1964), Vesper (1975) and  
54 Rosenfeld and Vesper (1977), it is known that the living anomalohaline species *Cyprideis torosa*  
55 (Jones) undergoes morphometrical variations in size, nodding and sieve-pore shape linked to  
56 environmental physical and chemical parameters - especially salinity - showing a clear  
57 environmentally cued polymorphism. The species can withstand and thrive in a very wide range of  
58 salinity (0.4 to 150 psu according to Neale, 1988 and Griffiths and Holmes, 2000), thus it is  
59 commonly regarded as a valuable palaeosalinometer for the Quaternary marginal marine and  
60 athalassic brackish deposits (Marco-Barba, 2010; Pint et al., 2012 with references therein). Its low-  
61 Mg calcite shell represents also a source of biogenic carbonate for the geochemical analyses (trace  
62 elements, stable isotopes and  $^{87}\text{Sr}/^{86}\text{Sr}$  ratios) to infer the chemical composition of past waterbodies,  
63 because of its high rate of valve calcification. In many studies, morphometrical variations were  
64 coupled with the geochemical approach to make more detailed palaeoenvironmental reconstructions  
65 of brackish environments (Barbieri et al., 1999; Anadón et al., 2002; Marco-Barba, 2010; Curry et  
66 al., 2013; Pint et al., 2013; Rossi et al., 2013).

67 Several studies (Carbonel, 1982; Aladin, 1993; van Harten, 1996; 2000; Keiser and Aladin,  
68 2004; Keyser, 2005; Boomer and Frenzel, 2011; Frenzel et al., 2011; 2012 among others) showed  
69 that salinity values around 8-9 psu represent the osmoregulation threshold and also the turning point  
70 between smaller and greater valve dimensions and prevailingly noded against un-noded valves.  
71 Rosenfeld and Vesper (1977) showed an empiric logarithmic correlation between the variation of  
72 the percentage of round-, elongate- and irregular-shaped sieve-pores on the valves of *C. torosa* and  
73 the water salinity from 0 to 100 psu. This correlation has been confirmed by subsequent papers  
74 (Neale, 1988; Keating et al., 2007; Pint et al., 2012) and Frenzel et al. (2011) elaborated a transfer  
75 function based on the percentages of round sieve-pores.

76 In order to decipher the palaeosalinity changes during the end of the Messinian Salinity  
77 Crisis (Hsü et al., 1973; CIESM, 2008; [Roveri et al., 2014a](#)), Rosenfeld (1977) and Bonaduce and  
78 Sgarrella (1999) applied the counting of different sieve-pore shapes to the fossil species *Cyprideis*



79 *agrigentina* Decima, supposing that also this species could morphologically react as *C. torosa*. In  
80 both cases they obtained hyperhaline values for the waters hosting *C. agrigentina* specimens  
81 (respectively 35-50 psu and 50-70 psu) considering ~~this~~-those values reliable for the evaporative  
82 palaeoenvironment that yielded the deposition of the gypsum.

83 *C. agrigentina* (Fig. 1) is one of the most widespread ostracod that lived in the  
84 Palaeomediterranean during the latest Messinian Lago-Mare event (5.53–5.33 Ma, CIESM, 2008;  
85 5.55-5.33 Ma, Manzi et al., 2013; Roveri et al., 2014a). It seems to have been the first ostracod that  
86 colonized again the sterile bottoms of the Palaeomediterranean after the deposition of the Primary  
87 Lower Gypsum and the partial desiccation of the basin, and it has been recovered both in the  
88 Messinian sediments drilled on the Palaeomediterranean bottoms and in those cropping out along  
89 the peri-Mediterranean chains, from the most western area (Malaga Basin) to the easternmost  
90 Adana Basin (Benson, 1978; Iaccarino and Bossio, 1999; Bonaduce and Sgarrella, 1999; Grossi and  
91 Gennari, 2008; Guerra-Merchán et al., 2010; Cosentino et al., 2012; Faranda et al., 2013). In their  
92 study on the Messinian Lago-Mare palaeoenvironments inferred from the ostracod assemblages,  
93 Grossi et al. (2008) showed that *C. agrigentina* behaved as a very euryhaline species: it was  
94 associated a) with the benthic foraminifer *Ammonia tepida* (“*Cyprideis-Ammonia* assemblage”) in  
95 very oligotypic assemblages supposed to be typical of high mesohaline environments; b) with  
96 *Loxoconcha muelleri* (Mehés) and *Loxoconcha eichwaldi* Livaltal (“*Cyprideis-Loxoconcha*  
97 assemblage”) (low mesohaline environment); c) it was also a component, although not dominant, of  
98 the “pointed candonids-Leptocytheridae assemblage” and “pointed candonids assemblage”,  
99 supposed to be characteristic of oligohaline to low mesohaline environments.

100 Anyway, despite its apparent capability to withstand different salinities, no noded specimens  
101 of *C. agrigentina* have been ever found (Ligios and Gliozzi, 2012) and this could arise some  
102 questions about the possible ecophenotypical reaction of *C. agrigentina* to the environment.

103 In this paper we attempt to verify whether the ecophenotypical behavior of *C. agrigentina*  
104 was comparable with that of *C. torosa*. To reach this goal, adult male and female valves of *C.*

105 *agrigentina* from the long section of Eraclea Minoa (Agrigento, Sicily) were investigated and three  
106 morphometrical characters have been analysed: 1) size variability; 2) nodding and ornamentation; 3)  
107 variability of the percentage of the sieve-pore shapes. The palaeoenvironmental framework to  
108 which the ecophenotypical characters displayed by *C. agrigentina* will be compared has been built  
109 based on synecological analysis (assemblages taxonomic composition and diversity) (Chapter 3)  
110 and geochemical approaches [stable isotopes, trace elements, Sr-isotopes and natural radioactivity  
111 (NRD)] (Chapter 4).

Formatted: Highlight

112

## 113 2. Material and methods

114 One hundred fifty-two samples have been soaked in a H<sub>2</sub>O<sub>2</sub> 5%<sub>vol</sub> solution for 24 hours,  
115 sieved with 0.063 and 0.125 mm-mesh sieves and dried in oven at 40°C. Total manual picking has  
116 been carried out on the 0.125 mm dried sieved samples. When possible, up to 300 valves were  
117 hand-picked from each sample. Ostracods have been identified and their frequency counted; the  
118 obtained values have been normalized to 10 g in order to get comparable figures all along the  
119 section to perform a reliable palaeoenvironmental interpretation using the synecological approach  
120 proposed by Gliozzi and Grossi, 2008 and Grossi et al., 2008. Shannon-Wiener index has been  
121 calculated on the basis of the normalized matrix.

122 When possible, supplementary adult specimens of *C. agrigentina* were picked to increase  
123 the amount of material on which the morphometrical and geochemical analyses were performed.  
124 The morphometrical and geochemical analyses have been carried out on more than 3000 adult  
125 valves of *C. agrigentina*, and several thousand juvenile valves were added for Sr-analyses.

126

### 127 2.1 Morphometrical analyses

128 All juvenile and adult valves of *C. agrigentina* were observed under the stereo-microscope  
129 to investigate the ornamentation and nodding.

130 Over one thousand adult female and male valves of *C. agrigentina* from fifty-three selected  
131 samples were measured under the stereo-microscope, using the Leica Application Suite 2.5.0. Mean  
132 values were calculated for each sample.

133 Around 20 adult female and male valves of *C. agrigentina* from fifty-three samples, chosen  
134 on the basis of its high frequency, were observed under the Scanning Electron Microscope (LIME  
135 Laboratory, Roma Tre University). Following the methodology proposed by Rosenfeld and Vesper  
136 (1977), the rounded, elongated and irregular sieve-pores were counted and each percentage was  
137 calculated. To obtain the inferred salinity value, the following transfer function elaborated by  
138 Frenzel et al. (2011), based on the percentage of rounded sieve-pores was used:

139 
$$S = e^{-0.06RS + 4.7}$$

140 where S = salinity (psu) and RS = percentage of rounded sieve-pores.

141

## 142 2.2 Geochemical analyses

143

### 144 2.2.1 Stable isotopes

145 Carbon and oxygen stable isotope analyses ( $\delta^{13}\text{C}$  and  $\delta^{18}\text{O}$ ) were performed on fifty-three  
146 ostracod samples each consisting of ~~8~~eight *C. agrigentina* clean adult valves. Two splits of each  
147 sample (4 valves each) were reacted with anhydrous phosphoric acid at  $76^\circ\text{C} \pm 2^\circ\text{C}$  in a Finnigan  
148 MAT Kiel preparation device directly coupled to the inlet of a Finnigan MAT 251 triple collector  
149 isotope ratio mass spectrometer (Stable Isotope Laboratory, University of Michigan, Ann Arbor,  
150 MI, USA). The isotopic results of the mean of the two splits are reported in permil (‰) notation  
151 relative to the Pee Dee Belemnite (PDB) standard. The measured precision for the analyses was  
152 0.04 for  $\delta^{13}\text{C}$  and 0.07 for  $\delta^{18}\text{O}$ .

153

### 154 2.2.2 Trace elements

155 Trace and minor element analyses together with Ca on fifty-three ostracod samples,  
156 consisting each in 6 to 10 clean adult valves of *C. agrigentina*, were performed by inductively  
157 coupled plasma atomic emission spectrometry (ICP-AES). The ostracod valves were dissolved in 3  
158 ml of ultrapure HNO<sub>3</sub> acid (3%). The solutions were analysed for Ca (317.9 nm), Mg (285.2 nm),  
159 Na (589.5 nm) and Sr (215.2 nm) in the ICP-AES Thermo Jarrell IRIS Advantage Radial device of  
160 the Institute of Environmental Assessment and Water Research (IDAEA-CSIC, Barcelona, Spain).  
161 The limits of detection were 0.05 ppm for Ca and Mg, 0.01 ppm for Na and 0.005 ppm for Sr. All  
162 the analyses were run against multielemental standards prepared from Johnson Matthey™ stock  
163 solutions. The obtained results are expressed as metal/calcium ratios of the valves (Me/Ca<sub>v</sub>).

164

### 165 2.2.3 Sr isotope analyses

166 Strontium isotope measurements were obtained from 26 suitable samples of hand-picked  
167 valves of *C. agrigentina*, perfectly preserved. About 10 mg of each sample was subjected to the  
168 following procedure: ultrasonic cleaning in double distilled water to remove impurities; gentle  
169 crushing and re-washing in double-distilled water; fast dissolution in 4.0 N ultrapure HCl;  
170 centrifugation; loading onto standard BIO-RAD AG50-X12cation exchange resin. The total  
171 procedure blank was 0.5 ng. Sr was collected in 2.9 and 6.3 N HCl and evaporated.

172 Isotopic analyses were carried out at IGAG-CNR c/o Department of Earth Sciences,  
173 University of Rome — La Sapienza using a FINNIGAN MAT 262RPQ multicollector mass  
174 spectrometer with Re double filaments in static mode. The internal precision (within-run precision)  
175 of the single analytical value is given as two standard error of the mean. The <sup>87</sup>Sr/<sup>86</sup>Sr ratios of the  
176 samples were normalized to a <sup>86</sup>Sr/<sup>88</sup>Sr value of 0.1194. The internal precision (‘‘within-run’’  
177 precision) of a single analytical result is reported as 2 standard errors of the mean (2SE) and is  
178 obtained as the mean of more than 800–1000 ratios collected in each sample with a stable beam of  
179 > 2.0 V. Repeated analyses of NIST-987 during the period of the analyses gave a mean value  
180 <sup>87</sup>Sr/<sup>86</sup>Sr = 0.710251±15 (2σ, n = 15).

**Formatted:** Indent: First line: 1.27 cm, Don't adjust space between Latin and Asian text, Don't adjust space between Asian text and numbers

181

#### 182 2.2.4 Natural Radioactivity (NRD)

183 Natural Radioactivity (NRD) was measured on 27 bulk sediment samples. Uranium, thorium and  
184 potassium were determined by high resolution gamma spectrometry using a low background (GEM-  
185 EG&G ORTEC) HPGe coaxial detector in a PopTop capsule including detector element,  
186 preamplifier and high voltage filter at the Institute of Environmental Geology and Geoengineering  
187 (IGAG, CNR, Rome - Italy). The multichannel buffer (16,384 channels, Ethernim-ORTEC 919E),  
188 including ADC with extended live time correction, was connected into an Ethernet environment  
189 under Windows XP and its control and spectral display was achieved by the use of MAESTRO  
190 application software. In particular,  $^{232}\text{Th}$  and K were estimated from 583 keV ( $^{208}\text{Tl}$ ) and 1461 keV  
191 ( $^{40}\text{K}$ ) peaks, while  $^{238}\text{U}$  was estimated -by the weighted average of U1 and U2, -where U1 is the  
192 product of the known  $^{238}\text{U}/^{235}\text{U}$  natural activity ratio by the  $^{235}\text{U}$  activity (calculated by the 186 keV  
193 peak corrected by the  $^{226}\text{Ra}$  contribution) and U2 is the  $^{238}\text{U}$  activity -estimated by the 352 keV peak  
194 ( $^{214}\text{Pb}$ ) assuming full equilibrium in the  $^{238}\text{U}$  radioactive series.  
195 Capo di Bove leucitite (Voltaggio et al., 2004) was used as standard, while counting time and  
196 amount of each sample were, respectively, 86,400 sec and 150 grams.

197

#### 198 2.3 Statistical analyses

199 A raw matrix of data has been was constructed taking into account those samples that have provided  
200 all the results for the considered types of analyses (9 variables): stratigraphic position, lithology,  
201  $\delta^{13}\text{C}$ ,  $\delta^{18}\text{O}$ , Mg/Ca, Sr/Ca, Na/Ca, Th/U, assumed salinity after the sieve-pore analysis and the  
202  $^{87}\text{Sr}/^{86}\text{Sr}$  ratio. The statistical software used was STATISTICA 7.0. From the raw matrix, with 9  
203 variables and 20 cases (samples), a correlation matrix was obtained. Moreover from the raw matrix,  
204 a set of multivariate analysis techniques, as cluster and principal-component analysis (PCA) was  
205 applied. Cluster analysis defines groups of more or less related variables and the corresponding  
206 dendrogram (tree clustering) corresponds to the graphic display of the groups. PCA defines

Formatted: Highlight

Formatted: Highlight

Formatted: Highlight

Formatted: Highlight

Formatted: Highlight

Formatted: Highlight

Formatted: Highlight

207 ~~eigenvectors showing the position of the variables in the factor plane and revealing the underlying~~  
208 ~~structure of the data set. From the raw matrix, with 8 variables and 26 cases (samples), a correlation~~  
209 ~~matrix is obtained. Moreover from the raw matrix, a set of multivariate analysis techniques, as~~  
210 ~~cluster and principal component analysis (PCA) have been applied. Cluster analysis defines groups~~  
211 ~~of more or less related variables and the corresponding dendrogram (tree clustering) corresponds to~~  
212 ~~the graphic display of the groups. PCA defines eigenvectors showing the position of the variables in~~  
213 ~~the factor plane and revealing the underlying structure of the data set. An additional analysis with 9~~  
214 ~~variables, the 8 ones mentioned above and the Th/U ratio, has been performed. In this case the~~  
215 ~~number of suitable samples is reduced to 10.~~

216

### 217 **3. The Eraclea Minoa section and its palaeoenvironments inferred from ostracod assemblages**

218 The ca. 266 m-thick Messinian Lago-Mare succession of Eraclea Minoa crops out along the  
219 south-western coast of Sicily (lat. 37°23'30"N, long. 13°16'50"E) along the cliff which borders the  
220 village (Fig. 42). The section has been extensively studied since 1971 (Decima and Wezel, 1971)  
221 because it is one of the most complete Messinian Lago-Mare section of the Palaeomediterranean  
222 where several gypsum levels referred to the Upper Gypsum Unit crop out (among the most recent  
223 papers: Schreiber, 1997; Caruso and Rouchy, 2006; Van der Laan et al., 2006; Manzi et al., 2009  
224 with references therein), and because it represents the GSSP of the Messinian/Zanclean boundary  
225 (Van Couvering et al., 2000 with references therein) (Fig. 23).

226 The succession is made of a rhythmic alternation of clays and marls interbedded with sandy  
227 and fine grained carbonates and seven gypsum bodies made by multiple strata of finely-laminated  
228 gypsum and gypsarenites/selenites (Fig. 34). The astrochronological tuning of the Eraclea Minoa  
229 section is different according to several authors. As stated by Caruso and Rouchy (2006), six  
230 sedimentary cycles covered by the Arenazzolo Fm. up to the Messinian/Zanclean boundary are  
231 recognizable, with a possible seventh basal cycle represented by an intensively deformed gypsum  
232 deposit located along the fault contact at the base of the succession. Van der Laan et al. (2006)

233 consider the presence of seven cycles and a half, including the Arenazzolo Fm. They are linked to  
234 the precessional cyclicity and date the deposition of the Eraclea Minoa succession between 5.508  
235 Ma to 5.332 Ma. Finally, Manzi et al. (2009; 2012) hypothesize the presence of nine to ten  
236 sedimentary cycles, including the Arenazzolo Fm., bracketing the depositional age between 5.53  
237 and 5.33 Ma.

238 Ostracods are discontinuously present at the base of the section, in the marls intercalated  
239 between the lowest six gypsum bodies and become abundant in the upper portion, below and above  
240 the seventh gypsum level. Assemblages show variable richness from 1 species (monotypic  
241 assemblages made only by *C. agrigentina*) up to 13 species mainly made by the typical Lago-Mare  
242 ostracod assemblages of Paratethyan origin.

243 In the lowest portion from 88 (sample EM 3-3) to 144 m (sample EM 6-7), *C. agrigentina* is  
244 scarce and the assemblages, made by *Loxoconcha muelleri* (Méhés), *L. kocki* Méhes, *L. eichwaldi*  
245 Livental, *Loxocorniculina djafarovi* (Schneider), *Loxocauda limata* (Schneider), *Camptocypria* sp.  
246 1, *Tyrrhenocythere pontica* (Livental), *Euxinocythere (Maeotocythere) praebaquana* (Livental),  
247 *Amnicythere propinqua* (Livental), *A. subcaspia* (Livental), *A. multituberculata* (Livental) and *A.*  
248 *accicularia* Olteanu, are rather diversified. These assemblages can be referred to the “*Cyprideis-*  
249 *Loxoconchidae* assemblage” (*sensu* Grossi et al., 2008), suggesting low mesohaline and shallow  
250 waterbodies (supposed salinities <10 psu).

251 Monotypic assemblages have been recovered in the central portion of the Eraclea Minoa  
252 section, from 153 m (sample EM 6'-1) to 227 m (sample EM 7-12) and the collected valves are  
253 abundant and well preserved. In this long interval, *C. agrigentina* is the only species present in the  
254 samples or is accompanied by the euryhaline benthic foraminifer *Ammonia tepida* (Cushman).  
255 Grossi and Gennari (2008) defined the “*Cyprideis-Ammonia* assemblage” for some ostracod and  
256 forams associations recovered in the Lago-Mare borehole of Montepetra (northern Apennines, Italy)  
257 in which, together with *C. agrigentina* and *A. tepida*, also other ~~two~~ benthic foraminifers, *Florilus*  
258 *boueanum* (d'Orbigny) and *Elphidium* spp. were seldom present or *A. tepida* was the dominant

259 species of the assemblage. The authors related such “*Cyprideis-Ammonia* assemblage” to high  
260 mesohaline to hyperhaline shallow waterbody. At Eraclea Minoa no other brackish benthic  
261 foraminifers have been recovered except *A. tepida*. Moreover, this latter species is not always  
262 present and generally ~~it~~ is far subordinated to *C. agrigentina*. Thus, the palaeoenvironmental  
263 interpretation of the interval from 153 to 227 m at Eraclea Minoa could be slightly different. At the  
264 moment, we can suppose for this new “*Cyprideis* assemblage” a relatively high salinity waterbody  
265 and/or a dysoxic bottom, based on the capability of the living species *C. torosa* and *Ammonia* spp.  
266 to withstand low oxygen contents (Jahn et al., 1996; Bernhard and Sen Gupta, 2002). Different  
267 assemblages, made only by scarce *C. agrigentina* and accompanying *Loxoconcha muelleri* were  
268 recovered in the Lago-Mare succession of Colle di Votta (Majella Mt., central Italy) (unpublished  
269 data), in oxygen-depleted sediments (Sampalmieri et al., 2010).

270 In this central portion of the succession there are only five scattered samples in which the  
271 dominant *C. agrigentina* is associated with few other species: with *L. djafarovi* (at 182 m, sample  
272 EM 6’-29a), pointing to a low mesohaline environment; with *Ilyocypris* sp. (at 198.5 and 201.0 m,  
273 respectively samples EM 6”-8 and 6”-11), suggesting two short oligohaline episodes; with  
274 *Fabaeformiscandona* sp. (at 213 m, EM 6”-19) pointing to a further oligohaline episode; with *A.*  
275 *accicularia* (at 220.6 m, EM 7-4) indicating a low mesohaline short interval.

276 Finally, in the uppermost part of the section [from 228 m (sample EM 7-13) to 265.5 m  
277 (sample EM 8-20)], *C. agrigentina* is again accompanied by the Paratethyan assemblage in which  
278 Loxoconchidae are slightly less abundant and two more leptocytherid species are included, even if  
279 with scarce frequency: *Ammicythere litica* (Livental) and *A. costata* (Olteanu). On the whole, this  
280 topmost interval seems again to be referable to the “*Cyprideis*-Loxoconchidae assemblage” (Grossi  
281 et al., 2008), pointing to shallow waterbodies with supposed salinities <10 psu). Within this  
282 uppermost interval, it is possible to identify three horizons (from 228 m (sample EM 7-13) to 232  
283 m (sample EM 7-19), at 234 m (sample EM 7-21) and from 235 m (sample EM 7-25) to 238 m  
284 (sample EM 7-28)) in which *C. agrigentina* shares its dominance only with two candonids



285 species, *Fabaeformiscandona* sp. and *Cypria* sp., testifying an oligohaline and shallow  
286 environment, and two short levels [at 252.8 m (sample EM 8-3) and 257.8 m (sample EM 8-7)] in  
287 which *C. agrigentina* is again the only ostracod species of the assemblage.

288

#### 289 4. Geochemical analyses ~~on *Cyprideis agrigentina* from Eraclea Minoa~~ and inferred 290 palaeoenvironmental features

291

##### 292 4.1 Stable isotopes

293 ~~Ostracod~~ *C. agrigentina* calcite valves display a wide range of stable isotopic values.  $\delta^{13}\text{C}$   
294 ranges from -6.40 to 1.91‰;  $\delta^{18}\text{O}$  ranges from -4.08 to 7.95‰ (Tab. 1; Figs. 45, 56). The  $\delta^{13}\text{C}$   
295 values of the ostracod valves show a slight increase from 153-189 m (interval A) to 198-225 m  
296 (interval B). Significant, rapid variations are shown around 198-204 m and in the upper portion of  
297 the section (around 253-260 m) (interval E).

298 The  $\delta^{18}\text{O}$  values of the ostracod valves show a slight increase from 153 to 189 m (interval  
299 A), a rapid variation around 198-204 m (lower interval B), and lowering in  $\delta^{18}\text{O}$  values decrease  
300 from 198-204 to 225 m (upper interval B). In the upper portion of the section, from 257.8 to 258.5  
301 m (interval E), a significant decrease in  $\delta^{18}\text{O}$  values, from 8‰ to -1.4‰ is observed.

302 The  $\delta^{13}\text{C}$  and  $\delta^{18}\text{O}$  values from 153 to 189 m (interval A) display small fluctuations,  
303 suggesting minor variations in the palaeohydrological conditions. On the contrary, the valves from  
304 198-204 m (interval B) and 253-260 m (interval E) display significant oscillations, both in  $\delta^{13}\text{C}$  and  
305  $\delta^{18}\text{O}$  values, suggesting instabilities in the palaeohydrological conditions related to these intervals.

306 In both cases the larger instabilities (major  $\delta^{13}\text{C}$  and  $\delta^{18}\text{O}$  oscillations) may be linked to significant  
307 detrital and freshwater inputs as reflected by the coarse-grained detrital beds at 199 m and 256-  
308 264.5 m.

Formatted: Highlight

Formatted: Font: Italic

Formatted: Strikethrough

Formatted: Highlight

Formatted: Highlight

Formatted: Highlight

Formatted: Highlight

Formatted: Highlight

Formatted: Highlight

Formatted: Highlight

Formatted: Highlight

Formatted: Highlight

Formatted: Highlight

Formatted: Highlight

Formatted: Highlight

309 The distribution in a X-Y plot (Fig. 46) shows that the isotopic values from 153 to 216 m  
310 (interval A and lower B) display a negative covariant trend with a significant correlation ( $R=$   
311 0.894). This is mainly due to the negative correlation of the interval ~~from~~ 198-216 m (lower B,  $R=$   
312 0.903) and the almost invariant values in the interval 153-189 m (interval A).

Formatted: Highlight

#### 314 4.2 Trace elements

315 For ~~ostracod~~ *C. agrigentina* calcite valves, the Mg, Sr and Na content expressed as  $Mg/Ca_v$ ,  
316  $Sr/Ca_v$  and  $Na/Ca_v$  molar ratios are listed in Table 1 and represented in Fig. 55. The  $Mg/Ca_v$  values  
317 range from 0.0052 to 0.0158, the  $Sr/Ca_v$  values range from 0.0022 to 0.0054 and the  $Na/Ca_v$  values  
318 range from 0.0032 to 0.0046.

Formatted: Font: Italic

Formatted: Highlight

319 The  $Mg/Ca_v$  values ~~from C. agrigentina valves~~ show a significant drop from 189- to 198.2  
320 m (intervals A and B boundary) towards the upper portion of the succession, with a rapid variation  
321 around 153-156 m (lower interval A). An overall increase trend in  $Mg/Ca_v$  is recorded in the  
322 interval 198.2-225 m (interval B) and a significant increase in  $Mg/Ca_v$  is observed also in the upper  
323 part of the section (interval E). This is parallelized with a similar increase in the  $\delta^{13}C$  values.

Formatted: Highlight

Formatted: Highlight

Formatted: Highlight

Formatted: Highlight

Formatted: Highlight

Formatted: Highlight

324 The  $Na/Ca_v$  values ~~from C. agrigentina~~ show a slight decrease from 153-189 m (interval A)  
325 to 198-216 m (interval B), with a rapid variation around 198.2—201 m. A significant decrease of  
326  $Na/Ca_v$  is observed in the upper portion of the section (interval B). This is parallelized with the  
327 decrease in  $Sr/Ca$  and  $\delta^{18}O$  values.

Formatted: Highlight

Formatted: Highlight

Formatted: Highlight

#### 329 4.3 Sr isotopes

330 Differently from the ratios of cation concentrations and oxygen isotopes, no Sr isotope  
331 fractionation occurs during chemical and biological processes within the marginal basin (Faure and  
332 Powell, 1972). Considering that Ostracoda are good monitors of the composition of the aquatic  
333 environment (De Deckker et al., 1988), the Sr isotopic compositions of ostracod shells allow us to

334 evaluate the connectivity of the basin with the open ocean and the paleoclimatic conditions and  
335 hydrography.

336 The Eraclea Minoa section shows that the  $^{87}\text{Sr}/^{86}\text{Sr}$  values from the *C. agrigentina* valves  
337 are comprised between 0.708510 and 0.708729 (Tab-le 1). The range of values is high in the lower  
338 analysed interval (153-189 m interval A) and decreases in the portion comprised between 198 to  
339 225 m interval B, reaching the minimum values (0.708510 and 0.708511) in the interval 204.2-  
340 210 m low interval B, in correspondence of low  $\delta^{18}\text{O}$ ,  $\text{Sr}/\text{Ca}_v$  and  $\text{Na}/\text{Ca}_v$  values. In the upper  
341 portion of the section (253-260 m interval E) the  $^{87}\text{Sr}/^{86}\text{Sr}$  values rise again, with a maximum  
342 (0.708704) at 253 m (Fig. 55). Sr isotopic data of *C. agrigentina* are markedly different with respect  
343 to coeval global ocean values (Henderson et al., 1994; McArthur et al., 2001) being significantly  
344 lower than the marine waters at that time, but this is a common feature for -latest Miocene-earliest  
345 Pliocene strontium values of the Mediterranean-Palaeomediterranean Basin carbonates.

346

#### 347 4.4 Natural Radioactivity

348  $^{232}\text{Th}$  and K measured in bulk sediment samples are highly correlated ( $r=-0.94$ ) suggesting that  
349  $^{232}\text{Th}$  is mainly contained in the detrital fraction. Detrital uranium, in turns, was calculated by the  
350 product of measured  $^{232}\text{Th}$  and the average  $^{238}\text{U}/^{232}\text{Th}$  weight ratio of pelagic sediments, considered  
351 close to 0.25 (Mangini et al., 2001). Finally, authigenic uranium,  $^{238}\text{U}_a$  was estimated by  
352 subtracting the detrital  $^{238}\text{U}$  from measured  $^{238}\text{U}$  (Tab-le 2). Authigenic uranium as well as the Th/U  
353 ratio was proposed by Wignall and Myers (1988) as an index of bottom-water oxygenation, the  $\text{U}_a$   
354 values trending to increase in a reducing environment, where uranium is immobile as tetravalent  
355 ion. According to Wignall (1994)  $\text{U}_a$  values comprised between 2 and 10 are indicative of dysoxic  
356 environments; similarly for Th/U values,  $\text{Th}/\text{U} \ll 1$  indicate anoxic conditions,  $\text{Th}/\text{U} > 1$  indicate oxic  
357 conditions, while values in the range  $1 < \text{Th}/\text{U} < 1$  point to dysoxic conditions. Even if the use of authigenic  
358 uranium as proxy for reducing conditions -is common in the chemiography of marine sediments  
359 (Pattan and Pearce, 2009), several authors have questioned the real preservation of the authigenic

Formatted: Highlight

Formatted: Highlight

Formatted: Highlight

Formatted: Highlight

Formatted: Highlight

Formatted: Highlight

Formatted: Highlight

Formatted: Highlight

Formatted: Highlight

Formatted: Subscript

Formatted: Highlight

Formatted: Highlight

Formatted: Highlight

Formatted: Highlight

Formatted: English (U.K.), Highlight

Formatted: Highlight

Formatted: English (U.K.), Highlight

Formatted: Highlight

Formatted: English (U.K.), Highlight

Formatted: Highlight

Formatted: English (U.K.), Highlight

Formatted: Highlight

360 uranium signal by different processes as burn down, fast change of sedimentation rate and oxygen  
361 ventilation or bioturbation (Zheng et al., 2002). Therefore any indication of oxygen depletion  
362 suggested by the authigenic uranium has to be regarded in a wider fitting context.

363 U<sub>a</sub> from the bulk sediment display values from 0.3 to 9.5 ppm (Table 2). The lowest values are  
364 attained in intervals A, B and lower C, with figures generally below 2. In the upper part of interval  
365 C, U<sub>a</sub> increases and maintains high values in interval D and E, where some fluctuations occur,  
366 similarly to what observed for the stable isotopes and trace elements ratios (Fig. 5). A similar trend  
367 is observed for the Th/U ratios, which show values greater than 1 in intervals A, B and C, and  
368 values mainly around 1 in intervals D and E (Table 2).

Formatted: Highlight

Formatted: Subscript, Highlight

Formatted: Highlight

Formatted: Highlight

Formatted: Highlight

Formatted: Highlight

Formatted: Highlight

Formatted: Highlight

Formatted: Highlight

Formatted: Highlight

Formatted: Highlight

Formatted: Highlight

#### 370 4.5 Palaeoenvironmental episodes inferred from the geochemical proxies

371 The geochemical analyses performed on the valves of *C. agrigentina* and bulk sediment  
372 samples collected from the 96.5-260 m portion of the post-evaporitic Messinian succession of  
373 Eraclea Minoa confirm the frame of a Palaeomediterranean waterbody discontinuous and isolated,  
374 characterised by diluted waters after the evaporative phase of the Lower Gypsum Unit, the closure  
375 of the Atlantic-Palaeomediterranean connection and the subsequent global humid climate phase  
376 (Griffin, 2002; CIESM, 2008; Grossi et al., 2008). In fact, notwithstanding the clear-well known  
377 saline character of the Palaeomediterranean waters, testified by the presence of brackish ostracod  
378 assemblages, all the geochemical indicators point to a clear differentiation with the Messinian  
379 oceanic seawater. On the other hand, the stable isotopes values reported in Fig. 45.6 does not  
380 show the overall covariant trend that would correspond to a marginal marine environment or a  
381 closed waterbody (Talbot, 1990; Utrilla et al., 1998; Ligios et al., 2012), and also trace elements  
382 behave in a different manner. The Mg/Ca<sub>v</sub> values from *C. agrigentina* (Mg/Ca<sub>v</sub>=0.0052-0.0152) are  
383 similar to most of the analyses from *Cyprideis* shells for the Messinian Lago-Mare horizons from  
384 DSDP sites (De Deckker et al., 1988). For these Mg/Ca<sub>v</sub> values, De Deckker et al. (1988) consider  
385 the host water had Mg/Ca values lesser than that of Messinian seawater, and in some cases similar

Formatted: Highlight

Formatted: Highlight

386 to most of the Mg/Ca shown by freshwaters (Mg/Ca=1). The Sr/Ca<sub>v</sub> values from *C. agrigentina* at  
387 153-189 m (Sr/Ca<sub>v</sub>=0.0025-0.0030) are similar to most of the analyses from *Cyprideis* shells from  
388 the Messinian Lago-Mare horizons from DSDP sites (De Deckker et al., 1988). For these Sr/Ca<sub>v</sub>  
389 values, these authors consider the host water had Sr/Ca values lesser than that of Messinian oceanic  
390 seawater. On the contrary, the Sr/Ca<sub>v</sub> values for most of the samples from 198-225 m and 252.8-  
391 257.8 m (Sr/Ca<sub>v</sub>=0.0038-0.0054) indicate that the host water frequently had Sr/Ca values greater  
392 than that of Messinian oceanic seawater. The values of Sr/Ca<sub>v</sub> and Mg/Ca<sub>v</sub> indicate that the waters  
393 where the *Eraclea Minoa* ostracods lived were very different than the Messinian seawater and there  
394 is no indication of connection with oceanic seawater. Furthermore, the <sup>87</sup>Sr/<sup>86</sup>Sr range of values  
395 obtained from the analyses of *C. agrigentina* valves ~~from Eraclea Minoa~~ is consistent with the  
396 isotopic values of the Upper Gypsum Unit from Sicily and other localities of the  
397 Palaeomediterranean (Müller and Mueller, 1991; Keogh and Butler, 1999; Flecker and Ellam, 2006;  
398 Roveri et al., 2014b). This range is also similar to the range (0.708600-0.70875) reported from most  
399 ostracod valves (*Cyprideis*) from Messinian Lago-Mare deposits from several DSDP sites of the  
400 Palaeomediterranean studied by McCulloch and De Deckker (1989). On the other hand, the Sr  
401 isotopic values from *Eraclea Minoa* are quite different from the value of the average ocean water  
402 during the deposition of the Upper Evaporite: 0.709012 (Howarth and McArthur, 1997; Flecker et  
403 al., 2002). The <sup>87</sup>Sr/<sup>86</sup>Sr values of the *Eraclea Minoa C. agrigentina*, as is the case of materials from  
404 other post-evaporitic Messinian localities, confirm to be the result of a large influence of freshwater  
405 on the Sr isotopic composition of the desiccating subbasins of the Palaeomediterranean (Müller et  
406 al., 1990). Finally, it is noteworthy that isotopic ratios anomalously low could result from  
407 reworking of older marine evaporites, or diagenetic overprinting. However, according to Keogh and  
408 Butler (1999), the reworking of Sr from the older marine evaporites implies mixing in different  
409 proportion between Sr deriving from continental run-off and coming from ground water circulating  
410 inside the buried evaporites. Such a process likely produces high variability in both salinity and  
411 <sup>87</sup>Sr/<sup>86</sup>Sr ratios.

Formatted: Highlight

412 Based on the geochemical signature of *C. agrigentina* valves and bulk sediment samples,  
413 five main palaeoenvironmental intervals may be differentiated along the studied portion of the  
414 Eraclea Minoa succession (Fig. 5):

415 Interval A (153-189 m), characterised by high  $\delta^{18}\text{O}$ ,  $\text{Na}/\text{Ca}_v$ ,  $\text{Mg}/\text{Ca}_v$  and  $^{87}\text{Sr}/^{86}\text{Sr}$  values,  
416 and low  $\delta^{13}\text{C}_a$  ~~and~~  $\text{Sr}/\text{Ca}_v$  ~~and~~  $\text{U}_a$ . This interval records relatively stable hydrochemical conditions  
417 as suggested by the small variation of each geochemical indicator, isotopically concentrated waters  
418 and high  $\text{Na}/\text{Ca}_v$  and  $\text{Mg}/\text{Ca}_v$  ratios that were attained after the deposition of the 6<sup>th</sup> gypsum level.

419 An overall evaporative environment (Fig. 45) with moderate salinity could be inferred for this  
420 interval. The high amount of Th and detrital U, the low content of authigenic uranium and the rather  
421 high Th/U ratios (Table 2) record possible well oxygenated bottoms.

422 Interval B (198-~~to~~ 225 m), characterised by low  $\delta^{18}\text{O}$ ,  $\text{Na}/\text{Ca}_v$ ,  $\text{Mg}/\text{Ca}_v$ , ~~and~~  $^{87}\text{Sr}/^{86}\text{Sr}$ , and  
423  $\text{U}_a$  values, and high  $\delta^{13}\text{C}$  and  $\text{Sr}/\text{Ca}_v$ . A major change is recorded at the base of this interval (198 m,  
424 sample EM 6<sup>7</sup>-8) where large shifts in all the geochemical indicators appear. A possible explanation  
425 for these features is to consider the noticeable detrital and freshwater inputs that increase the Ca  
426 dissolution, recorded both by the coarser lithologies, the high values of Th and detrital U and the  
427 low  $^{87}\text{Sr}/^{86}\text{Sr}$  values for most samples. Those inputs may explain the lowering of  $\delta^{18}\text{O}$  in the valves,  
428 the increase of  $\text{Sr}/\text{Ca}_v$  (recording Sr inputs from the  $\text{CaSO}_4$ -rich subsurface waters) and the lowering  
429 in  $\text{Mg}/\text{Ca}_v$  because of the high increase in Ca in the waterbody. The increase in  $\delta^{13}\text{C}$  values could  
430 be produced by an increase in the productivity, linked to the detrital and nutrient inputs and a trend  
431 to re-equilibration with the atmospheric  $\text{CO}_2$  (Fig. 45). As in the previous interval, NRD results  
432 (Table 2) testify for possible ~~The high amount of Th and detrital U and the low content of~~  
433 ~~authigenic uranium (Tab. 2) record~~ well oxygenated bottoms.

434 Interval C (225-240 m). In this interval, only NRD analyses have been performed due to the  
435 low frequency of *C. agrigentina* in the ostracod assemblages, that prevented the possibility to reach  
436 the suitable amount of biogenic carbonate for the analyses. The content of authigenic uranium in the

Formatted: Not Superscript/ Subscript

Formatted: Not Superscript/ Subscript

Formatted: Highlight

Formatted: Highlight

Formatted: Highlight

Formatted: Subscript

Formatted: Highlight

Formatted: Highlight

Formatted: Highlight

Formatted: Highlight

437 upper part of this interval, higher than in the previous one, (Table 2, Fig. 5) points to possibly  
438 progressively less oxygenated bottoms.

Formatted: Highlight

Formatted: Highlight

439 Interval D (240-242 m). This short interval is characterised by the highest values of  
440 authigenic U and low values of the Th/U ratios, suggesting possible dysoxic conditions at the  
441 bottom.

442 Interval E (252.8-259.1 m). In this interval two portions may be differentiated and a main  
443 change is recorded from the lower samples to the upper ones. The lower samples are characterised  
444 by high  $\delta^{18}\text{O}$ ,  $\text{Sr}/\text{Ca}_v$ ,  $\text{Na}/\text{Ca}_v$ , and  $^{87}\text{Sr}/^{86}\text{Sr}$  values, and low  $\delta^{13}\text{C}$  and  $\text{Mg}/\text{Ca}_v$  values. The low

Formatted: Highlight

445 content of authigenic uranium indicates possibly oxygenated bottoms. The upper samples are  
446 characterised by the opposite trends. The geochemical features of the ostracod valves from the  
447 lower part may be explained by the evaporitic concentration of the waterbody (Figs. 5, 46) leading  
448 to high  $\delta^{18}\text{O}$ ,  $\text{Sr}/\text{Ca}_v$  and  $\text{Na}/\text{Ca}_v$  values. A subsequent large input of freshwater produced the  
449 lowering of  $\delta^{18}\text{O}$ ,  $\text{Sr}/\text{Ca}_v$  and  $\text{Na}/\text{Ca}_v$ . At present, we have no explanation for the variations of the  
450  $\text{Mg}/\text{Ca}_v$  values in this interval. It is worth to note the high content of authigenic uranium that

Formatted: Highlight

451 reaches in one sample the value of 9.5 ppm, possibly indicating dysoxic conditions at the bottom.

Formatted: Highlight

Formatted: Highlight

452

### 453 5. Morphometrical analyses on *Cyprideis agrigentina* valves

454 Length and height of one thousand-sixty valves of adult males and females were measured.  
455 The obtained values fall within the variability field typical of the species (Decima, 1964; Ligios et  
456 al., 2012). The mean values of the length of the female left valve (the most numerous in the  
457 measured samples) have been compared. Generally the mean values of the length vary from 0.96 to  
458 1.00 mm, but in few samples the mean values are rather small: at 185 m (sample EM 6<sup>3</sup>-3, mean  
459 value 0.90 mm), 201 m (EM 6<sup>3</sup>-11, mean value 0.89 mm), 222 m (EM 7-6, mean value 0.85 mm),  
460 and 223.5 m (EM 7-8, mean value 0.88 mm) (Fig. 67). Only in four samples the mean values of the  
461 length result significantly large/high: at 165 m (sample EM 6<sup>2</sup>-12 mean value 1.05 mm), 176.2 m

462 | (sample EM 6<sup>2</sup>-24, mean value 1.06 mm), 180 m (EM 6<sup>2</sup>-27, mean value 1.04 mm), and 210 m (EM  
463 | 6<sup>2</sup>-17, mean value 1.14 mm).

464 | The several thousands specimens of *C. agrigentina* investigated for the ornamentation and  
465 | nodding, showed rather homogeneous ornamentation: no noded specimens have been observed all  
466 | along the section among both juveniles and adults; almost all valves were smooth (at least some of  
467 | them showed few small pits in the posterior surface); only two samples (EM 6<sup>2</sup>-7 at 189.0 m and  
468 | EM 6<sup>2</sup>-20 at 216.0 m) showed, respectively, the 54.2% and 54.6% of valves pitted on the entire  
469 | surface (Fig. 67).

470 | The analysis of the percentage of the sieve-pore shape was carried out on fifty-three samples  
471 | from the middle and upper portion of the section, where *C. agrigentina* was more abundant, making  
472 | both monospecific and diversified assemblages. On average, more than 500 sieve-pores were  
473 | observed for each sample and counted on the basis of their shape: rounded, elongated, irregular,  
474 | following the indications by Rosenfeld and Vesper (1977). The results are reported in Fig. 67. In  
475 | most cases, the percentages of the rounded sieve-pores are comprised between 40 and 50%; in  
476 | twelve scattered samples they are higher, reaching the maximum value of 65% at 96.5 m (sample  
477 | EM 4-7) and only in a short interval from 198.5 m (sample EM 6<sup>2</sup>-8) to 216 m (sample EM 6<sup>2</sup>-20)  
478 | they are lower, comprised between 19 and 30%, reaching their minimum values (19-21%) in the  
479 | interval 204.5-216 m. Applying the transfer function elaborated by Frenzel et al. (2011) for *C.*  
480 | *torosa*, the resulting salinities expressed in psu shows values included in the mesohaline range (5-18  
481 | psu, Venice Symposium, 1958) for most samples. Only few scattered samples in the lower and  
482 | upper portions of the section point to the oligohaline range (0.5-5 psu), while higher salinities  
483 | (polyhaline to euhaline ranges, 18-40 psu) are recorded only in a limited portion of the section, from  
484 | 198.5 to 216 m (Fig. 78).

485

## 486 | 6. Discussion



487 As explained in the introduction, the living species *C. torosa* is considered to be one of the  
488 most valuable tools to detect past salinities in the marginal marine environments, owing to its  
489 environmentally cued polymorphism that induces variations in size, nodding and sieve-pore shapes  
490 depending on salinity. Large sizes, presence of nodes and high percentages (around 40-45%) of  
491 rounded sieve-pores point to salinity less than 8-9 psu that is considered an important  
492 osmoregulation threshold for the species (Keiser and Aladin, 2004; Keyser, 2005).

493 It is not clear when *Cyprideis torosa* appeared for the first time, owing to the difficulty to  
494 identify the species. Often in the Neogene sediments *Cyprideis* remains have been recorded as  
495 *Cyprideis* gr. *torosa* or *Cyprideis* sp. (Bossio et al., 1993; 1996; Testa, 1995). According to Decima  
496 (1964) and Ligios and Gliozzi (2012) the species is the only survivor of a stem that started in the  
497 Palaeomediterranean area with *Cyprideis ruggierii* Decima (late Tortonian-early Messinian),  
498 including *Cyprideis agrigentina* Decima (post-evaporitic Messinian) and *Cyprideis crotonensis*  
499 Decima (post-evaporitic Messinian-Late Pliocene). The great morphological similarity of the  
500 species of the stem lead some authors to suppose that the same environmentally cued polymorphism  
501 displayed by *C. torosa* could affect also its relatives (Neale, 1988), notwithstanding no noded  
502 specimens of the other species had never been recorded. Thus, Rosenfeld (1977) and Bonaduce and  
503 Sgarrella (1999) inferred hyperhaline post-evaporitic Messinian environments respectively for the  
504 Mavqi'im Formation (Israel) and at Eraclea Minoa, applying on *C. agrigentina* valves the empirical  
505 methods of the percentage of the rounded sieve-pores elaborated by Rosenfeld and Vesper (1977)  
506 on *C. torosa*.

507 As a first step to investigate whether *C. agrigentina* shared with *C. torosa* the same  
508 ecophenotypical behavior, we have analyzed size, ornamentation and sieve-pore shapes on some  
509 thousand of specimens from the post-evaporitic Messinian section of Eraclea Minoa. The expected  
510 results, in case of a comparable behavior, is a positive correlation between large size, nodding (or  
511 strongly pitted valve surface), and high percentages of rounded sieve-pores. Fig. 6-7 shows that this  
512 correlation lacks: the largest sizes (thus the supposed lowest salinities, below 8-9 psu) are attained

513 by specimens recovered in samples bearing smooth valves (supposed high salinities) and  
514 percentages of rounded sieve-pores less than 40% (above the 8-9 psu threshold). In particular, in  
515 sample EM 6"-17 (at 210 m) the largest *C. agrigentina* valves matches with one of the lowest  
516 percentages of rounded sieve-pores (22,7%); the smallest sizes (supposed high salinities) correlates  
517 with smooth valve surfaces (supposed high salinities) but to percentages of rounded sieve-pores  
518 greater than 40% except in one case (sample EM 6"-11 at 201 m) in which the percentage is low  
519 (23.1%); the only two samples in which *C. agrigentina* valves are densely pitted (supposed low  
520 salinities), corresponds, on average, to intermediate dimensions and high percentage values.

521 From those comparisons it is possible to conclude that size and ornamentation/noding in *C.*  
522 *agrigentina* are not correlated. In particular, pitted ornamentation and noding seem to be,  
523 respectively, very rare and totally absent in *C. agrigentina*, despite the species seems to be strongly  
524 euryhaline as it is its living relative (Ligios and Gliozzi, 2012). Thus, it seems that those characters  
525 do not display in *C. agrigentina* the same salinity-dependant polymorphism of *C. torosa*.

526 A further question is to investigate whether the percentage variations of the sieve-pore  
527 shapes are correlated with salinity variations as in *C. torosa*. To test this hypothesis we have based  
528 the comparisons of the salinity curve obtained applying the transfer function elaborated by Frenzel  
529 et al. (2011) with the salinity inferred by the synecological analysis and with the palaeohydrological  
530 variations inferred by the geochemical analyses (Figs. [78](#), [89](#), [910](#)).

531 Based on the synecological analysis and the Shannon-Wiener diversity curve, it is possible  
532 to observe that the "Cyprideis assemblage", correlatable with the minimum diversity values  
533 (monotypic ostracod assemblages) corresponds to different inferred salinities: oligo-low mesohaline  
534 in the intervals 153-171, 218-225 and 253-257.8 m; high mesohaline from 174 to 189 m;  
535 polyhaline-euhaline from 198.5 to 216.5 m. Moreover, it is worth to note that the two oligohaline  
536 levels with *Cyprideis* and *Ilyocypris*, included in the "Cyprideis" long interval at 198.5 and 201 m,  
537 according to the salinity curve based on sieve-pore percentage should have deposited in  
538 polyhaline/euhaline waters. We should conclude that there is no correspondence between the

539 salinities inferred by the method of the sieve-pore percentages and the synecological  
540 palaeoenvironmental interpretation. This conclusion contradicts the statement by Bonaduce and  
541 Sgarrella (1999) who, on the basis of the percentage of sieve-pore shapes, inferred for the Eraclea  
542 Minoa portion of succession with monospecific *Cyprideis* assemblage hyperhaline environments  
543 (50-70 psu). Probably their conclusions are affected by the very few analyzed samples along the  
544 succession (only two) and the scarcity of counted sieve-pores for each sample (respectively 74 and  
545 161).

546 The calculation of past salinities from the results of the geochemical analyses on the valves  
547 of *C. agrigentina* is difficult to assess. Although Na/Ca<sub>v</sub> could be tentatively perceived as a proxy of  
548 the salinity (assuming salinity dominated by NaCl solute), the obtained data must be considered  
549 with caution because of the poor knowledge of the Na uptake in the ostracod calcite shell (Holmes  
550 and De Deckker, 2012). However, recent attempts to use Na/Ca ratios from ostracod valves for  
551 palaeoenvironmental reconstructions must be taken into account (Gouramanis et al., 2010;  
552 Devriendt, 2011). On the other hand, Sr/Ca and Mg/Ca from ostracod valves just may inform about  
553 the Sr/Ca and Mg/Ca of the waters (De Deckker et al., 1999; [Dettman and Dwyer, 2012](#); Holmes  
554 and De Deckker, 2012; ~~[Dettman and Dwyer, 2012](#)~~), and only in some cases (i.e. some estuarine  
555 environments) these ratios could correlate with the salinity of the waters. On the other hand,  $\delta^{18}\text{O}$   
556 variations in closed non-marine environments are linked usually to evaporation/precipitation  
557 processes (Talbot, 1990), that in some cases are associated to salinity variations. Anyway, the  
558 decreasing Na/Ca<sub>v</sub> ratios from Interval A to Interval B (Fig. 5) is consistent with the interpretation  
559 of more diluted waters in this latter interval, as pointed by the low  $\delta^{18}\text{O}$  values in B. However, this  
560 is in contradiction with the higher salinity assumed for interval B than for interval A based on the  
561 sieve-pore analysis of *C. agrigentina* (Fig. [78](#)).

562 We have tried to test the correlation between the geochemical results and the salinities  
563 assumed from the analysis of the sieve-pore percentages using a multivariate approach. The  
564 correlation matrix obtained for [eight-nine](#) variables is shown in [Table 3](#). Significant correlations

565 ( $p < 0.01$ ) are displayed only by the pairs  $\delta^{18}\text{O}$  and  $\text{Na}/\text{Ca}_v$ ,  $\text{Na}/\text{Ca}_v$  and  $\text{Mg}/\text{Ca}_v$ ,  $\text{Sr}/\text{Ca}_v$  and  
566 stratigraphic position. Significant negative correlations are shown by  $\delta^{13}\text{C}$  and  $\text{Na}/\text{Ca}_v$ ,  $\delta^{13}\text{C}$  and  
567  $\delta^{18}\text{O}$ ,  $\delta^{13}\text{C}$  and  $\text{Mg}/\text{Ca}_v$ ,  $\text{Mg}/\text{Ca}_v$  and  $\text{Sr}/\text{Ca}_v$ . In fact salinity assumed from sieve-pore analysis (N  
568 pores), and Sr isotopic ratios of the valves do not show significant correlation with any of the other  
569 considered variables.

570 Principal Component Analysis (PCA) delineates similar patterns. About ~~34.92~~43.09% of the  
571 total variance is explained by the first eigenvector (Fig. 89), which is tied to concentration-  
572 evaporation processes, indicated by the relations among  $\delta^{18}\text{O}$ ,  $\text{Na}/\text{Ca}_v$ ,  $\text{Mg}/\text{Ca}_v$ , ~~Th/U~~ and  $^{87}\text{Sr}/^{86}\text{Sr}$   
573 in the positive field. This factor is related to the precipitation/evaporation balance and residence  
574 time and probably to the resedimentation of evaporites. Inputs of ~~oxygenated~~  $\text{SO}_4$ -rich solutions  
575 would lead to lowering of  $\delta^{18}\text{O}$ ,  $\text{Na}/\text{Ca}_v$ ,  $\text{Mg}/\text{Ca}_v$  and  $^{87}\text{Sr}/^{86}\text{Sr}$ . On the negative field, the variables  
576 are  ~~$\delta^{13}\text{C}$ ,  $\text{Sr}/\text{Ca}_v$ , the stratigraphic position and the percentages of rounded sieve-pores that are~~  
577 ~~linked to DIC (Dissolved Inorganic Carbon) changes, probably are linked to the productivity~~  
578 ~~nutrient inputs, OM decomposition and at the end DIC (Dissolved Inorganic Carbon) changes and~~  
579 ~~the environmental evolution.~~ On the other hand, factor 2 that accounts for 20.6872% of the  
580 variance, in the positive area contains a group formed by  $\delta^{18}\text{O}$ ,  $\text{Sr}/\text{Ca}_v$ , stratigraphic position and  
581  $\text{Na}/\text{Ca}_v$ , whereas in the negative area a group formed by ~~N pores~~,  $\delta^{13}\text{C}$ , ~~Th/U~~ and  $\text{Mg}/\text{Ca}_v$  exists.  
582 Factor 2 probably is linked to detrital, freshwater and nutrient inputs related to ~~the environmental~~  
583 ~~evolution~~ climate.

584 Results from the cluster analysis reveal several groups (Fig. 910). One of the groups shown  
585 by the dendrogram reflects the relationship between  $\delta^{18}\text{O}$  and  $\text{Na}/\text{Ca}_v$ , revealing the control of the  
586  $\text{Na}/\text{Ca}_v$  exerted by the P/E balance ( $\delta^{18}\text{O}$ ). They are associated with  $\text{Mg}/\text{Ca}_v$ , ~~Th/U~~ and Sr isotopic  
587 ratios in the ostracod valve that, into a lesser extent, seem ~~also~~ to be influenced by the P/E balance.  
588 The pair  $\text{Sr}/\text{Ca}_v$ —position of the sample is associated to the pair  $\delta^{13}\text{C}$ —percentage of rounded  
589 sieve-pores. This pair reveals the link between DIC changes and the changes in sieve-pore shapes.

Formatted: Highlight

Formatted: Highlight

Formatted: Highlight

Formatted: Highlight

Formatted: Highlight

Formatted: Highlight

Formatted: Highlight

Formatted: Highlight

590 ~~If we add the Th/U ratios in the sediments to the other variables in order to perform a new statistical~~  
591 ~~analysis (9 variables), the number of available samples for this analysis is reduced to 10. In this new~~  
592 ~~examination, the percentages of rounded sieve pores is associated to Th/U and this pair is linked to~~  
593  ~~$\delta^{13}\text{C}$ . The links among these 3 variables reflect the relationship between the number of rounded~~  
594 ~~sieve pores in *C. agrigentina* and the environmental changes in the bottom of the basin in relation~~  
595 ~~with the cycling of carbon (OM decomposition), oxygen availability and redox conditions.~~  
596 ~~Nevertheless, for this analysis the correlations are low and weak. We need additional data to fully~~  
597 ~~confirm these links with Th/U in the sediments.~~ It is worth to note that, although some authors  
598 consider both the  $U_{\text{a}}$  and Th/U values as good proxies to detect past oxic/dysoxic conditions  
599 (Adams and Weaver, 1958; Wignall and Myers, 1988 ; Wignall, 1994; Jones and Manning, 1994),  
600 Wignall and Meyers (1988) suggest to couple the  $U_{\text{a}}$  results with the Shannon-Weaver dominance-  
601 diversity index (H) since, under low-oxygen conditions, assemblages are dominated by a few  
602 eurypotic forms, and values of H are typically low. If we compare the H-index curve (Fig. 8) with  
603 the oxygen availability at the bottom derived from the  $U_{\text{a}}$  curve of Fig. 5, we notice that they are  
604 contradictory: when  $U_{\text{a}}$  values are high (comprised between 2 and 10 and indicate possible dysoxic  
605 bottoms) the H-index values are high (rather well diversified assemblages). This negative  
606 correlation suggest, as supposed by Zheng et al. (2002) that the accumulation of  $U_{\text{a}}$  in sediments  
607 could due also to physico-chemical variables other than the oxygen availability.

608 The results of the statistical analyses underline that there is no significant relationship  
609 between the salinity assumed from the sieve-pore analyses on the valves of *C. agrigentina* and the  
610 variables linked to the hydrochemical changes ( $\delta^{18}\text{O}$ ,  $\text{Na}/\text{Ca}_v$  and  $\text{Mg}/\text{Ca}_v$ , i.e. the salinity changes).  
611 On the other hand, the number of rounded sieve pores in *C. agrigentina* seems to be mainly linked  
612 to  $\delta^{13}\text{C}$  (~~OM decomposition, DIC-cycling of C~~), ~~oxygen availability and redox condition in the~~  
613 ~~bottom.~~

Formatted: Indent: First line: 0 cm, Don't adjust space between Latin and Asian text, Don't adjust space between Asian text and numbers

Formatted: Highlight

Formatted: Subscript, Highlight

Formatted: Highlight

Formatted: Subscript, Highlight

Formatted: Highlight

Formatted: Highlight

Formatted: Font: 12 pt, Highlight

Formatted: Font: 12 pt, English (U.K.), Highlight

Formatted: Font: 12 pt, Highlight

Formatted: Font: 12 pt, English (U.K.), Highlight

Formatted: Font: 12 pt, English (U.K.), Highlight

Formatted: Font: 12 pt, English (U.K.), Highlight

Formatted: Font: 12 pt, Highlight

Formatted: Font: 12 pt, English (U.K.), Highlight

Formatted: Font: 12 pt, English (U.K.), Highlight

Formatted: Font: 12 pt, Highlight

Formatted: Font: 12 pt, English (U.K.), Highlight

Formatted: Font: 12 pt, English (U.K.), Highlight

Formatted: Font: 12 pt, Not Italic, English (U.K.), Highlight

Formatted: Font: 12 pt, English (U.K.), Highlight

Formatted: Font: 12 pt, Highlight

Formatted: Font: 12 pt, English (U.K.), Highlight

Formatted: Font: 12 pt, Highlight

Formatted: Font: 12 pt, English (U.K.), Highlight

Formatted: Highlight

Formatted: Highlight

Formatted: Subscript, Highlight

Formatted: Highlight

Formatted: Highlight

Formatted: Subscript, Highlight

Formatted: Highlight

Formatted: Highlight

Formatted: Highlight

Formatted: Highlight

Formatted: Subscript, Highlight

Formatted: Highlight

614 In conclusion, this puzzly set of data does not confirm that the percentages variation of the  
615 sieve-pore shapes in *C. agrigentina* is a reliable salinity indicator for the Lago-Mare episode of the  
616 Messinian Salinity Crisis. On the other hand, the complexity of the hydrochemical evolution due to  
617 the ~~deposition-re-sedimentation~~ of the Upper Gypsum Unit and scattered inputs of detrital materials  
618 and meteoric waters accounts for a complex palaeohydrological and palaeohydrochemical scenario  
619 in which it seems that the factors responsible for the changes in the shape of the pores in the valves  
620 of *C. agrigentina* could be the behaviour of the DIC and the oxygen availability.

621 On the other hand, the geochemical data give a negative response to the hypothesis that the  
622 “*Cyprideis* assemblage” could be related to dysoxia at the bottom. Data from the percentage of the  
623 authigenic U, Th/U ratios indicate that some ~~episodes of oxygen depletion~~ accumulation of U<sub>238</sub>  
624 occurred at the bottom of the Eraclea Minoa waterbody, but it seems that they were not so important  
625 to affect the benthic ostracod assemblages.

626 Although it is beyond the aim of this paper, in order to try to understand the  
627 palaeoenvironmental meaning of the “*Cyprideis* assemblage” we have tried to extend our  
628 investigations comparing other Lago-Mare successions of the Mediterranean area that included  
629 monotypic *C. agrigentina* assemblages. In the first case, such assemblage, represented by very  
630 scarce specimens, has been recovered in the lower portion of the Lago-Mare succession of the  
631 Adana Basin (Turkey) during the deposition of resedimented evaporites and marls, where a very  
632 high sedimentation rate was recorded (Faranda et al., 2013). The authors linked the low diversity  
633 and the scattered distribution of the ostracod assemblage of the Adana Basin to the high siliciclastic  
634 input connected with the high subsidence rate that affected the Adana Basin during the Lago-Mare  
635 phase. At Eraclea Minoa the “*Cyprideis* assemblage” is present with high frequencies and  
636 continuously recovered along the entire interval, but it is rather confined to the thick marly-sandy  
637 succession included between gypsum bodies 6 and 7. If we hypothesize that this portion of  
638 succession represents one precessional cycle, as supposed by Van der Laan et al. (2006), high  
639 sedimentation rates affected both Adana (12.5 mm/yr) (Radeff et al., submitted) and Eraclea Minoa

Formatted: Highlight

Formatted: Subscript, Highlight

Formatted: Not Highlight

640 (4.3 mm/yr) successions. Similar stratigraphical, sedimentological and paleontological conditions  
641 have been found also in the lower portion of the Lago-Mare succession cropping out in the Iraklion  
642 Basin (central Crete) (unpublished data). Unfortunately, not everywhere high sedimentation rates  
643 and siliciclastic inputs support only the “*Cyprideis* assemblage”: in the Mondragone 1 well  
644 (Garigliano Plain, Campania, southern Italy) around one-thousand meters of sediments deposited  
645 within the short temporal frame of the *Loxocorniculina djafarovi* zone (5.40-5.33 Ma), thus a very  
646 high sedimentation rate above 13 mm/yr was calculated, but the recovered Lago-Mare ostracod  
647 assemblages were highly diversified (Cosentino et al., 2006).

648 In conclusion, at the moment no plausible hypothesis can be arised on the  
649 palaeoenvironmental meaning of the “*Cyprideis* assemblage”, once again stressing the peculiar and  
650 complex geological and palaeoenvironmental history of the Eraclea Minoa succession.

651

## 652 7. Conclusion

653 The ostracod assemblages of the post-evaporitic Messinian section of Eraclea Minoa (Sicily)  
654 have been studied in a palaeoenvironmental perspective to decipher the environmental changes  
655 verified during the deposition of the Upper Gypsum Unit. Rich and diversified assemblages made  
656 mainly by Paratethyan species, have been recovered in the lower and upper portion of the  
657 succession, pointing to shallow and low mesohaline waterbodies. In the central portion of the  
658 succession, very abundant monospecific assemblages made only by *C. agrigentina* were  
659 recognized, suggesting high mesohaline to hyperhaline shallow waterbody with low oxygen  
660 content. To test this latter interpretation, morphometric and geochemical analyses (stable isotopes,  
661 trace elements,  $^{87}\text{Sr}/^{86}\text{Sr}$ , and NRD) have been performed on *C. agrigentina* ostracod valves and  
662 bulk sediment samples in order to verify if *C. agrigentina* ecophenotypical behavior was  
663 comparable with that of the living species *C. torosa*.

664 The results have shown that:

665 1) *C. agrigentina* sizes and ornamentations are not affected by salinity variations;

Formatted: Indent: First line: 1.06 cm

Formatted: Font: Not Italic

Formatted: Font: Italic

666 2) The percentages of sieve-pore shapes do not depend from the water salinity, as in *C. torosa*,  
667 but seem linked to the [behavior of the DIC and the](#) oxygen availability at the bottom.

668 Thus, it is possible to conclude that *C. agrigentina* cannot be considered as a  
669 palaeosalinometer for the Messinian Salinity Crisis.

670 Furthermore, the geochemical analyses have shown that the deposition of the Eraclea Minoa  
671 succession occurred in a complex palaeohydrological and palaeohydrochemical scenario.

672

673

#### 674 Acknowledgements

675

676 The research of F.G. and E.G. has been founded by the Italian National Research Project PRIN  
677 2009-2010. P.A. work is supported by Project CGL2011-23438. The authors are grateful to Rafael  
678 Bartrolí (ICTJA and IDAEA, CSIC) for the ICP-AES analyses and to Lora Wingate (Stable Isotope  
679 Laboratory, University of Michigan) for the stable isotope analyses on the ostracod valves.

680

#### 681 REFERENCES

682

683 [Adams J.A. & Weaver C.E., 1958. Thorium-uranium ratios as indicators of sedimentary processes:  
684 example of concept of geochemical facies. Bulletin American Association of Petroleum  
685 Geologists 42\(2\), 387-430.](#)

686 Aladin, N.V., 1993. Salinity tolerance, morphology and physiology of the osmoregulation organs in  
687 Ostracoda with special reference to Ostracoda from the Aral Sea. In Jones, P. and McKenzie  
688 K. (Eds.), Ostracoda in Earth and Life Sciences, A.A. Balkema, Rotterdam, 387-404.

689 Anadón, P., Gliozzi, E., Mazzini, I., 2002. Paleoenvironmental reconstruction of marginal marine  
690 environments from combined paleoecological and geochemical analyses on Ostracods. In:

Formatted: Highlight

Formatted: Highlight

Formatted: Indent: Left: 0 cm,  
Hanging: 1.06 cm

Formatted: Font: (Default) Times  
New Roman, 12 pt, English (U.K.),

Formatted: Font: (Default) Times  
New Roman, 12 pt, English (U.K.),

Formatted: Font: (Default) Times  
New Roman, 12 pt, Not Italic, Highlight

Formatted: Font: (Default) Times  
New Roman, 12 pt, Not Italic, English  
(U.K.), Highlight

Formatted: Highlight

Formatted: Font: (Default) Times  
New Roman, 12 pt, Highlight

Formatted: Font: (Default) Times  
New Roman, 12 pt, Not Bold, English  
(U.K.), Highlight

Formatted: Font: (Default) Times  
New Roman, 12 pt, English (U.K.)

Formatted: Font: Italic, English (U.K.)



691 Holmes, J., Chivas, A. (Eds), *The Ostracoda: Applications in Quaternary Research*,  
692 *Geophysical Monograph* 131, 227–247.

693 Barbieri, M., Carrara, C., Castorina, F., Dai Pra, G., Esu, D., Gliozzi, E., Paganin, G., Sadori, L.,  
694 1999. Multidisciplinary study of Middle-Upper Pleistocene deposits in a core from the Piana  
695 Pontina (central Italy). *Giornale di Geologia* 61, 47–73.

696 Benson, R.H., 1978. The paleoecology of the ostracodes of DSDP Leg 42A. In: *Initial Reports of*  
697 *the Deep Sea Drilling Project* 42, 777–787, U.S. Government Printing Office, Washington,  
698 D.C.

699 Bernhard, J.M, Sen Gupta, B.K., 2002. Foraminifera of oxygen-depleted environment. In: Sen  
700 Gupta, B.K. (Ed.), *Modern Foraminifera*. Kluwer Academic Publishers, 201-216.

701 Bonaduce, G., Sgarrella, F., 1999. Paleoeological interpretation of the latest Messinian sediments  
702 from southern Sicily (Italy). *Memorie della Società Geologica Italiana* 54, 83–91.

703 Boomer, I., Frenzel, P., 2011. Possible environmental and biological controls on carapace size in  
704 *Cyprideis torosa* (Jones, 1850). *Joannea Geologie und Paläontologie* 11, 26–27.

705 Bossio, A., Costantini, A., Lazzarotto, A., Liotta, D., Mazzanti, R., Mazzei, R., Salvatorini, G.,  
706 Sandrelli, F., 1993. Rassegna delle conoscenze sulla stratigrafia del Neautoctono toscano.  
707 *Memorie della Società Geologica Italiana* 49, 17–98.

708 Bossio, A., Cerri, R., Mazzei, R., Salvatorini, G., Sandrelli, F., 1996. Geologia dell'area  
709 Spicchiaiola-Pignano (Settore orientale del Bacino di Volterra). *Bollettino della Società*  
710 *Geologica Italiana* 115, 393-422.

711 Carbonel, P., 1982. Les Ostracodes, traceurs des variations hydrologiques dans des systèmes de  
712 transition eaux douces-eaux salées. *Mémoires de la Société géologique de France* 8(144),  
713 117–128.

714 Caruso, A., Rouchy, J.-M., 2006. The Upper Gypsum Unit. In: Roveri, M., Manzi, V., Lugli, S.,  
715 Schreiber, B.C., Caruso, A., Rouchy, J.-M., Iaccarino, S.M., Gennari, R., Vitale, F.P., Ricci

716 Lucchi, F. (Eds.), Clastic vs. primary precipitated evaporites in the Messinian Sicilian  
717 basins. *Acta Naturalia de "L'Ateneo Parmense"* 42(4), 157-159.

718 CIESM (Commission Internationale pour l'Exploration de la Mer ~~Méditerranée~~Mediterranee,  
719 Monaco), 2008. The Messinian Salinity Crisis from Mega-Deposits to Microbiology: A  
720 Consensus Report. CIESM Workshop Monograph 33, 1-168.

721 Cosentino, D., Bertini, A., Cipollari, P., Florindo, F., Gliozzi, E., Grossi, F., Lo Mastro, S.,  
722 Sprovieri, M., 2012. Orbitally-forced palaeoenvironmental and palaeoclimate changes in the  
723 late post-evaporitic Messinian stage of the central Mediterranean Basin. *Geological Society*  
724 *of America Bulletin* 124(3-4), 499-516.

725 Cosentino, D., Federici, I., Cipollari, P., Gliozzi, E., 2006. Environments and tectonic instability in  
726 central Italy (Garigliano Basin) during the late Messinian *Lago-Mare* episode: New data  
727 from the onshore Mondragone well (Garigliano Plain, central Italy). *Sedimentary Geology*  
728 188-189, 293-317.

729 Curry, B., Mesquita-Joanes, F., Fanta, S., Sterner, D., Calò, C., Tinner, W., 2013. Two coastal  
730 sinkhole lakes in SW Sicily (Italy) reveal low-salinity excursion during Greek and Roman  
731 occupation. *Naturalista Siciliano* 4, 37(1), 93-95.

732 De Deckker, P., Chivas, A.R., Shelley, J.M.G., 1988. Palaeoenvironment of the Messinian  
733 Mediterranean "Lago Mare" from strontium and magnesium in ostracode shells. *Palaios*, 3,  
734 352-358.

735 De Deckker, P., Chivas, A.R., Shelley, J.M.G., 1999. Uptake of Mg and Sr in the euryhaline  
736 ostracod *Cyprideis* determined from in vitro experiments. *Palaeogeography,*  
737 *Palaeoclimatology, Palaeoecology* 148, 105-116.

738 Decima, A., 1964. Ostracodi del genere *Cyprideis* Jones del Neogene e del Quaternario italiani.  
739 *Palaeontographia Italica*, 57(1962), 81-133.

740 Decima, A., Wezel, F.C., 1971. Osservazioni sulle evaporiti messiniane della Sicilia centro-  
741 meridionale. *Rivista mineraria siciliana* 130-132, 172-187.

Formatted: Highlight

742 Dettman, D.L., Dwyer, G.S., 2012. Biological and environmental controls on ostracod shell trace-  
743 element chemistry. In: D. J. Horne, J. Holmes, J. Rodriguez-Lazaro and F. Viehberg (Eds.).  
744 Ostracoda as proxies for Quaternary climate change. Developments in Quaternary Sciences.  
745 Elsevier, v. 17, -145-163.

746 Devriendt, L.S.J., 2011. Late Quaternary environment of paleolake Carpentaria inferred from the  
747 chemistry of ostracod valves. Master of Sciences Research Thesis, University of  
748 Wollongong, Australia, 175 pp. <http://ro.uow.edu.au/theses/3319/>

749 Faranda, C., Gliozzi, E., Cipollari, P., Grossi, F., Darbaş, G., Gürbüz, K., Nazik, A., Gennari, R.,  
750 Cosentino, D., 2013. Messinian paleoenvironmental changes in the easternmost  
751 Mediterranean Basin: Adana Basin, southern Turkey. Turkish J Earth Sci 22, 839-863.

752 Faure, G., Powell, J.L., 1972. Strontium Isotope Geology. Springer-Verlag, Berlin, 1-188.

753 Flecker, R., de Villiers, S., Ellam, R.M., 2002. Modelling the effect of evaporation on the salinity–  
754  $^{87}\text{Sr}/^{86}\text{Sr}$  relationship in modern and ancient marginal–marine systems: the Mediterranean  
755 Messinian Salinity Crisis. Earth Planet. Sci. Lett. 203 (1), 221– 233.

756 Flecker, R., Ellam, R.M., 2006. Identifying Late Miocene episodes of connection and isolation in  
757 the Mediterranean–Paratethyan realm using Sr isotopes. Sediment. Geol. 188–189, 189–203.

758 Frenzel, P., Schulze, I., Pint, A., 2011. Salinity dependant morphological variation in *Cyprideis*  
759 *torosa*. Joanea Geologie und Paläontologie 11, 59–61.

760 Frenzel, P., Schulze, I., Pint, A., 2012. Noding of *Cyprideis torosa* valves (Ostracoda) – a proxy for  
761 salinity? New data from field observations and a long-term microcosm experiment.  
762 International Review of Hydrobiology 97(4), 314–329.

763 Gliozzi, E., Grossi, F., 2008. Late Messinian Lago-mare ostracod palaeoecology: a correspondence  
764 analysis approach. Palaeogeography, Palaeoclimatology, Palaeoecology 264, 288-295.

765 Gouramanis, C., Wilkins, D., De Deckker, P., 2010. 6000 years of environmental changes recorded  
766 in Blue Lake, South Australia, based on ostracod ecology and valve chemistry.  
767 Palaeogeography, Palaeoecology, Palaeoclimatology 297, 223-237.

768 | [Graham, D.W., Bender, M.L., Williams, D.F., Keigwin, L.D., 1982. Strontium calcium ratios in the](#)  
769 | [Cenozoic planktonic foraminifera. \*Geochim. Cosmochim. Acta\* 46, 1281–1292.](#)

770 | Griffin, D.L., 2002. Aridity and humidity: Two aspects of the late Miocene climate of North Africa  
771 | and the Mediterranean. *Palaeogeography, Palaeoclimatology, Palaeoecology* 182, 65–91.

772 | Griffiths, H.I., Holmes, J.A., 2000. Non-marine ostracods & Quaternary palaeoenvironments.  
773 | Quaternary Research Association, Technical Guide 8, 1-179.

774 | Grossi, F., Gennari, R., 2008. Palaeoenvironmental reconstruction across the Messinian/Zanclean  
775 | boundary by means of ostracods and foraminifers: the Montepetra borehole (Northern  
776 | Apennine, Italy). *Atti del Museo Civico di Storia Naturale di Trieste* 53(suppl), 67-88.

777 | Grossi, F., Cosentino, D., Gliozzi, E., 2008. Palaeoenvironmental reconstruction of the late  
778 | Messinian lago-mare successions in central and eastern Mediterranean using ostracod  
779 | assemblages. *Bollettino della Società Paleontologica Italiana* 47(2), 131–146.

780 | Guerra-Merchán, A., Serrano, F., Garcés, M., Gofas, S., Esu, D., Gliozzi, E., Grossi, F., 2010.  
781 | Messinian Lago-Mare deposits near the Strait of Gibraltar (Malaga Basin, S Spain).  
782 | *Palaeogeography, Palaeoclimatology, Palaeoecology* 285, 264–276.

783 | Henderson, G. M., Martel, D. J., O’Nions, R. K., Shackleton, N. J., 1994. Evolution of seawater  
784 |  $^{87}\text{Sr}/^{86}\text{Sr}$  over the last 400 ka: the absence of glacial/interglacial cycles. *Earth Planetary*  
785 | *Sciences and Letters* 128, 643–651.

786 | Holmes, J., De Deckker, P., 2012. Introduction to ostracod shell chemistry and its application to  
787 | Quaternary palaeoclimate studies. In: D. J. Horne, J. Holmes, J. Rodriguez-Lazaro and F.  
788 | Viehberg (Eds.). *Ostracoda as proxies for Quaternary climate change. Developments in*  
789 | *Quaternary Sciences*. Elsevier, v. 17, 131-144.

790 | Howarth, R., McArthur, J.M., 1997. Statistics for Strontium Isotope Stratigraphy: a robust  
791 | LOWESS fit to the marine Sr-isotope curve for 0 to 206 Ma, with look-up table for  
792 | derivation of numeric age. *J. Geol.* 105, 441–456.

793 Hsü, K.J., Ryan, W.F.B., Cita, M.B., 1973. Late Miocene desiccation of the Mediterranean. *Nature*  
794 242, 240–244.

795 Iaccarino, S., Bossio, A., 1999. Paleoenvironment of uppermost Messinian sequences in the  
796 Western Mediterranean (sites 974, 975 and 978). In: Zahn, R., Comas, M.C., Klaus, A., et  
797 al. (Eds.), *Proceedings of Ocean Drilling Program, Scientific Results 161*, 529–541, College  
798 Station, Texas.

799 Jahn, A., Gamenick, I., Theede, H., 1996. Physiological adaptations of *Cyprideis torosa* (Crustacea,  
800 Ostracoda) to hydrogen sulphide. *Marine Ecology Progress Series* 142, 215–223.

801 Jones, B. and Manning, D.A.C., 1994. Comparison of geochemical indices used for the  
802 interpretation of paleoredox conditions in ancient mudstones. *Chemical Geology* 111, 111–  
803 129.

804 Keating, K.W., Hawkes, I., Holmes, J.A., Flower, R.J., Leng, M.J., Abu-Zied, R.H., Lord, A.R.,  
805 2007. Evaluation of ostracod-based palaeoenvironmental reconstruction with instrumental  
806 data from the arid Faiyum Depression. *Egyptian Journal of Paleolimnology* 38, 261–283.

807 Keogh, S.M., Butler, R.W.H., 1999. The Mediterranean water body in the late Messinian:  
808 interpreting the record from marginal basins on Sicily. *J. Geol. Soc. (Lond.)* 156, 837–846.

809 Keyser, D., 2005. Histological peculiarities of the nodding process in *Cyprideis torosa* (Jones)  
810 (Crustacea, Ostracoda). *Hydrobiologia* 538, 95–106.

811 Keyser, D., Aladin, N., 2004. Noding in *Cyprideis torosa* and its causes. *Studia Quaternaria* 2, 19–  
812 24.

813 Ligios, S., Anadón, P., Castorina, F., D’Amico, C., Esu, D., Gliozzi, E., Gramigna, P., Mola, M.,  
814 Monegato, G., 2012. Ostracoda and Mollusca biodiversity and hydrochemical features of  
815 Late Miocene brackish basins of Italy. *Geobios* 45, 351–367.

816 Ligios, S., Gliozzi, E., 2012. The genus *Cyprideis* Jones, 1857 (Crustacea, Ostracoda) in the  
817 Neogene of Italy: A geometric morphometric approach. *Revue de micropaléontologie* 55,  
818 171–207.

**Formatted:** Font: (Default) Times New Roman, 12 pt, English (U.K.),

**Formatted:** Font: (Default) Times New Roman, 12 pt, English (U.K.),

**Formatted:** Justified

**Formatted:** Font: (Default) Times New Roman, 12 pt, Highlight

**Formatted:** Font: (Default) Times New Roman, 12 pt, Highlight

**Formatted:** Font: (Default) Times New Roman, 12 pt, English (U.K.),

**Formatted:** Font: (Default) Times New Roman, 12 pt, Highlight

**Formatted:** Font: (Default) Times New Roman, 12 pt, English (U.K.),

**Formatted:** Font: (Default) Times New Roman, 12 pt, Highlight

**Formatted:** Font: (Default) Times New Roman, 12 pt, English (U.K.),

**Formatted:** Font: (Default) Times New Roman, 12 pt, English (U.K.),

**Formatted:** English (U.K.)

- 819 Mangini, A., Jung, M., Laukenmann, S., 2001. What do we learn from peaks of uranium and of  
820 manganese in deep sea sediments? *Marine Geology* 177(1), 63-78.
- 821 Manzi, V., Lugli, S., Roveri, M., Schreiber, C., 2009. A new facies model for the Upper Gypsum of  
822 Sicily (Italy): chronological and palaeoenvironmental constraints for the Messinian salinity  
823 crisis in the Mediterranean. *Sedimentology* 56, 1937-1960.
- 824 Manzi, V., Gennari, R., Lugli, S., Roveri, M., Scafetta, N., Schreiber, B.C., 2012. High-frequency  
825 cyclicity in the Mediterranean Messinian evaporites: evidence for solar-lunar climate  
826 forcing. *Journal of Sedimentary Research* 82, 991-1005.
- 827 Manzi, V., Gennari, R., Hilgen, F., Krijgsman, W., Lugli, S., Roveri, M., Sierro F.J., 2013. Age  
828 refinement of the Messinian salinity crisis onset in the Mediterranean. *Terra Nova*, doi:  
829 10.1111/ter.12038
- 830 Marco-Barba, J., 2010. Freshwater ostracods ecology and geochemistry as paleoenvironmental  
831 indicators in marginal marine ecosystems: a case of study the Albufera of Valencia. Ph. D.  
832 thesis, Univ. of Valencia.
- 833 McArthur, J.M., Howarth, R.J., Bailey T.R., 2001. Strontium isotope stratigraphy: LOWESS  
834 version 3: Best fit to the marine Sr-isotope curve for 0-509 Ma and accompanying look-up  
835 table for deriving numerical age. *Journal of Geology* 109, 155-170.
- 836 McCulloch, M.T., De Deckker, P., 1989. Sr-isotope constraints on the Mediterranean environment  
837 at the end of the Messinian salinity crisis. *Nature* 342, 63- 65.
- 838 Müller, D.W., Mueller, P.A., 1991. Origin and age of the Mediterranean Messinian evaporites:  
839 implications from Sr isotopes. *Earth Planet. Sci. Lett.* 107, 1 -12.
- 840 Müller, D.W., Mueller, P.A., McKenzie, J.A., 1990. Strontium isotopic ratios as fluid tracers in  
841 Messinian evaporites of the Tyrrhenian sea (western Mediterranean sea). *Proc. ODP Sci.*  
842 *Res.* 107, 603-614.

Formatted: No underline

843 Neale, J.V., 1988. Ostracods and paleosalinity reconstruction. In: De Deckker, P., Colin, J.-P.,  
844 Peypouquet, J.-P. (Eds.), Ostracoda in the Earth Sciences. Elsevier, Amsterdam, pp. 125–  
845 155.

846 Pattan, J.N., Pearce, N.J.G., 2009. Bottom water oxygenation history in southeastern Arabian Sea  
847 during the past 140 ka: Results from redox-sensitive elements. *Palaeogeography,*  
848 *Palaeoclimatology, Palaeoecology* 280(3-4), 396-405.

849 Pint, A., Frenzel, P., Fuhrmann, R., Scharf, B., Wennrich, V., 2012. Distribution of *Cyprideis*  
850 *torosa* (Ostracoda) in Quaternary athalassic sediments in Germany and its application for  
851 palaeoecological reconstructions. *International Review of Hydrobiology* 97(4), 330-335.

852 Pint, A., Melzer, S., Frenzel, P., Engel, M., Brückner, H., 2013. Monospecific occurrence of  
853 *Cyprideis torosa* associated with micro- and macrofauna of marine origin in sabkha  
854 sediments of the Northern Arabian Peninsula. *Naturalista Siciliano* 4, 37(1), 277-278.

855 Radeff, G., Schildgen, T.F., Cosentino, D., Strecker, M.R., Cipollari, P., Darbaş, G., Gürbüz, K.,  
856 (submitted). Sedimentary evidence for late Miocene uplift of the SE margin of the central  
857 Anatolian Plateau: Adana Basin, Southern Turkey. *Geological Society of America Bulletin*.

858

859 Rosenfeld, A, Vesper, B., 1977. The variability of the sieve-pores in recent and fossil species of  
860 *Cyprideis torosa* (Jones, 1850) as an indicator for salinity and paleosalinity. In: Löffler, H.,  
861 Danielopol, D. (Eds.), Aspects of ecology and zoogeography of recent and fossil Ostracoda.  
862 Junk Publishers, The Hague, 55–67.

863 Rosenfeld, A., 1977. The Sieve-pores of *Cyprideis torosa* (Jones, 1850) from the Messinian  
864 Mavqi'im Formation in the Coastal Plain and Continental Shelf of Israel as an Indicator of  
865 Paleoenvironment. *Israel Journal of Earth-Sciences* 26, 89-93.

866 Rossi, V., Amorosi, A., Sammartino, I., Sarti, G., 2013. Environmental changes in the lacustrine  
867 ancient harbour of Magdala (Kinneret Lake, Israel) inferred from ostracod, geochemical and  
868 sedimentological analyses. *Naturalista Siciliano* 4, 37(1), 331-332.

**Formatted:** Font: Times New Roman,  
Font color: Auto, English (U.K.)

**Formatted:** Line spacing: single,  
Don't adjust space between Latin and  
Asian text, Don't adjust space between  
Asian text and numbers

- 869 Roveri, M., Flecker, R., Krijgsman, W., Lofi, J., Lugli, S., Manzi, V., Sierro, F.J., Bertini, A.,  
870 Camerlenghi, A., De Lange, G., Govers, R., Hilgen, F.J., Hübscher, C., Meijer, P.Th.,  
871 Stoica, M., 2014a, The Messinian Salinity Crisis: Past and future of a great challenge for  
872 marine sciences. Marine Geology 352, 25-58.
- 873 Roveri, M., Lugli, S., Manzi, V., Gennari, R., Schreiber, B.C., 2014b. High-resolution strontium  
874 isotope stratigraphy of the Messinian deep Mediterranean basins: Implications for marginal  
875 to central basins correlation, Marine Geology, doi: [10.1016/j.margeo.2014.01.002](https://doi.org/10.1016/j.margeo.2014.01.002)
- 876 Sampalmieri, G., Iadanza, A., Cipollari, P., Cosentino, D., Lo Mastro, S., 2010.  
877 Palaeoenvironments of the Mediterranean Basin at the Messinian hypersaline/hyposaline  
878 transition: evidence from natural radioactivity and microfacies of post-evaporitic  
879 successions of the Adriatic sub-basin. Terra Nova 22, 239-250.
- 880 Sandberg, P., 1964. The ostracod genus *Cyprideis* in the Americas. Stockholm Contributions in  
881 Geology 12, 1-178.
- 882 Schäfer, H.W., 1953. Über Meeres- und Brackwasserostacoden aus dem Deutschen Küstengebiet  
883 mit 2. Mitteilung über die Ostracodenfauna Griechenlands. Hydrobiologia 5(4), 351-389.
- 884 Schreiber, B.C., 1997. Field trip to Eraclea Minoa: Upper Messinian. "Neogene Mediterranean  
885 Paleooceanography". Excursion Guide Book Palermo-Caltanissetta Agrigento. Erice (Sicily),  
886 24-27 September 1997, 72-80.
- 887 Talbot, M.R., 1990. A review of the palaeohydrological interpretation of carbon and oxygen  
888 isotopic ratios in primary lacustrine carbonates. Chemical Geology (Isot. Geosci. Sect.) 80,  
889 261-279.
- 890 Testa, G., 1995. Upper Miocene extensional tectonics and synrift sedimentation in the western  
891 sector of the Volterra Basin (Tuscany, Italy). Studi Geologici Camerti vol. spec. 1, 617-630.
- 892 Utrilla, R., Vazquez, A., Anadón, P., 1998. Paleohydrology of the Upper Miocene Bicorn Lake (E  
893 Spain) as inferred from stable isotopic data from inorganic carbonates. Sedimentary  
894 Geology 121, 191-206.

Formatted: Italian (Italy)

Formatted: Italian (Italy)



- 895 Van Couvering, J.A., Castradori, D., Cita, M.B., Hilgen, F.J., Rio, D., 2000. The base of the  
896 Zanclean Stage and of the Pliocene Series. *Episodes* 23(3), 179-187.
- 897 Van der Laan, E., Snel, E., de Kaenel, E., Hilgen, F.J., Krijgsman, W., 2006. No major deglaciation  
898 across the Miocene-Pliocene boundary: integrated stratigraphy and astronomical tuning of  
899 the Loulja sections (Bou Regreg area, NW Morocco). *Paleoceanography* 21, PA3011,  
900 doi:10.1029/2005PA001193.
- 901 Van Harten, D., 1996. *Cyprideis torosa* (Ostracoda) revisited. Of salinity, nodes and shell size. In:  
902 Keen, C. (Ed.), *Proceedings of the second European Ostracodologists Meeting*. British  
903 Micropalaeontological Society, London, pp. 191–194.
- 904 Van Harten, D., 2000. Variable nodding in *Cyprideis torosa* (Ostracoda, Crustacea): an overview,  
905 experimental results and a model from Catastrophe Theory. *Hydrobiologia* 419, 131–139.
- 906 Venice Symposium on the Classification of Brackish Waters, Venice 8-14 April 1958 in Remane,  
907 A., Schlieper, C. (eds.), *Die Biologie der Brackwassers*. Schweizerbartsche Verlag,  
908 Stuttgart, 1-348.
- 909 Vesper, B., 1975. To the problem of nodding on *Cyprideis torosa* (Jones, 1850). In: Swain, F.,  
910 Kornicker, L.S., Lundin, R.F. (Eds.), *Biology and Paleobiology of Ostracoda*. *Bulletin of*  
911 *American Paleontology* 65(282), 205-216.
- 912 Voltaggio, M., Branca, M., Tedesco, D., Tuccimei, P., Di Pietro, L., 2004. <sup>226</sup>Ra-excess during the  
913 1631-1944 activity period of -Vesuvius (Italy): a model of alpha recoil enrichment in a  
914 metasomatized mantle and implications on the current state of the magmatic system.  
915 *Geochimica et Cosmochimica Acta* 68, 167-181.
- 916 Wignall, P.B., 1994. Black Shales. Claredon Press, Oxford, 127 pp.
- 917 Wignall, P.B., Myers, K.J., 1988. Interpreting benthic oxygen levels in mudrocks: anew approach.  
918 *Geology* 16, 452-455.

**Formatted:** Font: (Default) Times New Roman, 12 pt, English (U.K.),

**Formatted:** Normal, Don't adjust space between Latin and Asian text, Don't adjust space between Asian text and numbers

**Formatted:** Highlight

**Formatted:** Font: 8 pt, Italian (Italy)

919 Zheng, Y., Anderson, R.F., Van Geen, A., Fleisher, M.Q., 2002. Remobilization of authigenic  
920 uranium in marine sediments by bioturbation. *Geochimica et Cosmochimica Acta* 66 (10),  
921 1759–1772.  
922  
923

FIGURE CAPTIONS

Fig. 1 – SEM pictures of *Cyprideis agrigentina* Decima. a. male left valve, sample EM 8-3; b. male right valve, sample EM 7-2; c. female left valve, sample EM 7-2; d. female right valve, sample EM 8-3. White bar corresponds to 0.1 mm.

Fig. 2 – Geographical location of the Eraclea Minoa section.

Fig. 3 – Panoramic view of the Eraclea Minoa section. In evidence the gypsum levels of the Upper Gypsum Unit from gypsum body 3 to gypsum body 6 (marked by numbers) and the Messinian/Zanclean boundary.

Fig. 4 – Simplified stratigraphic log of the Eraclea Minoa section (modified from Manzi et al., 2009). Legend: 1. sapropels; 2. clays; 3. sandstones/sandy levels; 4. microconglomerate levels; 5. marls; 6. gypsum bodies (Upper Gypsum Unit); 7. samples for paleontological analyses; 8. samples for morphometrical analyses (ornamentation, dimensions and percentage of sieve-pore shapes) on *C. agrigentina* valves; 9. samples for stable isotopes analyses on *C. agrigentina* valves; 10. samples for trace elements analyses on *C. agrigentina* valves; 11. samples for Sr-isotopes analyses on *C. agrigentina* valves; 12. samples for NRD analyses on marls.

Fig. 5 – Stable isotopes, trace and minor elements,  $^{87}\text{Sr}/^{86}\text{Sr}$ , and authigenic uranium curves plotted against the stratigraphic log of the Eraclea Minoa section. For the descriptions of the intervals, see the text.

Fig. 6 – Stable isotopic composition ( $\delta^{13}\text{C}$  and  $\delta^{18}\text{O}$ ; PDB notation) of *Cyprideis agrigentina* calcite valves (Table 1). Note the negative correlation and regression line for samples from interval

Formatted: English (U.K.), Highlight

Formatted: Font: Italic, English (U.K.), Highlight

Formatted: English (U.K.), Highlight

Formatted: Highlight

Formatted: English (U.K.), Highlight

Formatted: Highlight

Formatted: English (U.K.), Highlight

Formatted: Highlight

Formatted: English (U.K.)

Formatted: Highlight

950 lower B. The larger variation of  $\delta^{13}\text{C}$  and  $\delta^{18}\text{O}$  along the regression line corresponds to samples EM  
951 6"-8 (198.2 m) to 6"-20 (216 m) from lower interval B. E/P: Evaporation /Precipitation ratio; PP:  
952 Primary productivity; Eq-Atm: Atmospheric  $\text{CO}_2$  equilibrium. See also Fig. 54.

953

954 ~~Fig. 5— Stable isotopes, trace and minor elements,  $^{87}\text{Sr}/^{86}\text{Sr}$ , and authigenic uranium curves plotted~~  
955 ~~against the stratigraphic log of the Eraclea-Minoa section. For the descriptions of the intervals, see~~  
956 ~~the text.~~

957

958 Fig. 6-7— Results of the morphometrical analyses (mean lengths, percentages of sieve-pore shape  
959 and ornamentation/noding) performed on *Cyprideis agrigentina* adult valves, plotted against the  
960 stratigraphic log of the Eraclea Minoa section.

961

962 Fig. 78— Comparisons among the palaeosalinity curve inferred by the analysis of the percentages  
963 of the sieve-pore shape on *Cyprideis agrigentina* and the palaeoenvironmental and  
964 palaeohydrochemistry changes inferred from synecological and Shannon-Wiener and geochemical  
965 proxies.

966

967 Fig. 8-9 - Principal Component Analysis (PCA) plot of the scores of the eigenvectors for the  
968 variables listed in Table 3. Abbreviations: N pores: variability of percentage of sieve pores (rounded  
969 sieve pores assumed as a proxy of salinity), Position: stratigraphic position of the samples, Sr isot:  
970  $^{87}\text{Sr}/^{86}\text{Sr}$  values. See the text for discussion.

971

972 Fig. 9-10 - Tree diagram for the considered variables defining the relationships between the groups  
973 of variables. Ward's method, 1-Pearson r. Abbreviations as in Fig. 8. See the text for discussion.

974

Formatted: Highlight

975

976

977

TABLE CAPTIONS

978

979 | Tab-le 1 – Stratigraphic position and lithology of the samples, and geochemical analytical results  
980 | from *C. agrigentina* valves: stable isotope data ( $\delta^{13}\text{C}$  and  $\delta^{18}\text{O}$ ; PDB notation), Mg/Ca<sub>v</sub>, Sr/Ca<sub>v</sub>, and  
981 | Na/Ca<sub>v</sub> in molar ratios, and  $^{87}\text{Sr}/^{86}\text{Sr}$  ratios.

982

983 | Tab-le 2 – Summary of natural radioactivity data, with the concentrations of U, Th and K (with  
984 | relative errors), values of authigenic uranium expressed in ppm and percentage and Th/U ratios.

985

986 | Table 3 – Correlation matrix for the data in Table 1 and Th/U ratios (9 variables, 20 samples). The  
987 | correlation coefficient r between the diverse variables is shown in the upper part of each division.  
988 | The p value is indicated in the lower part of each division. The r values are in bold when the  
989 | correlation is significant p<0.01. Abbreviations: N pores: variability of percentage of sieve pores  
990 | (rounded sieve pores assumed as a proxy of salinity), Position: stratigraphic position of the samples,  
991 | Sr isot:  $^{87}\text{Sr}/^{86}\text{Sr}$  values.

992

993

994

995

Formatted: Highlight

1 **Is *Cyprideis agrigentina* Decima a good palaeosalinometer for the Messinian Salinity Crisis?**  
2 **Morphometrical and geochemical analyses from the Eraclea Minoa section (Sicily)**

3  
4 F. Grossi <sup>a,\*</sup>, E. Gliozzi <sup>a,b</sup>, P. Anadón <sup>c</sup>, F. Castorina <sup>d</sup>, M. Voltaggio <sup>b</sup>

5  
6 <sup>a</sup> *Dipartimento di Scienze, Università Roma Tre, Largo S. Leonardo Murialdo, 1, I-00146, Roma, Italy*

7 <sup>b</sup> *IGAG, CNR, Area della Ricerca di Roma RM1, Via Salaria km 29,300, CP 10, I-00016, Monterotondo Stazione,*  
8 *Roma, Italy*

9 <sup>c</sup> *Institut de Ciències de la Terra “Jaume Almera” (CSIC), C. Lluís Solé Sabarís sn, 08028, Barcelona, Spain*

10 <sup>d</sup> *Dipartimento di Scienze della Terra, Università Roma La Sapienza, P.le A. Moro, 5, I-00185, Roma, Italy*

11

12

13

14

15 \* Corresponding author: Present address: Dipartimento di Scienze, Università Roma Tre, Largo S. Leonardo Murialdo,  
16 1, I-00146, Rome, Italy

17 e-mail address: [francesco.grossi@uniroma3.it](mailto:francesco.grossi@uniroma3.it) (F. Grossi)

18

19

20 **ABSTRACT**

21

22 The living euryhaline species *Cyprideis torosa* (Jones) undergoes morphometric variations in size,  
23 nodding and sieve-pore shape linked to the environmental salinity. In particular it is known that  
24 salinity values around 8-9 psu represent the osmoregulation threshold and also the turning point  
25 between smaller and greater valve dimensions and prevalingly noded against un-noded valves. The  
26 variation of the percentage of round-, elongate- and irregular-shaped sieve-pores on the valves has  
27 shown an empiric logarithmic correlation with the water salinity from 0 to 100 psu. Due to this

28 ecologically cued polymorphism, *C. torosa* represents an invaluable palaeosalinometer for the  
29 Quaternary brackish basins.

30 In this paper we attempt to verify whether the ecophenotypical behaviour of the post-evaporitic  
31 Messinian species *Cyprideis agrigentina* Decima was comparable with that of *C. torosa*. To reach  
32 this goal, three morphometric characters have been analysed: 1) size variability; 2) nodding and  
33 ornamentation; 3) variability of the percentage of the sieve-pore shapes. The palaeoenvironmental  
34 interpretation was made using synecological and geochemical approaches [stable isotopes, trace  
35 elements, Sr-isotopes and natural radioactivity (NRD)]. For this study, the 250 m-thick Messinian  
36 Lago-Mare succession of Eraclea Minoa (Agrigento, Sicily) was chosen for the presence of  
37 monotypic assemblages made only by *C. agrigentina* for around 70 m of thickness.

38 The results of the morphometric analyses showed that: 1) size variations are not related to the  
39 salinity changes recognized both from synecological and geochemical analyses; 2) no noded  
40 specimens have been recovered along the section; 3) the salinities calculated on the basis of the  
41 percentage of the sieve-pore shape are not correlated with the salinities inferred from the  
42 synecological and geochemical analyses. Thus, in this paper we conclude that *C. agrigentina* cannot  
43 be considered a palaeosalinometer for the Messinian Salinity Crisis.

44 There is a correlation of the  $\delta^{13}\text{C}$  with the percentages of sieve-pore shapes, linking them to the  
45 behavior of the dissolved inorganic carbon (DIC) and to the oxygen availability at the bottom of the  
46 basin.

47

#### 48 KEYWORDS

49 Ostracoda; morphometrical analyses; geochemical analyses; palaeoenvironmental reconstruction;  
50 post-evaporitic Messinian; Sicily (Italy).

51

#### 52 1. Introduction

53 Since the pioneering studies by Schäfer (1953), Sandberg (1964), Vesper (1975) and  
54 Rosenfeld and Vesper (1977), it is known that the living anomalohaline species *Cyprideis torosa*  
55 (Jones) undergoes morphometrical variations in size, nodding and sieve-pore shape linked to  
56 environmental physical and chemical parameters - especially salinity - showing a clear  
57 environmentally cued polymorphism. The species can withstand and thrive in a very wide range of  
58 salinity (0.4 to 150 psu according to Neale, 1988 and Griffiths and Holmes, 2000), thus it is  
59 commonly regarded as a valuable palaeosalinometer for the Quaternary marginal marine and  
60 athalassic brackish deposits (Marco-Barba, 2010; Pint et al., 2012 with references therein). Its low-  
61 Mg calcite shell represents also a source of biogenic carbonate for the geochemical analyses (trace  
62 elements, stable isotopes and  $^{87}\text{Sr}/^{86}\text{Sr}$  ratios) to infer the chemical composition of past waterbodies,  
63 because of its high rate of valve calcification. In many studies, morphometrical variations were  
64 coupled with the geochemical approach to make more detailed palaeoenvironmental reconstructions  
65 of brackish environments (Barbieri et al., 1999; Anadón et al., 2002; Marco-Barba, 2010; Curry et  
66 al., 2013; Pint et al., 2013; Rossi et al., 2013).

67 Several studies (Carbonel, 1982; Aladin, 1993; van Harten, 1996; 2000; Keiser and Aladin,  
68 2004; Keyser, 2005; Boomer and Frenzel, 2011; Frenzel et al., 2011; 2012 among others) showed  
69 that salinity values around 8-9 psu represent the osmoregulation threshold and also the turning point  
70 between smaller and greater valve dimensions and prevailingly noded against un-noded valves.  
71 Rosenfeld and Vesper (1977) showed an empiric logarithmic correlation between the variation of  
72 the percentage of round-, elongate- and irregular-shaped sieve-pores on the valves of *C. torosa* and  
73 the water salinity from 0 to 100 psu. This correlation has been confirmed by subsequent papers  
74 (Neale, 1988; Keating et al., 2007; Pint et al., 2012) and Frenzel et al. (2011) elaborated a transfer  
75 function based on the percentages of round sieve-pores.

76 In order to decipher the palaeosalinity changes during the end of the Messinian Salinity  
77 Crisis (Hsü et al., 1973; CIESM, 2008; Roveri et al., 2014a), Rosenfeld (1977) and Bonaduce and  
78 Sgarrella (1999) applied the counting of different sieve-pore shapes to the fossil species *Cyprideis*



79 *agrigentina* Decima, supposing that also this species could morphologically react as *C. torosa*. In  
80 both cases they obtained hyperhaline values for the waters hosting *C. agrigentina* specimens  
81 (respectively 35-50 psu and 50-70 psu) considering those values reliable for the evaporative  
82 palaeoenvironment that yielded the deposition of the gypsum.

83 *C. agrigentina* (Fig. 1) is one of the most widespread ostracod that lived in the  
84 Palaeomediterranean during the latest Messinian Lago-Mare event (5.53–5.33 Ma, CIESM, 2008;  
85 5.55-5.33 Ma, Manzi et al., 2013; Roveri et al., 2014a). It seems to have been the first ostracod that  
86 colonized again the sterile bottoms of the Palaeomediterranean after the deposition of the Primary  
87 Lower Gypsum and the partially desiccation of the basin. It has been recovered both in the  
88 Messinian sediments drilled on the Palaeomediterranean bottoms and in those cropping out along  
89 the peri-Mediterranean chains, from the most western area (Malaga Basin) to the easternmost  
90 Adana Basin (Benson, 1978; Iaccarino and Bossio, 1999; Bonaduce and Sgarrella, 1999; Grossi and  
91 Gennari, 2008; Guerra-Merchán et al., 2010; Cosentino et al., 2012; Faranda et al., 2013). In their  
92 study on the Messinian Lago-Mare palaeoenvironments inferred from the ostracod assemblages,  
93 Grossi et al. (2008) showed that *C. agrigentina* behaved as a very euryhaline species: it was  
94 associated a) with the benthic foraminifer *Ammonia tepida* (“*Cyprideis-Ammonia* assemblage”) in  
95 very oligotypic assemblages supposed to be typical of high mesohaline environments; b) with  
96 *Loxococoncha muelleri* (Mehés) and *Loxococoncha eichwaldi* Livialtal (“*Cyprideis-Loxococoncha*  
97 assemblage”) (low mesohaline environment); c) it was also a component, although not dominant, of  
98 the “pointed candonids-Leptocytheridae assemblage” and “pointed candonids assemblage”,  
99 supposed to be characteristic of oligohaline to low mesohaline environments.

100 Anyway, despite its apparent capability to withstand different salinities, no noded specimens  
101 of *C. agrigentina* have been ever found (Ligios and Gliozzi, 2012) and this could arise some  
102 questions about the possible ecophenotypical reaction of *C. agrigentina* to the environment.

103 In this paper we attempt to verify whether the ecophenotypical behavior of *C. agrigentina*  
104 was comparable with that of *C. torosa*. To reach this goal, adult male and female valves of *C.*

Formatted: Not Highlight

105 *agrigentina* from the long section of Eraclea Minoa (Agrigento, Sicily) were investigated and three  
106 morphometrical characters have been analysed: 1) size variability; 2) nodding and ornamentation; 3)  
107 variability of the percentage of the sieve-pore shapes. The palaeoenvironmental framework to  
108 which the ecophenotypical characters displayed by *C. agrigentina* will be compared has been built  
109 based on synecological analysis (assemblages taxonomic composition and diversity) (Chapter 3)  
110 and geochemical approaches [stable isotopes, trace elements, Sr-isotopes and natural radioactivity  
111 (NRD)] (Chapter 4).

112

## 113 2. Material and methods

114 One hundred fifty-two samples have been soaked in a H<sub>2</sub>O<sub>2</sub> 5%<sub>vol</sub> solution for 24 hours,  
115 sieved with 0.063 and 0.125 mm-mesh sieves and dried in oven at 40°C. Total manual picking has  
116 been carried out on the 0.125 mm dried sieved samples. When possible, up to 300 valves were  
117 hand-picked from each sample. Ostracods have been identified and their frequency counted; the  
118 obtained values have been normalized to 10 g in order to get comparable figures all along the  
119 section to perform a reliable palaeoenvironmental interpretation using the synecological approach  
120 proposed by Gliozzi and Grossi, 2008 and Grossi et al., 2008. Shannon-Wiener index has been  
121 calculated on the basis of the normalized matrix.

122 When possible, supplementary adult specimens of *C. agrigentina* were picked to increase  
123 the amount of material on which the morphometrical and geochemical analyses were performed.  
124 The morphometrical and geochemical analyses have been carried out on more than 3000 adult  
125 valves of *C. agrigentina*, and several thousand juvenile valves were added for Sr-analyses.

126

### 127 2.1 Morphometrical analyses

128 All juvenile and adult valves of *C. agrigentina* were observed under the stereo-microscope  
129 to investigate the ornamentation and nodding. Over one thousand adult female and male valves of *C.*

Formatted: Not Highlight

Formatted: Not Highlight

Formatted: Not Highlight

130 *agrigentina* from fifty-three selected samples were measured under the stereo-microscope, using the  
131 Leica Application Suite 2.5.0. Mean values were calculated for each sample.

132         Around 20 adult female and male valves of *C. agrigentina* from fifty-three samples, chosen  
133 on the basis of its high frequency, were observed under the Scanning Electron Microscope (LIME  
134 Laboratory, Roma Tre University). Following the methodology proposed by Rosenfeld and Vesper  
135 (1977), the rounded, elongated and irregular sieve-pores were counted and each percentage was  
136 calculated. To obtain the inferred salinity value, the following transfer function elaborated by  
137 Frenzel et al. (2011), based on the percentage of rounded sieve-pores was used:

$$138 \quad S = e^{-0.06RS+4.7}$$

139 where S = salinity (psu) and RS = percentage of rounded sieve-pores.

140

## 141 *2.2 Geochemical analyses*

142

### 143 *2.2.1 Stable isotopes*

144         Carbon and oxygen stable isotope analyses ( $\delta^{13}\text{C}$  and  $\delta^{18}\text{O}$ ) were performed on fifty-three  
145 ostracod samples each consisting of eight *C. agrigentina* clean adult valves. Two splits of each  
146 sample (4 valves each) were reacted with anhydrous phosphoric acid at  $76^\circ\text{C} \pm 2^\circ\text{C}$  in a Finnigan  
147 MAT Kiel preparation device directly coupled to the inlet of a Finnigan MAT 251 triple collector  
148 isotope ratio mass spectrometer (Stable Isotope Laboratory, University of Michigan, Ann Arbor,  
149 MI, USA). The isotopic results of the mean of the two splits are reported in permil (‰) notation  
150 relative to the Pee Dee Belemnite (PDB) standard. The measured precision for the analyses was  
151 0.04 for  $\delta^{13}\text{C}$  and 0.07 for  $\delta^{18}\text{O}$ .

152

### 153 *2.2.2 Trace elements*

154         Trace and minor element analyses together with Ca on fifty-three ostracod samples,  
155 consisting each in 6 to 10 clean adult valves of *C. agrigentina*, were performed by inductively

156 coupled plasma atomic emission spectrometry (ICP-AES). The ostracod valves were dissolved in 3  
157 ml of ultrapure HNO<sub>3</sub> acid (3%). The solutions were analysed for Ca (317.9 nm), Mg (285.2 nm),  
158 Na (589.5 nm) and Sr (215.2 nm) in the ICP-AES Thermo Jarrell IRIS Advantage Radial device of  
159 the Institute of Environmental Assessment and Water Research (IDAEA-CSIC, Barcelona, Spain).  
160 The limits of detection were 0.05 ppm for Ca and Mg, 0.01 ppm for Na and 0.005 ppm for Sr. All  
161 the analyses were run against multielemental standards prepared from Johnson Matthey™ stock  
162 solutions. The obtained results are expressed as metal/calcium ratios of the valves (Me/Ca<sub>v</sub>).

163

### 164 2.2.3 Sr isotope analyses

165 Strontium isotope measurements were obtained from 26 suitable samples of hand-picked  
166 valves of *C. agrigentina*, perfectly preserved. About 10 mg of each sample was subjected to the  
167 following procedure: ultrasonic cleaning in double distilled water to remove impurities; gentle  
168 crushing and re-washing in double-distilled water; fast dissolution in 4.0 N ultrapure HCl;  
169 centrifugation; loading onto standard BIO-RAD AG50-X12cation exchange resin. The total  
170 procedure blank was 0.5 ng. Sr was collected in 2.9 and 6.3 N HCl and evaporated. Isotopic  
171 analyses were carried out at IGAG-CNR c/o Department of Earth Sciences, University of Rome -  
172 La Sapienza using a FINNIGAN MAT 262RPQ multicollector mass spectrometer with Re double  
173 filaments in static mode. The internal precision (within-run precision) of the single analytical value  
174 is given as two standard error of the mean. The <sup>87</sup>Sr/<sup>86</sup>Sr ratios of the samples were normalized to a  
175 <sup>86</sup>Sr/<sup>88</sup>Sr value of 0.1194. The internal precision (within-run' precision) of a single analytical result  
176 is reported as 2 standard errors of the mean (2SE) and is obtained as the mean of more than 800–  
177 1000 ratios collected in each sample with a stable beam of > 2.0 V. Repeated analyses of NIST-987  
178 during the period of the analyses gave a mean value <sup>87</sup>Sr/<sup>86</sup>Sr = 0.710251±15 (2σ, n = 15).

179

### 180 2.2.4 Natural Radioactivity (NRD)

181 Natural Radioactivity (NRD) was measured on 27 bulk sediment samples. Uranium, thorium and  
182 potassium were determined by high resolution gamma spectrometry using a low background (GEM-  
183 EG&G ORTEC) HPGe coaxial detector in a PopTop capsule including detector element,  
184 preamplifier and high voltage filter at the Institute of Environmental Geology and Geoengineering  
185 (IGAG, CNR, Rome - Italy). The multichannel buffer (16,384 channels, Ethernim-ORTEC 919E),  
186 including ADC with extended live time correction, was connected into an Ethernet environment  
187 under Windows XP and its control and spectral display was achieved by the use of MAESTRO  
188 application software. In particular,  $^{232}\text{Th}$  and K were estimated from 583 keV ( $^{208}\text{Tl}$ ) and 1461 keV  
189 ( $^{40}\text{K}$ ) peaks, while  $^{238}\text{U}$  was estimated by the weighted average of U1 and U2, where U1 is the  
190 product of the known  $^{238}\text{U}/^{235}\text{U}$  natural activity ratio by the  $^{235}\text{U}$  activity (calculated by the 186 keV  
191 peak corrected by the  $^{226}\text{Ra}$  contribution) and U2 is the  $^{238}\text{U}$  activity estimated by the 352 keV peak  
192 ( $^{214}\text{Pb}$ ) assuming full equilibrium in the  $^{238}\text{U}$  radioactive series. Capo di Bove leucitite (Voltaggio et  
193 al., 2004) was used as standard, while counting time and amount of each sample were, respectively,  
194 86,400 sec and 150 grams.

Formatted: Not Highlight

Formatted: Not Highlight

### 196 2.3 Statistical analyses

197 A raw matrix of data was constructed taking into account those samples that provided all the results  
198 for the considered types of analyses (9 variables): stratigraphic position,  $\delta^{13}\text{C}$ ,  $\delta^{18}\text{O}$ ,  $\text{Mg}/\text{Ca}_v$ ,  
199  $\text{Sr}/\text{Ca}_v$ ,  $\text{Na}/\text{Ca}_v$ ,  $\text{Th}/\text{U}$ , assumed salinity after the sieve-pore analysis and the  $^{87}\text{Sr}/^{86}\text{Sr}$  ratio. The  
200 statistical software used was STATISTICA 7.0. From the raw matrix, with 9 variables and 20 cases  
201 (samples), a correlation matrix was obtained. Moreover from the raw matrix, a set of multivariate  
202 analysis techniques, as cluster and principal-component analysis (PCA) was applied. Cluster  
203 analysis defines groups of more or less related variables and the corresponding dendrogram (tree  
204 clustering) corresponds to the graphic display of the groups. PCA defines eigenvectors showing the  
205 position of the variables in the factor plane and revealing the underlying structure of the data set.

Formatted: Not Highlight

Formatted: Not Highlight

Formatted: Not Highlight

206

207 **3. The Eraclea Minoa section and its palaeoenvironments inferred from ostracod assemblages**

208 The ca. 266 m-thick Messinian Lago-Mare succession of Eraclea Minoa crops out along the  
209 south-western coast of Sicily (lat. 37°23'30"N, long. 13°16'50"E) along the cliff which borders the  
210 village (Fig. 2). The section has been extensively studied since 1971 (Decima and Wezel, 1971)  
211 because it is one of the most complete Messinian Lago-Mare section of the Palaeomediterranean  
212 where several gypsum levels referred to the Upper Gypsum Unit crop out (among the most recent  
213 papers: Schreiber, 1997; Caruso and Rouchy, 2006; Van der Laan et al., 2006; Manzi et al., 2009  
214 with references therein), and because it represents the GSSP of the Messinian/Zanclean boundary  
215 (Van Couvering et al., 2000 with references therein) (Fig. 3).

216 The succession is made of a rhythmic alternation of clays and marls interbedded with sandy  
217 and fine grained carbonates and seven gypsum bodies made by multiple strata of finely-laminated  
218 gypsum and gypsarenites/selenites (Fig. 4). The astrochronological tuning of the Eraclea Minoa  
219 section is different according to several authors. As stated by Caruso and Rouchy (2006), six  
220 sedimentary cycles covered by the Arenazzolo Fm. up to the Messinian/Zanclean boundary are  
221 recognizable, with a possible seventh basal cycle represented by an intensively deformed gypsum  
222 deposit located along the fault contact at the base of the succession. Van der Laan et al. (2006)  
223 consider the presence of seven cycles and a half, including the Arenazzolo Fm. They are linked to  
224 the precessional cyclicity and date the deposition of the Eraclea Minoa succession between 5.508  
225 Ma to 5.332 Ma. Finally, Manzi et al. (2009; 2012) hypothesize the presence of nine to ten  
226 sedimentary cycles, including the Arenazzolo Fm., bracketing the depositional age between 5.53  
227 and 5.33 Ma.

228 Ostracods are discontinuously present at the base of the section, in the marls intercalated  
229 between the lowest six gypsum bodies and become abundant in the upper portion, below and above  
230 the seventh gypsum level. Assemblages show variable richness from 1 species (monotypic  
231 assemblages made only by *C. agrigentina*) up to 13 species mainly made by the typical Lago-Mare  
232 ostracod assemblages of Paratethyan origin.

233 In the lowest portion from 88 (sample EM 3-3) to 144 m (sample EM 6-7), *C. agrigentina* is  
234 scarce and the assemblages, made by *Loxococoncha muelleri* (Méhes), *L. kocki* Méhes, *L. eichwaldi*  
235 Livental, *Loxocorniculina djafarovi* (Schneider), *Loxocauda limata* (Schneider), *Camptocypria* sp.  
236 1, *Tyrrhenocythere pontica* (Livental), *Euxinocythere (Maeotocythere) praebaquana* (Livental),  
237 *Amnicythere propinqua* (Livental), *A. subcaspia* (Livental), *A. multituberculata* (Livental) and *A.*  
238 *accicularia* Olteanu, are rather diversified. These assemblages can be referred to the “*Cyprideis-*  
239 *Loxoconchidae* assemblage” (*sensu* Grossi et al., 2008), suggesting low mesohaline and shallow  
240 waterbodies (supposed salinities <10 psu).

241 Monotypic assemblages have been recovered in the central portion of the Eraclea Minoa  
242 section, from 153 m (sample EM 6'-1) to 227 m (sample EM 7-12) and the collected valves are  
243 abundant and well preserved. In this long interval, *C. agrigentina* is the only species present in the  
244 samples or is accompanied by the euryhaline benthic foraminifer *Ammonia tepida* (Cushman).  
245 Grossi and Gennari (2008) defined the “*Cyprideis-Ammonia* assemblage” for some ostracod and  
246 forams associations recovered in the Lago-Mare borehole of Montepetra (northern Apennines, Italy)  
247 in which, together with *C. agrigentina* and *A. tepida*, also other benthic foraminifers, *Florilus*  
248 *boueanum* (d'Orbigny) and *Elphidium* spp. were seldom present or *A. tepida* was the dominant  
249 species of the assemblage. The authors related such “*Cyprideis-Ammonia* assemblage” to high  
250 mesohaline to hyperhaline shallow waterbody. At Eraclea Minoa no other brackish benthic  
251 foraminifers have been recovered except *A. tepida*. Moreover, this latter species is not always  
252 present and generally is far subordinated to *C. agrigentina*. Thus, the palaeoenvironmental  
253 interpretation of the interval from 153 to 227 m at Eraclea Minoa could be slightly different. At the  
254 moment, we can suppose for this new “*Cyprideis* assemblage” a relatively high salinity waterbody  
255 and/or a dysoxic bottom, based on the capability of the living species *C. torosa* and *Ammonia* spp.  
256 to withstand low oxygen contents (Jahn et al., 1996; Bernhard and Sen Gupta, 2002). Different  
257 assemblages, made only by scarce *C. agrigentina* and accompanying *Loxococoncha muelleri* were

Formatted: Not Highlight

Formatted: Not Highlight

Formatted: Not Highlight

Formatted: Not Highlight

Formatted: Not Highlight

Formatted: Not Highlight

258 recovered in the Lago-Mare succession of Colle di Votta (Majella Mt., central Italy) (unpublished  
259 data), in oxygen-depleted sediments (Sampalmieri et al., 2010).

260 In this central portion of the succession there are only five scattered samples in which the  
261 dominant *C. agrigentina* is associated with few other species: with *L. djafarovi* (at 182 m, sample  
262 EM 6'-29a), pointing to a low mesohaline environment; with *Ilyocypris* sp. (at 198.5 and 201.0 m,  
263 respectively samples EM 6''-8 and 6''-11), suggesting two short oligohaline episodes; with  
264 *Fabaeformiscandona* sp. (at 213 m, EM 6''-19) pointing to a further oligohaline episode; with *A.*  
265 *accicularia* (at 220.6 m, EM 7-4) indicating a low mesohaline short interval.

266 Finally, in the uppermost part of the section [from 228 m (sample EM 7-13) to 265.5 m  
267 (sample EM 8-20)], *C. agrigentina* is again accompanied by the Paratethyan assemblage in which  
268 Loxoconchidae are slightly less abundant and two more leptocytherid species are included, even if  
269 with scarce frequency: *Amnicythere litica* (Livental) and *A. costata* (Olteanu). On the whole, this  
270 topmost interval seems again to be referable to the “*Cyprideis*-Loxoconchidae assemblage” (Grossi  
271 et al., 2008), pointing to shallow waterbodies with supposed salinities <10 psu. Within this  
272 uppermost interval, it is possible to identify three horizons [from 228 m (sample EM 7-13) to 232 m  
273 (sample EM 7-19), at 234 m (sample EM 7-21) and from 235 m (sample EM 7-25) to 238 m  
274 (sample EM 7-28)] in which *C. agrigentina* shares its dominance only with two candonids species,  
275 *Fabaeformiscandona* sp. and *Cypria* sp., testifying an oligohaline and shallow environment, and  
276 two short levels [at 252.8 m (sample EM 8-3) and 257.8 m (sample EM 8-7)] in which *C.*  
277 *agrigentina* is again the only ostracod species of the assemblage.

278

#### 279 **4. Geochemical analyses and inferred palaeoenvironmental features**

Formatted: Not Highlight

280

##### 281 *4.1 Stable isotopes*

282 *C. agrigentina* calcite valves display a wide range of stable isotopic values.  $\delta^{13}\text{C}$  ranges  
283 from -6.40 to 1.91‰;  $\delta^{18}\text{O}$  ranges from -4.08 to 7.95‰ (Tab. 1; Figs. 5, 6). The  $\delta^{13}\text{C}$  values of the



284 ostracod valves show a slight increase from 153-189 m (interval A) to 198-225 m (interval B).  
285 Significant, rapid variations are shown around 198-204 m and in the upper portion of the section  
286 around 253-260 m (interval E).

Formatted: Not Highlight

Formatted: Not Highlight

287 The  $\delta^{18}\text{O}$  values of the ostracod valves show a slight increase from 153 to 189 m (interval  
288 A), a rapid variation around 198-204 m (lower interval B), and decrease from 204 to 225 m (upper  
289 interval B). In the upper portion of the section, from 257.8 to 258.5 m (interval E), a significant  
290 decrease in  $\delta^{18}\text{O}$  values, from 8‰ to -1.4‰ is observed.

Formatted: Not Highlight

Formatted: Not Highlight

Formatted: Not Highlight

Formatted: Not Highlight

Formatted: Not Highlight

Formatted: Not Highlight

Formatted: Not Highlight

291 The  $\delta^{13}\text{C}$  and  $\delta^{18}\text{O}$  values from 153 to 189 m (interval A) display small fluctuations,  
292 suggesting minor variations in the palaeohydrological conditions. On the contrary, the valves from  
293 198-204 m (interval B) and 253-260 m (interval E) display significant oscillations, both in  $\delta^{13}\text{C}$  and  
294  $\delta^{18}\text{O}$  values, suggesting instabilities in the palaeohydrological conditions related to these intervals.

Formatted: Not Highlight

295 In both cases the larger instabilities (major  $\delta^{13}\text{C}$  and  $\delta^{18}\text{O}$  oscillations) may be linked to significant  
296 detrital and freshwater inputs as reflected by the coarse-grained detrital beds at 199 m and 256-  
297 264.5 m.

Formatted: Not Highlight

Formatted: Not Highlight

298 The distribution in a X-Y plot (Fig. 6) shows that the isotopic values from 153 to 216 m  
299 (interval A and lower B) display a negative covariant trend with a significant correlation ( $R=-$   
300 0.894). This is mainly due to the negative correlation of the interval 198-216 m (lower B,  $R=-0.903$ )  
301 and the almost invariant values in the interval 153-189 m (interval A).

#### 302 303 4.2 Trace elements

304 For *C. agrigentina* calcite valves, the Mg, Sr and Na content expressed as Mg/Ca<sub>v</sub>, Sr/Ca<sub>v</sub>  
305 and Na/Ca<sub>v</sub> molar ratios are listed in Table 1 and represented in Fig. 5. The Mg/Ca<sub>v</sub> values range  
306 from 0.0052 to 0.0158, the Sr/Ca<sub>v</sub> range from 0.0022 to 0.0054 and the Na/Ca<sub>v</sub> from 0.0032 to  
307 0.0046.

308 The Mg/Ca<sub>v</sub> values show a significant drop from 189 to 198.2 m (intervals A and B  
309 boundary) towards the upper portion of the succession, with a rapid variation around 153-156 m  
310 (lower interval A). An overall increase trend in Mg/Ca<sub>v</sub> is recorded in the interval 198.2-225 m  
311 (interval B) and a significant increase is observed also in the upper part of the section (interval E).  
312 This is parallelized with a similar increase in the δ<sup>13</sup>C values.

Formatted: Not Highlight

Formatted: Not Highlight

Formatted: Not Highlight

Formatted: Not Highlight

Formatted: Not Highlight

Formatted: Not Highlight

313 The Na/Ca<sub>v</sub> values show a slight decrease from 153-189 m (interval A) to 198-216 m  
314 (interval B), with a rapid variation around 198.2-201 m. A significant decrease of Na/Ca<sub>v</sub> is  
315 observed in the upper portion of the section (interval B). This is parallelized with the decrease in  
316 Sr/Ca and δ<sup>18</sup>O values.

Formatted: Not Highlight

Formatted: Not Highlight

Formatted: Not Highlight

#### 318 4.3 Sr isotopes

319 Differently from the ratios of cation concentrations and oxygen isotopes, no Sr isotope  
320 fractionation occurs during chemical and biological processes within the marginal basin (Faure and  
321 Powell, 1972). Considering that Ostracoda are good monitors of the composition of the aquatic  
322 environment (De Deckker et al., 1988), the Sr isotopic composition of ostracod shells allow us to  
323 evaluate the connectivity of the basin with the open ocean and the paleoclimatic conditions and  
324 hydrography.

325 The Eraclea Minoa section shows that the <sup>87</sup>Sr/<sup>86</sup>Sr values from the *C. agrigentina* valves  
326 are comprised between 0.708510 and 0.708729 (Table 1). The range of values is high in the lower  
327 analysed interval (153-189 m - interval A) and decreases in the portion comprised between 198 to  
328 225 m (interval B), reaching the minimum values (0.708510 and 0.708511) in the interval 204.2-  
329 210 m (low interval B), in correspondence of low δ<sup>18</sup>O, Sr/Ca<sub>v</sub> and Na/Ca<sub>v</sub> values. In the upper  
330 portion of the section (253-260 m - interval E) the <sup>87</sup>Sr/<sup>86</sup>Sr values rise again, with a maximum  
331 (0.708704) at 253 m (Fig. 5). Sr isotopic data of *C. agrigentina* are markedly different with respect  
332 to coeval global ocean values (Henderson et al., 1994; McArthur et al., 2001) being significantly

Formatted: Not Highlight

Formatted: Not Highlight

Formatted: Not Highlight

Formatted: Not Highlight

333 lower than the marine waters at that time, but this is a common feature for latest Miocene–earliest  
334 Pliocene strontium values of the Palaeomediterranean Basin carbonates.

335  
336 *4.4 Natural Radioactivity*

337  $^{232}\text{Th}$  and K measured in bulk sediment samples are highly correlated ( $R=0.94$ ) suggesting that  
338  $^{232}\text{Th}$  is mainly contained in the detrital fraction. Detrital uranium, in turns, was calculated by the  
339 product of measured  $^{232}\text{Th}$  and the average  $^{238}\text{U}/^{232}\text{Th}$  weight ratio of pelagic sediments, considered  
340 close to 0.25 (Mangini et al., 2001). Finally, authigenic uranium,  $^{238}\text{U}_a$ , was estimated by  
341 subtracting the detrital  $^{238}\text{U}$  from measured  $^{238}\text{U}$  (Table 2). Authigenic uranium as well as the Th/U  
342 ratio was proposed by Wignall and Myers (1988) as an index of bottom-water oxygenation; the  $\text{U}_a$   
343 values trend to increase in a reducing environment, where uranium is immobile as tetravalent ion.  
344 According to Wignall (1994)  $\text{U}_a$  values comprised between 2 and 10 are indicative of dysoxic  
345 environments; similarly for Th/U values,  $\text{Th}/\text{U} \ll 1$  indicate anoxic conditions,  $\text{Th}/\text{U} \gg 1$  indicate oxic  
346 conditions, while values in the range  $1 < \text{Th}/\text{U} > 1$  point to dysoxic conditions. Even if the use of authigenic  
347 uranium as proxy for reducing conditions is common in the chemiography of marine sediments  
348 (Pattan and Pearce, 2009), several authors have questioned the real preservation of the authigenic  
349 uranium signal by different processes as burn down, fast change of sedimentation rate and oxygen  
350 ventilation or bioturbation (Zheng et al., 2002). Therefore any indication of oxigen depletion  
351 suggested by the authigenic uranium has to be regarded in a wider fitting context.

352  $\text{U}_a$  from the bulk sediment display values from 0.3 to 9.5 ppm (Table 2). The lowest values are  
353 attained in intervals A, B and lower C, with figures generally below 2. In the upper part of interval  
354 C,  $\text{U}_a$  increases and maintains high values in interval D and E, where some fluctuations occur,  
355 similarly to what observed for the stable isotopes and trace elements ratios (Fig. 5). A similar trend  
356 is observed for the Th/U ratios, which show values greater than 1 in intervals A, B and C, and  
357 values mainly around 1 in intervals D and E (Table 2).

Formatted: Not Highlight

Formatted: Not Highlight

Formatted: Not Highlight

Formatted: Not Highlight

Formatted: Not Highlight

Formatted: Not Highlight

Formatted: Not Highlight

359 4.5 Palaeoenvironmental episodes inferred from the geochemical proxies

360 The geochemical analyses performed on the valves of *C. agrigentina* and bulk sediment  
361 samples collected from the 96.5-260 m portion of the post-evaporitic Messinian succession of  
362 Eraclea Minoa confirm the frame of a Palaeomediterranean waterbody discontinuous and isolated,  
363 characterised by diluted waters after the evaporative phase of the Lower Gypsum Unit, the closure  
364 of the Atlantic-Palaeomediterranean connection and the subsequent global humid climate phase  
365 (Griffin, 2002; CIESM, 2008; Grossi et al., 2008). In fact, notwithstanding the well known saline  
366 character of the Palaeomediterranean waters, testified by the presence of brackish ostracod  
367 assemblages, all the geochemical indicators point to a clear differentiation with the Messinian  
368 oceanic seawater. On the other hand, the stable isotopes values reported in Figs. 5, 6 do not show  
369 the overall covariant trend that would correspond to a marginal marine environment or a closed  
370 waterbody (Talbot, 1990; Utrilla et al., 1998; Ligios et al., 2012), and also trace elements behave in  
371 a different manner. The Mg/Ca<sub>v</sub> values from *C. agrigentina* (0.0052-0.0152) are similar to most of  
372 the analyses from *Cyprideis* shells for the Messinian Lago-Mare horizons from DSDP sites (De  
373 Deckker et al., 1988). For these Mg/Ca<sub>v</sub> values, De Deckker et al. (1988) consider the host water  
374 had Mg/Ca values lesser than that of Messinian seawater, and in some cases similar to most of the  
375 Mg/Ca shown by freshwaters (Mg/Ca=1). The Sr/Ca<sub>v</sub> values from *C. agrigentina* at 153-189 m  
376 (0.0025-0.0030) are similar to most of the analyses from *Cyprideis* shells from the Messinian Lago-  
377 Mare horizons from DSDP sites (De Deckker et al., 1988). For these Sr/Ca<sub>v</sub> values, these authors  
378 consider the host water had Sr/Ca values lesser than that of Messinian oceanic seawater. On the  
379 contrary, the Sr/Ca<sub>v</sub> values for most of the samples from 198-225 m and 252.8-257.8 m (0.0038-  
380 0.0054) indicate that the host water frequently had Sr/Ca values greater than that of Messinian  
381 oceanic seawater. The values of Sr/Ca<sub>v</sub> and Mg/Ca<sub>v</sub> indicate that the waters where the Eraclea  
382 Minoa ostracods lived were very different than the Messinian seawater and there is no indication of  
383 connection with oceanic seawater. Furthermore, the <sup>87</sup>Sr/<sup>86</sup>Sr range of values obtained from the  
384 analyses of *C. agrigentina* valves is consistent with the isotopic values of the Upper Gypsum Unit

Formatted: Not Highlight

Formatted: Not Highlight

Formatted: Not Highlight

385 from Sicily and other localities of the Palaeomediterranean (Müller and Mueller, 1991; Keogh and  
386 Butler, 1999; Flecker and Ellam, 2006; Roveri et al., 2014b). This range is also similar to the range  
387 (0.708600-0.70875) reported from most ostracod valves (*Cyprideis*) from Messinian Lago-Mare  
388 deposits from several DSDP sites of the Palaeomediterranean studied by McCulloch and De  
389 Deckker (1989). On the other hand, the Sr isotopic values from Eraclea Minoa are quite different  
390 from the value of the average ocean water during the deposition of the Upper Evaporite: 0.709012  
391 (Howarth and McArthur, 1997; Flecker et al., 2002). The  $^{87}\text{Sr}/^{86}\text{Sr}$  values of the Eraclea Minoa *C.*  
392 *agrigentina*, as is the case of materials from other post-evaporitic Messinian localities, confirm to  
393 be the result of a large influence of freshwater on the Sr isotopic composition of the desiccating  
394 subbasins of the Palaeomediterranean (Müller et al., 1990). Finally, it is noteworthy that isotopic  
395 ratios anomalously low could result from reworking of older marine evaporites, or diagenetic  
396 overprinting. However, according to Keogh and Butler (1999), the reworking of Sr from the older  
397 marine evaporites implies mixing in different proportion between Sr deriving from continental run-  
398 off and coming from ground water circulating inside the buried evaporites. Such a process likely  
399 produces high variability in both salinity and  $^{87}\text{Sr}/^{86}\text{Sr}$  ratios.

Formatted: Not Highlight

400 Based on the geochemical signature of *C. agrigentina* valves and bulk sediment samples,  
401 five main palaeoenvironmental intervals may be differentiated along the studied portion of the  
402 Eraclea Minoa succession (Fig. 5):

403 Interval A (153-189 m), characterised by high  $\delta^{18}\text{O}$ ,  $\text{Na}/\text{Ca}_v$ ,  $\text{Mg}/\text{Ca}_v$  and  $^{87}\text{Sr}/^{86}\text{Sr}$  values,  
404 and low  $\delta^{13}\text{C}$ ,  $\text{Sr}/\text{Ca}_v$ , and  $\text{U}_a$ . This interval records relatively stable hydrochemical conditions as  
405 suggested by the small variation of each geochemical indicator, isotopically concentrated waters  
406 and high  $\text{Na}/\text{Ca}_v$  and  $\text{Mg}/\text{Ca}_v$  ratios that were attained after the deposition of the 6<sup>th</sup> gypsum level.  
407 An overall evaporative environment (Fig. 5) with moderate salinity could be inferred for this  
408 interval. The high amount of Th and detrital U, the low content of authigenic uranium and the rather  
409 high Th/U ratios (Table 2) record possible well oxygenated bottoms.

Formatted: Not Highlight

410 Interval B (198-225 m), characterised by low  $\delta^{18}\text{O}$ ,  $\text{Na}/\text{Ca}_v$ ,  $\text{Mg}/\text{Ca}_v$ ,  $^{87}\text{Sr}/^{86}\text{Sr}$ , and  $U_a$   
411 values, and high  $\delta^{13}\text{C}$  and  $\text{Sr}/\text{Ca}_v$ . A major change is recorded at the base of this interval (198 m,  
412 sample EM 6''-8) where large shifts in all the geochemical indicators appear. A possible explanation  
413 for these features is to consider the noticeable detrital and freshwater inputs that increase the Ca  
414 dissolution, recorded both by the coarser lithologies, the high values of Th and detrital U and the  
415 low  $^{87}\text{Sr}/^{86}\text{Sr}$  values for most samples. Those inputs may explain the lowering of  $\delta^{18}\text{O}$  in the valves,  
416 the increase of  $\text{Sr}/\text{Ca}_v$  (recording Sr inputs from the  $\text{CaSO}_4$ -rich subsurface waters) and the lowering  
417 in  $\text{Mg}/\text{Ca}_v$  because of the high increase in Ca in the waterbody. The increase in  $\delta^{13}\text{C}$  values could  
418 be produced by an increase in the productivity, linked to the detrital and nutrient inputs and a trend  
419 to re-equilibration with the atmospheric  $\text{CO}_2$  (Fig. 5). As in the previous interval, NRD results  
420 (Table 2) testify for possible well oxygenated bottoms.

Formatted: Not Highlight

Formatted: Not Highlight

421 Interval C (225-240 m). In this interval, only NRD analyses have been performed due to the  
422 low frequency of *C. agrigentina* in the ostracod assemblages that prevented the possibility to reach  
423 the suitable amount of biogenic carbonate for the analyses. The content of authigenic uranium in the  
424 upper part of this interval, higher than in the previous one, (Table 2, Fig. 5) points to possibly  
425 progressively less oxygenated bottoms.

Formatted: Not Highlight

Formatted: Not Highlight

426 Interval D (240-242 m). This short interval is characterised by the highest values of  
427 authigenic U and low values of the Th/U ratios, suggesting possible dysoxic conditions at the  
428 bottom.

429 Interval E (252.8-259.1 m). In this interval two portions may be differentiated and a main  
430 change is recorded from the lower samples to the upper ones. The lower samples are characterised  
431 by high  $\delta^{18}\text{O}$ ,  $\text{Sr}/\text{Ca}_v$ ,  $\text{Na}/\text{Ca}_v$ , and  $^{87}\text{Sr}/^{86}\text{Sr}$  values, and low  $\delta^{13}\text{C}$  and  $\text{Mg}/\text{Ca}_v$  values. The low  
432 content of authigenic uranium indicates possibly oxygenated bottoms. The upper samples are  
433 characterised by the opposite trend. The geochemical features of the ostracod valves from the lower  
434 part may be explained by the evaporitic concentration of the waterbody (Figs. 5, 6) leading to high

Formatted: Not Highlight

435  $\delta^{18}\text{O}$ , Sr/Ca<sub>v</sub> and Na/Ca<sub>v</sub> values. A subsequent large input of freshwater produced the lowering of  
436  $\delta^{18}\text{O}$ , Sr/Ca<sub>v</sub> and Na/Ca<sub>v</sub>. At present, we have no explanation for the variations of the Mg/Ca<sub>v</sub>  
437 values in this interval. It is worth to note the high content of authigenic uranium that reaches in one  
438 sample the value of 9.5 ppm, possibly indicating dysoxic conditions at the bottom.

Formatted: Not Highlight

439

## 440 **5. Morphometrical analyses on *Cyprideis agrigentina* valves**

441 Length and height of one thousand-sixty valves of adult males and females were measured.

Formatted: Not Highlight

442 The obtained values fall within the variability field typical of the species (Decima, 1964; Ligios et  
443 al., 2012). The mean values of the length of the female left valve (the most numerous in the  
444 measured samples) have been compared. Generally the mean values of the length vary from 0.96 to  
445 1.00 mm, but in few samples the mean values are rather small: at 185 m (sample EM 6''-3, mean  
446 value 0.90 mm), 201 m (EM 6''-11, mean value 0.89 mm), 222 m (EM 7-6, mean value 0.85 mm),  
447 and 223.5 m (EM 7-8, mean value 0.88 mm) (Fig. 7). Only in four samples the mean values of the  
448 length result significantly high: at 165 m (sample EM 6'-12 mean value 1.05 mm), 176.2 m (EM 6'-  
449 24, mean value 1.06 mm), 180 m (EM 6'-27, mean value 1.04 mm), and 210 m (EM 6''-17, mean  
450 value 1.14 mm).

451 The several thousands specimens of *C. agrigentina* investigated for the ornamentation and  
452 nodding, showed rather homogeneous ornamentation: no noded specimens have been observed all  
453 along the section among both juveniles and adults; almost all valves were smooth (at least some of  
454 them showed few small pits in the posterior surface); only two samples (EM 6''-7 at 189.0 m and  
455 EM 6''-20 at 216.0 m) showed, respectively, the 54.2% and 54.6% of valves pitted on the entire  
456 surface (Fig. 7).

457 The analysis of the percentage of the sieve-pore shape was carried out on fifty-three samples  
458 from the middle and upper portion of the section, where *C. agrigentina* was more abundant, making  
459 both monospecific and diversified assemblages. On average, more than 500 sieve-pores were  
460 observed for each sample and counted on the basis of their shape: rounded, elongated, irregular,

461 following the indications by Rosenfeld and Vesper (1977). The results are reported in Fig. 7. In  
462 most cases, the percentages of the rounded sieve-pores are comprised between 40 and 50%; in  
463 twelve scattered samples they are higher, reaching the maximum value of 65% at 96.5 m (sample  
464 EM 4-7) and only in a short interval from 198.5 m (sample EM 6''-8) to 216 m (sample EM 6''-20)  
465 they are lower, comprised between 19 and 30%, reaching their minimum values (19-21%) in the  
466 interval 204.5-216 m. Applying the transfer function elaborated by Frenzel et al. (2011) for *C.*  
467 *torosa*, the resulting salinities expressed in psu shows values included in the mesohaline range (5-18  
468 psu, Venice Symposium, 1958) for most samples. Only few scattered samples in the lower and  
469 upper portions of the section point to the oligohaline range (0.5-5 psu), while higher salinities  
470 (polyhaline to euhaline ranges, 18-40 psu) are recorded only in a limited portion of the section, from  
471 198.5 to 216 m (Fig. 8).

472

## 473 **6. Discussion**

474 As explained in the introduction, the living species *C. torosa* is considered to be one of the  
475 most valuable tools to detect past salinities in the marginal marine environments, owing to its  
476 environmentally cued polymorphism that induces variations in size, nodding and sieve-pore shapes  
477 depending on salinity. Large sizes, presence of nodes and high percentages (around 40-45%) of  
478 rounded sieve-pores point to salinity less than 8-9 psu that is considered an important  
479 osmoregulation threshold for the species (Keiser and Aladin, 2004; Keyser, 2005).

480 It is not clear when *Cyprideis torosa* appeared for the first time, owing to the difficulty to  
481 identify the species. Often in the Neogene sediments *Cyprideis* remains have been recorded as  
482 *Cyprideis* gr. *torosa* or *Cyprideis* sp. (Bossio et al., 1993; 1996; Testa, 1995). According to Decima  
483 (1964) and Ligios and Gliozzi (2012) the species is the only survivor of a stem that started in the  
484 Palaeomediterranean area with *Cyprideis ruggierii* Decima (late Tortonian-early Messinian),  
485 including *Cyprideis agrigentina* Decima (post-evaporitic Messinian) and *Cyprideis crotonensis*  
486 Decima (post-evaporitic Messinian-Late Pliocene). The great morphological similarity of the



487 species of the stem lead some authors to suppose that the same environmentally cued polymorphism  
488 displayed by *C. torosa* could affect also its relatives (Neale, 1988), notwithstanding no noded  
489 specimens of the other species had never been recorded. Thus, Rosenfeld (1977) and Bonaduce and  
490 Sgarrella (1999) inferred hyperhaline post-evaporitic Messinian environments respectively for the  
491 Mavqi'im Formation (Israel) and at Eraclea Minoa, applying on *C. agrigentina* valves the empirical  
492 methods of the percentage of the rounded sieve-pores elaborated by Rosenfeld and Vesper (1977)  
493 on *C. torosa*.

494 As a first step to investigate whether *C. agrigentina* shared with *C. torosa* the same  
495 ecophenotypical behavior, we have analyzed size, ornamentation and sieve-pore shapes on some  
496 thousand of specimens from the post-evaporitic Messinian section of Eraclea Minoa. The expected  
497 results, in case of a comparable behavior, is a positive correlation between large size, nodding (or  
498 strongly pitted valve surface), and high percentages of rounded sieve-pores. Fig. 7 shows that this  
499 correlation lacks: the largest sizes (thus the supposed lowest salinities, below 8-9 psu) are attained  
500 by specimens recovered in samples bearing smooth valves (supposed high salinities) and  
501 percentages of rounded sieve-pores less than 40% (above the 8-9 psu threshold). In particular, in  
502 sample EM 6"-17 (at 210 m) the largest *C. agrigentina* valves matches with one of the lowest  
503 percentages of rounded sieve-pores (22,7%); the smallest sizes (supposed high salinities) correlates  
504 with smooth valve surfaces (supposed high salinities) but to percentages of rounded sieve-pores  
505 greater than 40% except in one case (sample EM 6"-11 at 201 m) in which the percentage is low  
506 (23.1%); the only two samples in which *C. agrigentina* valves are densely pitted (supposed low  
507 salinities), corresponds, on average, to intermediate dimensions and high percentage values.

508 From those comparisons it is possible to conclude that size and ornamentation/nodding in *C.*  
509 *agrigentina* are not correlated. In particular, pitted ornamentation and nodding seem to be,  
510 respectively, very rare and totally absent in *C. agrigentina*, despite the species seems to be strongly  
511 euryhaline as it is its living relative (Ligios and Gliozzi, 2012). Thus, it seems that those characters  
512 do not display in *C. agrigentina* the same salinity-dependant polymorphism of *C. torosa*.

513 A further question is to investigate whether the percentage variations of the sieve-pore  
514 shapes are correlated with salinity variations as in *C. torosa*. To test this hypothesis we have based  
515 the comparisons of the salinity curve obtained applying the transfer function elaborated by Frenzel  
516 et al. (2011) with the salinity inferred by the synecological analysis and with the palaeohydrological  
517 variations inferred by the geochemical analyses (Figs. 8, 9, 10).

518 Based on the synecological analysis and the Shannon-Wiener diversity curve, it is possible  
519 to observe that the “*Cyprideis* assemblage”, correlatable with the minimum diversity values  
520 (monotypic ostracod assemblages) corresponds to different inferred salinities: oligo-low mesohaline  
521 in the intervals 153-171, 218-225 and 253-257.8 m; high mesohaline from 174 to 189 m;  
522 polyhaline-euhaline from 198.5 to 216.5 m. Moreover, it is worth to note that the two oligohaline  
523 levels with *Cyprideis* and *Ilyocypris*, included in the “*Cyprideis*” long interval at 198.5 and 201 m,  
524 according to the salinity curve based on sieve-pore percentage should have deposited in  
525 polyhaline/euhaline waters. We should conclude that there is no correspondence between the  
526 salinities inferred by the method of the sieve-pore percentages and the synecological  
527 palaeoenvironmental interpretation. This conclusion contradicts the statement by Bonaduce and  
528 Sgarrella (1999) who, on the basis of the percentage of sieve-pore shapes, inferred for the Eraclea  
529 Minoa portion of succession with monospecific *Cyprideis* assemblage hyperhaline environments  
530 (50-70 psu). Probably their conclusions are affected by the very few analyzed samples along the  
531 succession (only two) and the scarcity of counted sieve-pores for each sample (respectively 74 and  
532 161).

533 The calculation of past salinities from the results of the geochemical analyses on the valves  
534 of *C. agrigentina* is difficult to assess. Although  $\text{Na}/\text{Ca}_v$  could be tentatively perceived as a proxy of  
535 the salinity (assuming salinity dominated by NaCl solute), the obtained data must be considered  
536 with caution because of the poor knowledge of the Na uptake in the ostracod calcite shell (Holmes  
537 and De Deckker, 2012). However, recent attempts to use Na/Ca ratios from ostracod valves for  
538 palaeoenvironmental reconstructions must be taken into account (Gouramanis et al., 2010;

539 Devriendt, 2011). On the other hand, Sr/Ca and Mg/Ca from ostracod valves just may inform about  
540 the Sr/Ca and Mg/Ca of the waters (De Deckker et al., 1999; Dettman and Dwyer, 2012; Holmes  
541 and De Deckker, 2012), and only in some cases (i.e. some estuarine environments) these ratios  
542 could correlate with the salinity of the waters. On the other hand,  $\delta^{18}\text{O}$  variations in closed non-  
543 marine environments are linked usually to evaporation/precipitation processes (Talbot, 1990), that  
544 in some cases are associated to salinity variations. Anyway, the decreasing Na/Ca<sub>v</sub> ratios from  
545 Interval A to Interval B (Fig. 5) is consistent with the interpretation of more diluted waters in this  
546 latter interval, as pointed by the low  $\delta^{18}\text{O}$  values in B. However, this is in contradiction with the  
547 higher salinity assumed for interval B than for interval A based on the sieve-pore analysis of *C.*  
548 *agrigenina* (Fig. 8).

549 We have tried to test the correlation between the geochemical results and the salinities  
550 assumed from the analysis of the sieve-pore percentages using a multivariate approach. The  
551 correlation matrix obtained for nine variables is shown in Table 3. Significant correlations ( $p < 0.01$ )  
552 are displayed only by the pairs  $\delta^{18}\text{O}$  and Na/Ca<sub>v</sub>, Na/Ca<sub>v</sub> and Mg/Ca<sub>v</sub>, Sr/Ca<sub>v</sub> and stratigraphic  
553 position. Significant negative correlations are shown by  $\delta^{13}\text{C}$  and Na/Ca<sub>v</sub>,  $\delta^{13}\text{C}$  and  $\delta^{18}\text{O}$ ,  $\delta^{13}\text{C}$  and  
554 Mg/Ca<sub>v</sub>, Mg/Ca<sub>v</sub> and Sr/Ca<sub>v</sub>. In fact salinity assumed from sieve-pore analysis (N pores), and Sr  
555 isotopic ratios of the valves do not show significant correlation with any of the other considered  
556 variables.

557 Principal Component Analysis (PCA) delineates similar patterns. About 34.92% of the total  
558 variance is explained by the first eigenvector (Fig. 9), which is tied to concentration-evaporation  
559 processes, indicated by the relations among  $\delta^{18}\text{O}$ , Na/Ca<sub>v</sub>, Mg/Ca<sub>v</sub>, Th/U and  $^{87}\text{Sr}/^{86}\text{Sr}$  in the  
560 positive field. This factor is related to the precipitation/evaporation balance and residence time and  
561 probably to the resedimentation of evaporites. Inputs of oxygenated, SO<sub>4</sub>-rich solutions would lead  
562 to lowering of  $\delta^{18}\text{O}$ , Na/Ca<sub>v</sub>, Mg/Ca<sub>v</sub> and  $^{87}\text{Sr}/^{86}\text{Sr}$ . On the negative field, the variables are Sr/Ca<sub>v</sub>,  
563 the stratigraphic position and the percentages of rounded sieve-pores that are linked to DIC

Formatted: Not Highlight

Formatted: Not Highlight

Formatted: Not Highlight

Formatted: Not Highlight

Formatted: Not Highlight

564 (Dissolved Inorganic Carbon) changes. On the other hand, factor 2 that accounts for 20.72% of the  
565 variance, in the positive area contains a group formed by  $\delta^{18}\text{O}$ , Sr/Ca<sub>v</sub>, stratigraphic position and  
566 Na/Ca<sub>v</sub>, whereas in the negative area a group formed by N pores,  $\delta^{13}\text{C}$ , Th/U and Mg/Ca<sub>v</sub> exists.  
567 Factor 2 probably is linked to detrital, freshwater and nutrient inputs related to the environmental  
568 evolution.

Formatted: Not Highlight

Formatted: Not Highlight

Formatted: Not Highlight

Formatted: Not Highlight

Formatted: Not Highlight

569 Results from the cluster analysis reveal several groups (Fig. 10). One of the groups shown  
570 by the dendrogram reflects the relationship between  $\delta^{18}\text{O}$  and Na/Ca<sub>v</sub> revealing the control of the  
571 Na/Ca<sub>v</sub> exerted by the P/E balance ( $\delta^{18}\text{O}$ ). They are associated with Mg/Ca<sub>v</sub>, Th/U, and Sr isotopic  
572 ratios in the ostracod valve that, into a lesser extent, seem also to be influenced by the P/E balance.  
573 The pair Sr/Ca<sub>v</sub>-position of the sample is associated to the pair  $\delta^{13}\text{C}$ -percentage of rounded sieve-  
574 pores. This pair reveals the link between DIC changes and the changes in sieve-pore shapes.

Formatted: Not Highlight

Formatted: Not Highlight

575 It is worth to note that, although some authors consider both the U<sub>a</sub> and Th/U values as good  
576 proxies to detect past oxic/dysoxic conditions (Adams and Weaver, 1958; Wignall and Myers,  
577 1988 ; Wignall, 1994; Jones and Manning, 1994), Wignall and Meyers (1988) suggest to couple the  
578 U<sub>a</sub> results with the Shannon-Weaver dominance-diversity index (H) since, under low-oxygen  
579 conditions, assemblages are dominated by a few eurytopic forms, and values of H are typically low.  
580 If we compare the H-index curve (Fig. 8) with the oxygen availability at the bottom derived from  
581 the U<sub>a</sub> curve of Fig. 5, we notice that they are contradictory: when U<sub>a</sub> values are high (comprised  
582 between 2 and 10 and indicate possible dysoxic bottoms) the H-index values are high (rather well  
583 diversified assemblages). This negative correlation suggest, as supposed by Zheng et al. (2002) that  
584 the accumulation of U<sub>a</sub> in sediments could due also to physico-chemical variables other than the  
585 oxygen availability.

Formatted: Not Highlight

586 The results of the statistical analyses underline that there is no significant relationship  
587 between the salinity assumed from the sieve-pore analyses on the valves of *C. agrigentina* and the  
588 variables linked to the hydrochemical changes ( $\delta^{18}\text{O}$ , Na/Ca<sub>v</sub> and Mg/Ca<sub>v</sub>, i.e. the salinity changes).

589 On the other hand, the number of rounded sieve pores in *C. agrigentina* seems to be mainly linked  
590 to  $\delta^{13}\text{C}$  (DIC-cycling of C).

591 In conclusion, this puzzly set of data does not confirm that the percentages variation of the  
592 sieve-pore shapes in *C. agrigentina* is a reliable salinity indicator for the Lago-Mare episode of the  
593 Messinian Salinity Crisis. On the other hand, the complexity of the hydrochemical evolution due to  
594 the re-sedimentation of the Upper Gypsum Unit and scattered inputs of detrital materials and  
595 meteoric waters accounts for a complex palaeohydrological and palaeohydrochemical scenario in  
596 which it seems that the factor responsible for the changes in the shape of the pores in the valves of  
597 *C. agrigentina* could be the behaviour of the DIC and the oxygen availability.

598 On the other hand, the geochemical data give a negative response to the hypothesis that the  
599 “*Cyprideis* assemblage” could be related to dysoxia at the bottom. Data from the percentage of the  
600 authigenic U, Th/U ratios indicate that some accumulation of  $U_a$  occurred at the bottom of the  
601 Eraclea Minoa waterbody, but it seems that they were not so important to affect the benthic  
602 ostracod assemblages.

603 Although it is beyond the aim of this paper, in order to try to understand the  
604 palaeoenvironmental meaning of the “*Cyprideis* assemblage” we have tried to extend our  
605 investigations comparing other Lago-Mare successions of the Mediterranean area that included  
606 monotypic *C. agrigentina* assemblages. In the first case, such assemblage, represented by very  
607 scarce specimens, has been recovered in the lower portion of the Lago-Mare succession of the  
608 Adana Basin (Turkey) during the deposition of resedimented evaporites and marls, where a very  
609 high sedimentation rate was recorded (Faranda et al., 2013). The authors linked the low diversity  
610 and the scattered distribution of the ostracod assemblage of the Adana Basin to the high siliciclastic  
611 input connected with the high subsidence rate that affected the Adana Basin during the Lago-Mare  
612 phase. At Eraclea Minoa the “*Cyprideis* assemblage” is present with high frequencies and  
613 continuously recovered along the entire interval, but it is rather confined to the thick marly-sandy  
614 succession included between gypsum bodies 6 and 7. If we hypothesize that this portion of

Formatted: Not Highlight

615 succession represents one precessional cycle, as supposed by Van der Laan et al. (2006), high  
616 sedimentation rates affected both Adana (12.5 mm/yr) (Radeff et al., submitted) and Eraclea Minoa  
617 (4.3 mm/yr) successions. Similar stratigraphical, sedimentological and paleontological conditions  
618 have been found also in the lower portion of the Lago-Mare succession cropping out in the Iraklion  
619 Basin (central Crete) (unpublished data). Unfortunately, not everywhere high sedimentation rates  
620 and siliciclastic inputs support only the “*Cyprideis* assemblage”: in the Mondragone 1 well  
621 (Garigliano Plain, Campania, southern Italy) around one-thousand meters of sediments deposited  
622 within the short temporal frame of the *Loxocorniculina djafarovi* zone (5.40-5.33 Ma), thus a very  
623 high sedimentation rate above 13 mm/yr was calculated, but the recovered Lago-Mare ostracod  
624 assemblages were highly diversified (Cosentino et al., 2006).

625 In conclusion, at the moment no plausible hypothesis can be arised on the  
626 palaeoenvironmental meaning of the “*Cyprideis* assemblage”, once again stressing the peculiar and  
627 complex geological and palaeoenvironmental history of the Eraclea Minoa succession.

628

## 629 **7. Conclusion**

630 The ostracod assemblages of the post-evaporitic Messinian section of Eraclea Minoa (Sicily)  
631 have been studied in a palaeoenvironmental perspective to decipher the environmental changes  
632 verified during the deposition of the Upper Gypsum Unit. Rich and diversified assemblages made  
633 mainly by Paratethyan species, have been recovered in the lower and upper portion of the  
634 succession, pointing to shallow and low mesohaline waterbodies. In the central portion of the  
635 succession, very abundant monospecific assemblages made only by *C. agrigentina* were  
636 recognized, suggesting high mesohaline to hyperhaline shallow waterbody with low oxygen  
637 content. To test this latter interpretation, morphometric and geochemical analyses (stable isotopes,  
638 trace elements,  $^{87}\text{Sr}/^{86}\text{Sr}$ , and NRD) have been performed on ostracod valves and bulk sediment  
639 samples in order to verify if *C. agrigentina* ecophenotypical behavior was comparable with that of  
640 the living species *C. torosa*.

641 The results have shown that:

- 642 1) *C. agrigentina* sizes and ornamentations are not affected by salinity variations;  
643 2) The percentages of sieve-pore shapes do not depend from the water salinity, as in *C. torosa*,  
644 but seem linked to the behavior of the DIC and the oxygen availability at the bottom.

645 Thus, it is possible to conclude that *C. agrigentina* cannot be considered as a  
646 palaeosalinometer for the Messinian Salinity Crisis.

647 Furthermore, the geochemical analyses have shown that the deposition of the Eraclea Minoa  
648 succession occurred in a complex palaeohydrological and palaeohydrochemical scenario.

649

650

#### 651 **Acknowledgements**

652

653 The research of F.G. and E.G. has been founded by the Italian National Research Project PRIN  
654 2009-2010. P.A. work is supported by Project CGL2011-23438. The authors are grateful to Rafael  
655 Bartroli (ICTJA and IDAEA, CSIC) for the ICP-AES analyses and to Lora Wingate (Stable Isotope  
656 Laboratory, University of Michigan) for the stable isotope analyses on the ostracod valves.

657

#### 658 REFERENCES

659

660 Adams J.A. & Weaver C.E., 1958. Thorium-uranium ratios as indicators of sedimentary processes:  
661 example of concept of geochemical facies. Bulletin American Association of Petroleum  
662 Geologists 42(2), 387-430.

663 Aladin, N.V., 1993. Salinity tolerance, morphology and physiology of the osmoregulation organs in  
664 Ostracoda with special reference to Ostracoda from the Aral Sea. In Jones, P. and McKenzie  
665 K. (Eds.), Ostracoda in Earth and Life Sciences, A.A. Balkema, Rotterdam, 387-404.

Formatted: Not Highlight

- 666 Anadón, P., Gliozzi, E., Mazzini, I., 2002. Paleoenvironmental reconstruction of marginal marine  
667 environments from combined paleoecological and geochemical analyses on Ostracods. In:  
668 Holmes, J., Chivas, A. (Eds), *The Ostracoda: Applications in Quaternary Research*,  
669 *Geophysical Monograph* 131, 227–247.
- 670 Barbieri, M., Carrara, C., Castorina, F., Dai Pra, G., Esu, D., Gliozzi, E., Paganin, G., Sadori, L.,  
671 1999. Multidisciplinary study of Middle-Upper Pleistocene deposits in a core from the Piana  
672 Pontina (central Italy). *Giornale di Geologia* 61, 47–73.
- 673 Benson, R.H., 1978. The paleoecology of the ostracodes of DSDP Leg 42A. In: *Initial Reports of*  
674 *the Deep Sea Drilling Project* 42, 777–787, U.S. Government Printing Office, Washington,  
675 D.C.
- 676 Bernhard, J.M, Sen Gupta, B.K., 2002. Foraminifera of oxygen-depleted environment. In: Sen  
677 Gupta, B.K. (Ed.), *Modern Foraminifera*. Kluwer Academic Publishers, 201-216.
- 678 Bonaduce, G., Sgarrella, F., 1999. Paleoecological interpretation of the latest Messinian sediments  
679 from southern Sicily (Italy). *Memorie della Società Geologica Italiana* 54, 83–91.
- 680 Boomer, I., Frenzel, P., 2011. Possible environmental and biological controls on carapace size in  
681 *Cyprideis torosa* (Jones, 1850). *Joannea Geologie und Paläontologie* 11, 26–27.
- 682 Bossio, A., Costantini, A., Lazzarotto, A., Liotta, D., Mazzanti, R., Mazzei, R., Salvatorini, G.,  
683 Sandrelli, F., 1993. Rassegna delle conoscenze sulla stratigrafia del Neautoctono toscano.  
684 *Memorie della Società Geologica Italiana* 49, 17–98.
- 685 Bossio, A., Cerri, R., Mazzei, R., Salvatorini, G., Sandrelli, F., 1996. Geologia dell'area  
686 Spicchiaiola-Pignano (Settore orientale del Bacino di Volterra). *Bollettino della Società*  
687 *Geologica Italiana* 115, 393-422.
- 688 Carbonel, P., 1982. Les Ostracodes, traceurs des variations hydrologiques dans des systèmes de  
689 transition eaux douces-eaux salées. *Mémoires de la Société géologique de France* 8(144),  
690 117–128.



- 691 Caruso, A., Rouchy, J.-M., 2006. The Upper Gypsum Unit. In: Roveri, M., Manzi, V., Lugli, S.,  
692 Schreiber, B.C., Caruso, A., Rouchy, J.-M., Iaccarino, S.M., Gennari, R., Vitale, F.P., Ricci  
693 Lucchi, F. (Eds.), Clastic vs. primary precipitated evaporites in the Messinian Sicilian  
694 basins. Acta Naturalia de "L'Ateneo Parmense" 42(4), 157-159.
- 695 CIESM (Commission Internationale pour l'Exploration de la Mer Méditerranée, Monaco), 2008.  
696 The Messinian Salinity Crisis from Mega-Deposits to Microbiology: A Consensus Report.  
697 CIESM Workshop Monograph 33, 1-168.
- 698 Cosentino, D., Bertini, A., Cipollari, P., Florindo, F., Gliozzi, E., Grossi, F., Lo Mastro, S.,  
699 Sprovieri, M., 2012. Orbitally-forced palaeoenvironmental and palaeoclimate changes in the  
700 late post-evaporitic Messinian stage of the central Mediterranean Basin. Geological Society  
701 of America Bulletin 124(3-4), 499-516.
- 702 Cosentino, D., Federici, I., Cipollari, P., Gliozzi, E., 2006. Environments and tectonic instability in  
703 central Italy (Garigliano Basin) during the late Messinian *Lago-Mare* episode: New data  
704 from the onshore Mondragone well (Garigliano Plain, central Italy). Sedimentary Geology  
705 188-189, 293-317.
- 706 Curry, B., Mesquita-Joanes, F., Fanta, S., Sterner, D., Calò, C., Tinner, W., 2013. Two coastal  
707 sinkhole lakes in SW Sicily (Italy) reveal low-salinity excursion during Greek and Roman  
708 occupation. Naturalista Siciliano 4, 37(1), 93-95.
- 709 De Deckker, P., Chivas, A.R., Shelley, J.M.G., 1988. Palaeoenvironment of the Messinian  
710 Mediterranean "Lago Mare" from strontium and magnesium in ostracode shells. Palaios, 3,  
711 352-358.
- 712 De Deckker, P., Chivas, A.R., Shelley, J.M.G., 1999. Uptake of Mg and Sr in the euryhaline  
713 ostracod *Cyprideis* determined from in vitro experiments. Palaeogeography,  
714 Palaeoclimatology, Palaeoecology 148, 105-116.
- 715 Decima, A., 1964. Ostracodi del genere *Cyprideis* Jones del Neogene e del Quaternario italiani.  
716 Palaeontographia Italica, 57(1962), 81-133.

Formatted: Not Highlight

717 Decima, A., Wezel, F.C., 1971. Osservazioni sulle evaporiti messiniane della Sicilia centro-  
718 meridionale. *Rivista mineraria siciliana* 130-132, 172-187.

719 Dettman, D.L., Dwyer, G.S., 2012. Biological and environmental controls on ostracod shell trace-  
720 element chemistry. In: D. J. Horne, J. Holmes, J. Rodriguez-Lazaro and F. Viehberg (Eds.).  
721 *Ostracoda as proxies for Quaternary climate change. Developments in Quaternary Sciences.*  
722 Elsevier, v. 17, 145-163.

723 Devriendt, L.S.J., 2011. Late Quaternary environment of paleolake Carpentaria inferred from the  
724 chemistry of ostracod valves. Master of Sciences Research Thesis, University of  
725 Wollongong, Australia, 175 pp. <http://ro.uow.edu.au/theses/3319/>

726 Faranda, C., Gliozzi, E., Cipollari, P., Grossi, F., Darbaş, G., Gürbüz, K., Nazik, A., Gennari, R.,  
727 Cosentino, D., 2013. Messinian paleoenvironmental changes in the easternmost  
728 Mediterranean Basin: Adana Basin, southern Turkey. *Turkish J Earth Sci* 22, 839-863.

729 Faure, G., Powell, J.L., 1972. *Strontium Isotope Geology.* Springer-Verlag, Berlin, 1-188.

730 Flecker, R., de Villiers, S., Ellam, R.M., 2002. Modelling the effect of evaporation on the salinity–  
731  $^{87}\text{Sr}/^{86}\text{Sr}$  relationship in modern and ancient marginal–marine systems: the Mediterranean  
732 Messinian Salinity Crisis. *Earth Planet. Sci. Lett.* 203 (1), 221– 233.

733 Flecker, R., Ellam, R.M., 2006. Identifying Late Miocene episodes of connection and isolation in  
734 the Mediterranean–Paratethyan realm using Sr isotopes. *Sediment. Geol.* 188–189, 189–203.

735 Frenzel, P., Schulze, I., Pint, A., 2011. Salinity dependant morphological variation in *Cyprideis*  
736 *torosa*. *Joansea Geologie und Paläontologie* 11, 59–61.

737 Frenzel, P., Schulze, I., Pint, A., 2012. Noding of *Cyprideis torosa* valves (Ostracoda) – a proxy for  
738 salinity? New data from field observations and a long-term microcosm experiment.  
739 *International Review of Hydrobiology* 97(4), 314–329.

740 Gliozzi, E., Grossi, F., 2008. Late Messinian Lago-mare ostracod palaeoecology: a correspondence  
741 analysis approach. *Palaeogeography, Palaeoclimatology, Palaeoecology* 264, 288-295.

Field Code Changed

- 742 Gouramanis, C., Wilkins, D., De Deckker, P., 2010. 6000 years of environmental changes recorded  
743 in Blue Lake, South Australia, based on ostracod ecology and valve chemistry.  
744 Palaeogeography, Palaeoecology, Palaeoclimatology 297, 223-237.
- 745 Griffin, D.L., 2002. Aridity and humidity: Two aspects of the late Miocene climate of North Africa  
746 and the Mediterranean. Palaeogeography, Palaeoclimatology, Palaeoecology 182, 65-91.
- 747 Griffiths, H.I., Holmes, J.A., 2000. Non-marine ostracods & Quaternary palaeoenvironments.  
748 Quaternary Research Association, Technical Guide 8, 1-179.
- 749 Grossi, F., Gennari, R., 2008. Palaeoenvironmental reconstruction across the Messinian/Zanclean  
750 boundary by means of ostracods and foraminifers: the Montepetra borehole (Northern  
751 Apennine, Italy). Atti del Museo Civico di Storia Naturale di Trieste 53(suppl), 67-88.
- 752 Grossi, F., Cosentino, D., Gliozzi, E., 2008. Palaeoenvironmental reconstruction of the late  
753 Messinian lago-mare successions in central and eastern Mediterranean using ostracod  
754 assemblages. Bollettino della Società Paleontologica Italiana 47(2), 131-146.
- 755 Guerra-Merchán, A., Serrano, F., Garcés, M., Gofas, S., Esu, D., Gliozzi, E., Grossi, F., 2010.  
756 Messinian Lago-Mare deposits near the Strait of Gibraltar (Malaga Basin, S Spain).  
757 Palaeogeography, Palaeoclimatology, Palaeoecology 285, 264-276.
- 758 Henderson, G. M., Martel, D. J., O'Nions, R. K., Shackleton, N. J., 1994. Evolution of seawater  
759  $^{87}\text{Sr}/^{86}\text{Sr}$  over the last 400 ka: the absence of glacial/interglacial cycles. Earth Planetary  
760 Sciences and Letters 128, 643-651.
- 761 Holmes, J., De Deckker, P., 2012. Introduction to ostracod shell chemistry and its application to  
762 Quaternary palaeoclimate studies. In: D. J. Horne, J. Holmes, J. Rodriguez-Lazaro and F.  
763 Viehberg (Eds.). Ostracoda as proxies for Quaternary climate change. Developments in  
764 Quaternary Sciences. Elsevier, v. 17, 131-144.
- 765 Howarth, R., McArthur, J.M., 1997. Statistics for Strontium Isotope Stratigraphy: a robust  
766 LOWESS fit to the marine Sr-isotope curve for 0 to 206 Ma, with look-up table for  
767 derivation of numeric age. J. Geol. 105, 441-456.

Formatted: Not Highlight

768 Hsü, K.J., Ryan, W.F.B., Cita, M.B., 1973. Late Miocene desiccation of the Mediterranean. *Nature*  
769 242, 240–244.

770 Iaccarino, S., Bossio, A., 1999. Paleoenvironment of uppermost Messinian sequences in the  
771 Western Mediterranean (sites 974, 975 and 978). In: Zahn, R., Comas, M.C., Klaus, A., et  
772 al. (Eds.), *Proceedings of Ocean Drilling Program, Scientific Results 161*, 529–541, College  
773 Station, Texas.

774 Jahn, A., Gamenick, I., Theede, H., 1996. Physiological adaptations of *Cyprideis torosa* (Crustacea,  
775 Ostracoda) to hydrogen sulphide. *Marine Ecology Progress Series* 142, 215–223.

776 Jones, B. and Manning, D.A.C., 1994. Comparison of geochemical indices used for the  
777 interpretation of paleoredox conditions in ancient mudstones. *Chemical Geology* 111, 111–  
778 129.

779 Keating, K.W., Hawkes, I., Holmes, J.A., Flower, R.J., Leng, M.J., Abu-Zied, R.H., Lord, A.R.,  
780 2007. Evaluation of ostracod-based palaeoenvironmental reconstruction with instrumental  
781 data from the arid Faiyum Depression. *Egyptian Journal of Paleolimnology* 38, 261–283.

782 Keogh, S.M., Butler, R.W.H., 1999. The Mediterranean water body in the late Messinian:  
783 interpreting the record from marginal basins on Sicily. *J. Geol. Soc. (Lond.)* 156, 837–846.

784 Keyser, D., 2005. Histological peculiarities of the nodding process in *Cyprideis torosa* (Jones)  
785 (Crustacea, Ostracoda). *Hydrobiologia* 538, 95–106.

786 Keyser, D., Aladin, N., 2004. Noding in *Cyprideis torosa* and its causes. *Studia Quaternaria* 2, 19–  
787 24.

788 Ligios, S., Anadón, P., Castorina, F., D’Amico, C., Esu, D., Gliozzi, E., Gramigna, P., Mola, M.,  
789 Monegato, G., 2012. Ostracoda and Mollusca biodiversity and hydrochemical features of  
790 Late Miocene brackish basins of Italy. *Geobios* 45, 351–367.

791 Ligios, S., Gliozzi, E., 2012. The genus *Cyprideis* Jones, 1857 (Crustacea, Ostracoda) in the  
792 Neogene of Italy: A geometric morphometric approach. *Revue de micropaléontologie* 55,  
793 171–207.

Formatted: Not Highlight

- 794 Mangini, A., Jung, M., Laukenmann, S., 2001. What do we learn from peaks of uranium and of  
795 manganese in deep sea sediments? *Marine Geology* 177(1), 63-78.
- 796 Manzi, V., Lugli, S., Roveri, M., Schreiber, C., 2009. A new facies model for the Upper Gypsum of  
797 Sicily (Italy): chronological and palaeoenvironmental constraints for the Messinian salinity  
798 crisis in the Mediterranean. *Sedimentology* 56, 1937-1960.
- 799 Manzi, V., Gennari, R., Lugli, S., Roveri, M., Scafetta, N., Schreiber, B.C., 2012. High-frequency  
800 cyclicity in the Mediterranean Messinian evaporites: evidence for solar-lunar climate  
801 forcing. *Journal of Sedimentary Research* 82, 991-1005.
- 802 Manzi, V., Gennari, R., Hilgen, F., Krijgsman, W., Lugli, S., Roveri, M., Sierro F.J., 2013. Age  
803 refinement of the Messinian salinity crisis onset in the Mediterranean. *Terra Nova*, doi:  
804 10.1111/ter.12038
- 805 Marco-Barba, J., 2010. Freshwater ostracods ecology and geochemistry as paleoenvironmental  
806 indicators in marginal marine ecosystems: a case of study the Albufera of Valencia. Ph. D.  
807 thesis, Univ. of Valencia.
- 808 McArthur, J.M., Howarth, R.J., Bailey T.R., 2001. Strontium isotope stratigraphy: LOWESS  
809 version 3: Best fit to the marine Sr-isotope curve for 0-509 Ma and accompanying look-up  
810 table for deriving numerical age. *Journal of Geology* 109, 155-170.
- 811 McCulloch, M.T., De Deckker, P., 1989. Sr-isotope constraints on the Mediterranean environment  
812 at the end of the Messinian salinity crisis. *Nature* 342, 63- 65.
- 813 Müller, D.W., Mueller, P.A., 1991. Origin and age of the Mediterranean Messinian evaporites:  
814 implications from Sr isotopes. *Earth Planet. Sci. Lett.* 107, 1 -12.
- 815 Müller, D.W., Mueller, P.A., McKenzie, J.A., 1990. Strontium isotopic ratios as fluid tracers in  
816 Messinian evaporites of the Tyrrhenian sea (western Mediterranean sea). *Proc. ODP Sci.*  
817 *Res.* 107, 603-614.

Field Code Changed

818 Neale, J.V., 1988. Ostracods and paleosalinity reconstruction. In: De Deckker, P., Colin, J.-P.,  
819 Peypouquet, J.-P. (Eds.), Ostracoda in the Earth Sciences. Elsevier, Amsterdam, pp. 125–  
820 155.

821 Pattan, J.N., Pearce, N.J.G., 2009. Bottom water oxygenation history in southeastern Arabian Sea  
822 during the past 140 ka: Results from redox-sensitive elements. *Palaeogeography,*  
823 *Palaeoclimatology, Palaeoecology* 280(3-4), 396-405.

824 Pint, A., Frenzel, P., Fuhrmann, R., Scharf, B., Wennrich, V., 2012. Distribution of *Cyprideis*  
825 *torosa* (Ostracoda) in Quaternary atlantic sediments in Germany and its application for  
826 palaeoecological reconstructions. *International Review of Hydrobiology* 97(4), 330-335.

827 Pint, A., Melzer, S., Frenzel, P., Engel, M., Brückner, H., 2013. Monospecific occurrence of  
828 *Cyprideis torosa* associated with micro- and macrofauna of marine origin in sabkha  
829 sediments of the Northern Arabian Peninsula. *Naturalista Siciliano* 4, 37(1), 277-278.

830 Radeff, G., Schildgen, T.F., Cosentino, D., Strecker, M.R., Cipollari, P., Darbaş, G., Gürbüz, K.,  
831 (submitted). Sedimentary evidence for late Miocene uplift of the SE margin of the central  
832 Anatolian Plateau: Adana Basin, Southern Turkey. *Geological Society of America Bulletin*.

833 Rosenfeld, A., Vesper, B., 1977. The variability of the sieve-pores in recent and fossil species of  
834 *Cyprideis torosa* (Jones, 1850) as an indicator for salinity and paleosalinity. In: Löffler, H.,  
835 Danielopol, D. (Eds.), *Aspects of ecology and zoogeography of recent and fossil Ostracoda*.  
836 Junk Publishers, The Hague, 55–67.

837 Rosenfeld, A., 1977. The Sieve-pores of *Cyprideis torosa* (Jones, 1850) from the Messinian  
838 Mavqi'im Formation in the Coastal Plain and Continental Shelf of Israel as an Indicator of  
839 Paleoenvironment. *Israel Journal of Earth-Sciences* 26, 89-93.

840 Rossi, V., Amorosi, A., Sammartino, I., Sarti, G., 2013. Environmental changes in the lacustrine  
841 ancient harbour of Magdala (Kinneret Lake, Israel) inferred from ostracod, geochemical and  
842 sedimentological analyses. *Naturalista Siciliano* 4, 37(1), 331-332.

843 Roveri, M., Flecker, R., Krijgsman, W., Lofi, J., Lugli, S., Manzi, V., Sierro, F.J., Bertini, A.,  
844 Camerlenghi, A., De Lange, G., Govers, R., Hilgen, F.J., Hübscher, C., Meijer, P.Th.,  
845 Stoica, M., 2014a. The Messinian Salinity Crisis: Past and future of a great challenge for  
846 marine sciences. *Marine Geology* 352, 25-58.

847 Roveri, M., Lugli, S., Manzi, V., Gennari, R., Schreiber, B.C., 2014b. High-resolution strontium  
848 isotope stratigraphy of the Messinian deep Mediterranean basins: Implications for marginal  
849 to central basins correlation, *Marine Geology*, doi: [10.1016/j.margeo.2014.01.002](https://doi.org/10.1016/j.margeo.2014.01.002)

850 Sampalmieri, G., Iadanza, A., Cipollari, P., Cosentino, D., Lo Mastro, S., 2010.  
851 Palaeoenvironments of the Mediterranean Basin at the Messinian hypersaline/hyposaline  
852 transition: evidence from natural radioactivity and microfacies of post-evaporitic  
853 successions of the Adriatic sub-basin. *Terra Nova* 22, 239-250.

854 Sandberg, P., 1964. The ostracod genus *Cyprideis* in the Americas. *Stockholm Contributions in*  
855 *Geology* 12, 1-178.

856 Schäfer, H.W., 1953. Über Meeres- und Brackwasserostacoden aus dem Deutschen Küstengebiet  
857 mit 2. Mitteilung über die Ostracodenfauna Griechenlands. *Hydrobiologia* 5(4), 351-389.

858 Schreiber, B.C., 1997. Field trip to Eraclea Minoa: Upper Messinian. "Neogene Mediterranean  
859 Paleooceanography". Excursion Guide Book Palermo-Caltanissetta Agrigento. Erice (Sicily),  
860 24-27 September 1997, 72-80.

861 Talbot, M.R., 1990. A review of the palaeohydrological interpretation of carbon and oxygen  
862 isotopic ratios in primary lacustrine carbonates. *Chemical Geology (Isot. Geosci. Sect.)* 80,  
863 261-279.

864 Testa, G., 1995. Upper Miocene extensional tectonics and synrift sedimentation in the western  
865 sector of the Volterra Basin (Tuscany, Italy). *Studi Geologici Camerti vol. spec. 1*, 617-630.

866 Utrilla, R., Vazquez, A., Anadón, P., 1998. Paleohydrology of the Upper Miocene Bicorn Lake (E  
867 Spain) as inferred from stable isotopic data from inorganic carbonates. *Sedimentary*  
868 *Geology* 121, 191-206.

Formatted: Not Highlight

- 869 Van Couvering, J.A., Castradori, D., Cita, M.B., Hilgen, F.J., Rio, D., 2000. The base of the  
870 Zanclean Stage and of the Pliocene Series. *Episodes* 23(3), 179-187.
- 871 Van der Laan, E., Snel, E., de Kaenel, E., Hilgen, F.J., Krijgsman, W., 2006. No major deglaciation  
872 across the Miocene-Pliocene boundary: integrated stratigraphy and astronomical tuning of  
873 the Loulja sections (Bou Regreg area, NW Morocco). *Paleoceanography* 21, PA3011,  
874 doi:10.1029/2005PA001193.
- 875 Van Harten, D., 1996. *Cyprideis torosa* (Ostracoda) revisited. Of salinity, nodes and shell size. In:  
876 Keen, C. (Ed.), *Proceedings of the second European Ostracodologists Meeting*. British  
877 Micropalaeontological Society, London, pp. 191–194.
- 878 Van Harten, D., 2000. Variable nodding in *Cyprideis torosa* (Ostracoda, Crustacea): an overview,  
879 experimental results and a model from Catastrophe Theory. *Hydrobiologia* 419, 131–139.
- 880 Venice Symposium on the Classification of Brackish Waters, Venice 8-14 April 1958 in Remane,  
881 A., Schlieper, C. (eds.), *Die Biologie der Brackwassers*. Schweizerbartsche Verlag,  
882 Stuttgart, 1-348.
- 883 Vesper, B., 1975. To the problem of nodding on *Cyprideis torosa* (Jones, 1850). In: Swain, F.,  
884 Kornicker, L.S., Lundin, R.F. (Eds.), *Biology and Paleobiology of Ostracoda*. *Bulletin of*  
885 *American Paleontology* 65(282), 205-216.
- 886 Voltaggio, M., Branca, M., Tedesco, D., Tuccimei, P., Di Pietro, L., 2004. <sup>226</sup>Ra-excess during the  
887 1631-1944 activity period of Vesuvius (Italy): a model of alpha recoil enrichment in a  
888 metasomatized mantle and implications on the current state of the magmatic system.  
889 *Geochimica et Cosmochimica Acta* 68, 167-181.
- 890 Wignall, P.B., 1994. *Black Shales*. Claredon Press, Oxford, 127 pp.
- 891 Wignall, P.B., Myers, K.J., 1988. Interpreting benthic oxygen levels in mudrocks: anew approach.  
892 *Geology* 16, 452-455.

Formatted: Not Highlight



893 | Zheng, Y., Anderson, R.F., Van Geen, A., Fleisher, M.Q., 2002. Remobilization of authigenic  
894 | uranium in marine sediments by bioturbation. *Geochimica et Cosmochimica Acta* 66 (10),  
895 | 1759–1772.

896

897

898 FIGURE CAPTIONS

899  
900 Fig. 1 – SEM pictures of *Cyprideis agrigentina* Decima. a. male left valve, sample EM 8-3; b. male  
901 right valve, sample EM 7-2; c. female left valve, sample EM 7-2; d. female right valve, sample EM  
902 8-3. White bar corresponds to 0.1 mm.

903  
904 Fig. 2 – Geographical location of the Eraclea Minoa section.

905  
906 Fig. 3 – Panoramic view of the Eraclea Minoa section. In evidence the gypsum levels of the Upper  
907 Gypsum Unit from gypsum body 3 to gypsum body 6 (marked by numbers) and the  
908 Messinian/Zanclean boundary.

909  
910 Fig. 4 – Simplified stratigraphic log of the Eraclea Minoa section (modified from Manzi et al.,  
911 2009). Legend: 1. sapropels; 2. clays; 3. sandstones/sandy levels; 4. microconglomerate levels; 5.  
912 marls; 6. gypsum bodies (Upper Gypsum Unit); 7. samples for paleontological analyses; 8. samples  
913 for morphometrical analyses (ornamentation, dimensions and percentage of sieve-pore shapes) on  
914 *C. agrigentina* valves; 9. samples for stable isotopes analyses on *C. agrigentina* valves; 10. samples  
915 for trace elements analyses on *C. agrigentina* valves; 11. samples for Sr-isotopes analyses on *C.*  
916 *agrigentina* valves; 12. samples for NRD analyses on marls.

917  
918 Fig. 5 – Stable isotopes, trace and minor elements,  $^{87}\text{Sr}/^{86}\text{Sr}$ , and authigenic uranium curves plotted  
919 against the stratigraphic log of the Eraclea Minoa section. For the descriptions of the intervals, see  
920 the text.

921  
922 Fig. 6 - Stable isotopic composition ( $\delta^{13}\text{C}$  and  $\delta^{18}\text{O}$ ; PDB notation) of *Cyprideis agrigentina* calcite  
923 valves (Table 1). Note the negative correlation and regression line for samples from interval lower

Formatted: Not Highlight

Formatted: Not Highlight

924 B. The larger variation of  $\delta^{13}\text{C}$  and  $\delta^{18}\text{O}$  along the regression line corresponds to samples EM 6''-8  
925 (198.2 m) to 6''-20 (216 m) from lower interval B. E/P: Evaporation /Precipitation ratio; PP:  
926 Primary productivity; Eq-Atm: Atmospheric  $\text{CO}_2$  equilibrium. See also Fig. 4.

927

928

929 Fig. 7 – Results of the morphometrical analyses (mean lengths, percentages of sieve-pore shape and  
930 ornamentation/noding) performed on *Cyprideis agrigentina* adult valves, plotted against the  
931 stratigraphic log of the Eraclea Minoa section.

932

933 Fig. 8 - Comparisons among the palaeosalinity curve inferred by the analysis of the percentages of  
934 the sieve-pore shape on *Cyprideis agrigentina* and the palaeoenvironmental and  
935 palaeohydrochemistry changes inferred from synecological and Shannon-Wiener and geochemical  
936 proxies.

937

938 Fig. 9 - Principal Component Analysis (PCA) plot of the scores of the eigenvectors for the variables  
939 listed in Table 3. Abbreviations: N pores: variability of percentage of sieve pores (rounded sieve  
940 pores assumed as a proxy of salinity), Position: stratigraphic position of the samples, Sr isot:  
941  $^{87}\text{Sr}/^{86}\text{Sr}$  values. See the text for discussion.

942

943 Fig. 10 - Tree diagram for the considered variables defining the relationships between the groups of  
944 variables. Ward's method, 1-Pearson r. Abbreviations as in Fig. 8. See the text for discussion.

945

946  
947  
948  
949  
950  
951  
952  
953  
954  
955  
956  
957  
958  
959  
960  
961  
962  
963  
964  
965  
966

#### TABLE CAPTIONS

Table 1 – Stratigraphic position and lithology of the samples, and geochemical analytical results from *C. agrigentina* valves: stable isotope data ( $\delta^{13}\text{C}$  and  $\delta^{18}\text{O}$ ; PDB notation), Mg/Ca<sub>v</sub>, Sr/Ca<sub>v</sub>, and Na/Ca<sub>v</sub> in molar ratios, and  $^{87}\text{Sr}/^{86}\text{Sr}$  ratios.

Table 2 – Summary of natural radioactivity data, with the concentrations of U, Th and K (with relative errors), values of authigenic uranium expressed in ppm and percentage and Th/U ratios.

Table 3 – Correlation matrix for the data in Table 1 and Th/U ratios (9 variables, 20 samples). The correlation coefficient *r* between the diverse variables is shown in the upper part of each division. The *p* value is indicated in the lower part of each division. The *r* values are in bold when the correlation is significant  $p < 0.01$ . Abbreviations: N pores: variability of percentage of sieve pores (rounded sieve pores assumed as a proxy of salinity), Position: stratigraphic position of the samples, Sr isot:  $^{87}\text{Sr}/^{86}\text{Sr}$  values.

Formatted: Not Highlight

Figure 1  
[Click here to download high resolution image](#)

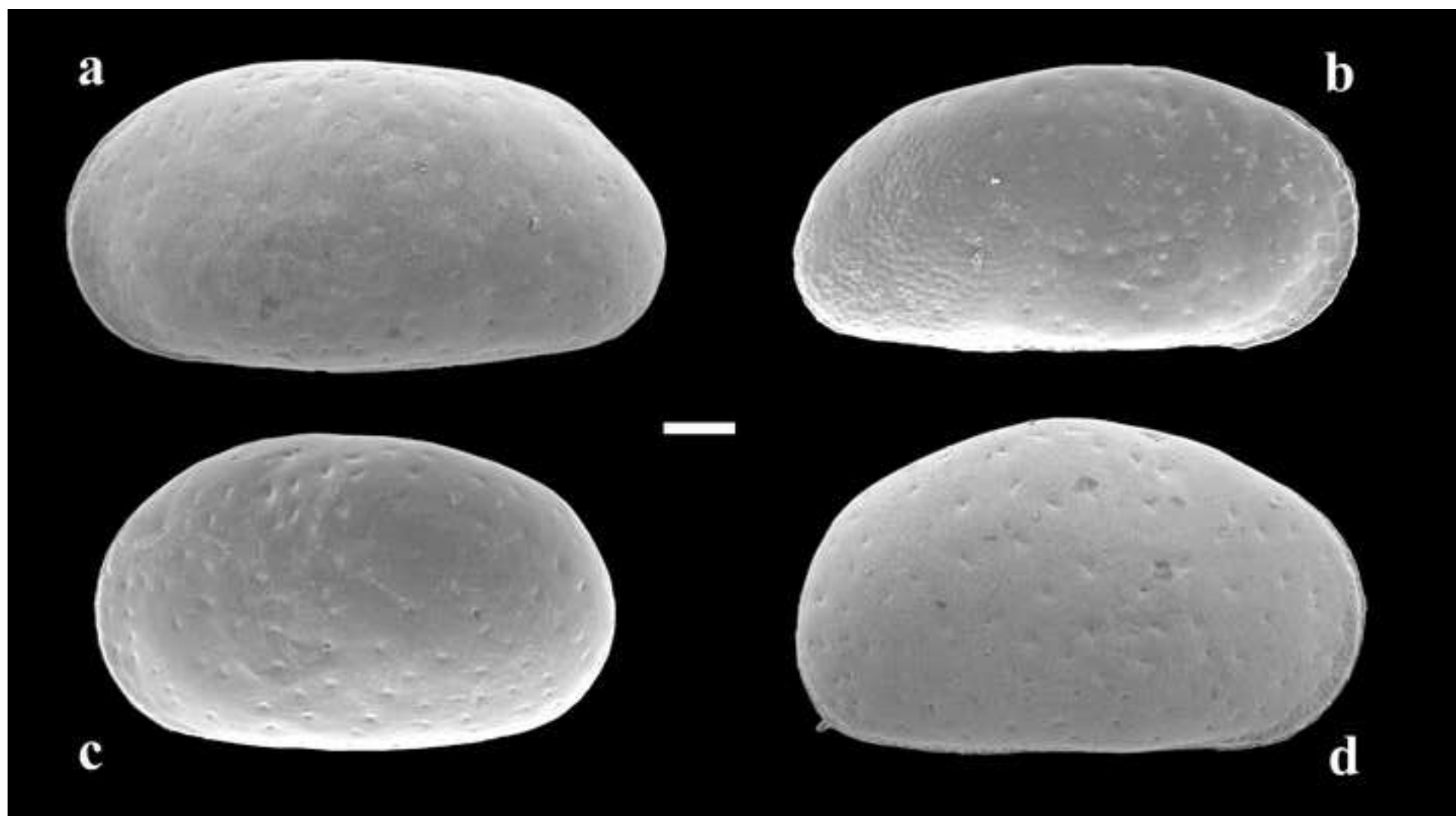


Figure 2  
[Click here to download high resolution image](#)



**Figure 3**  
[Click here to download high resolution image](#)



Figure 4  
[Click here to download high resolution image](#)

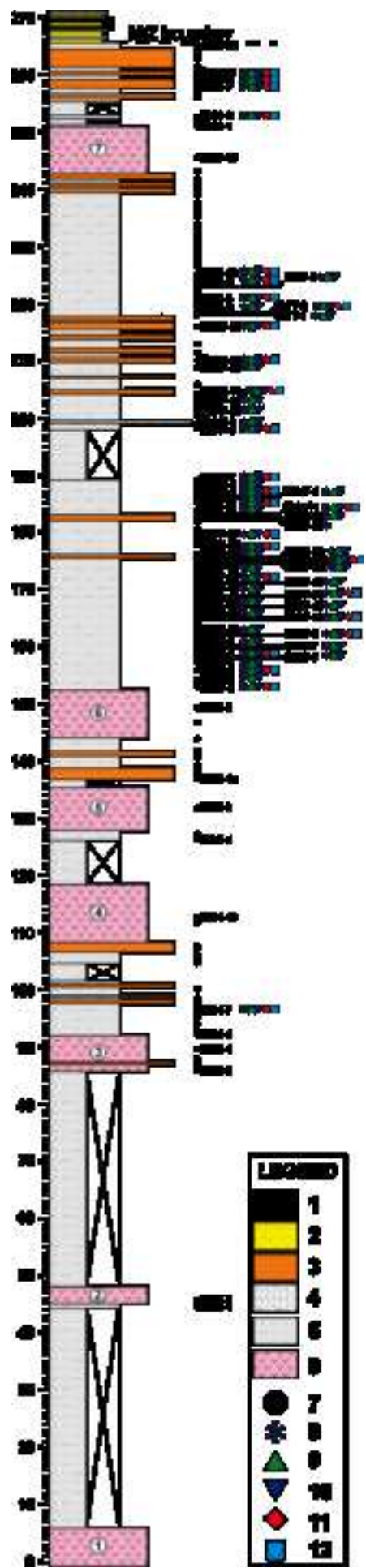




**Figure 5**  
[Click here to download high resolution image](#)

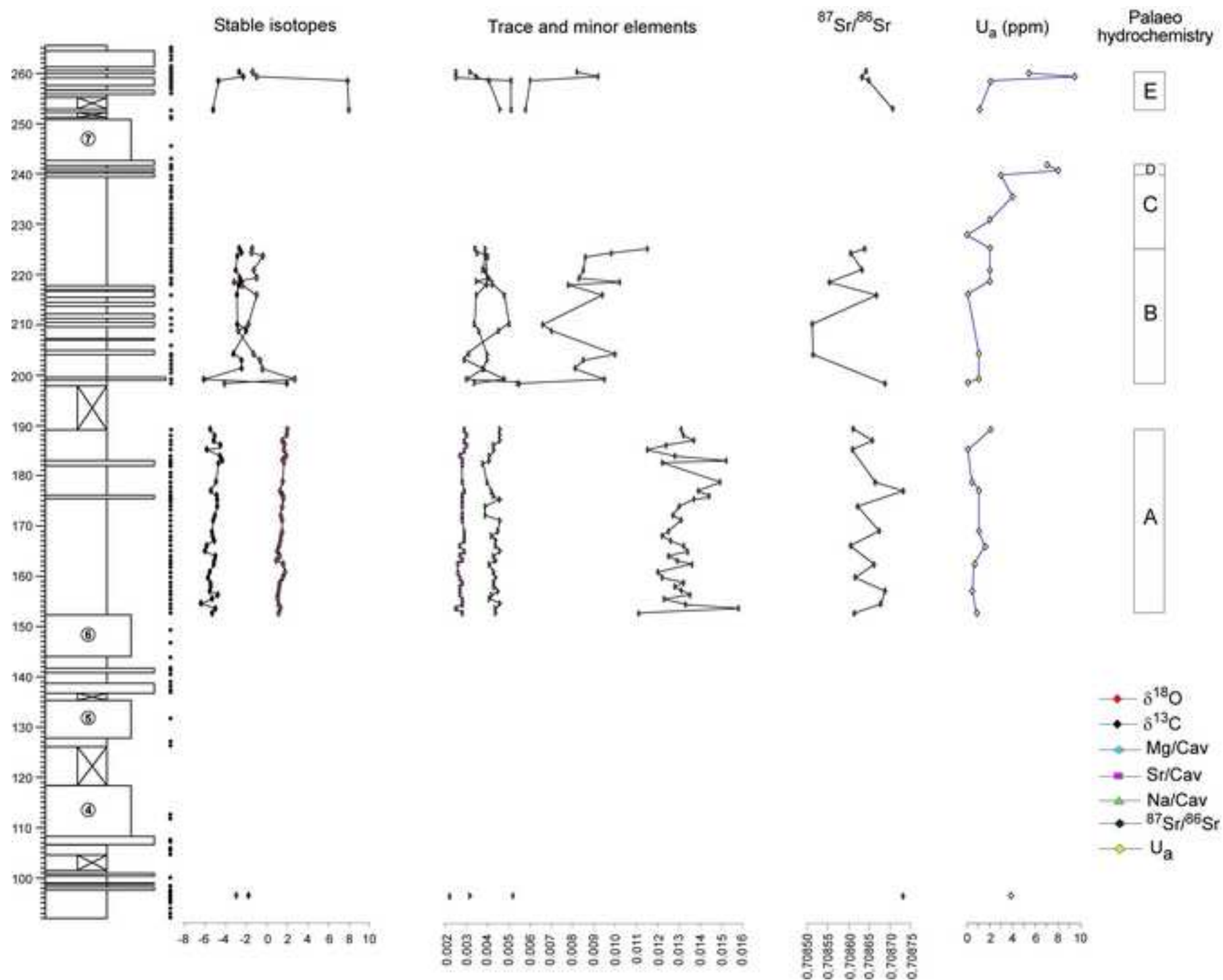


Figure 6  
[Click here to download high resolution image](#)

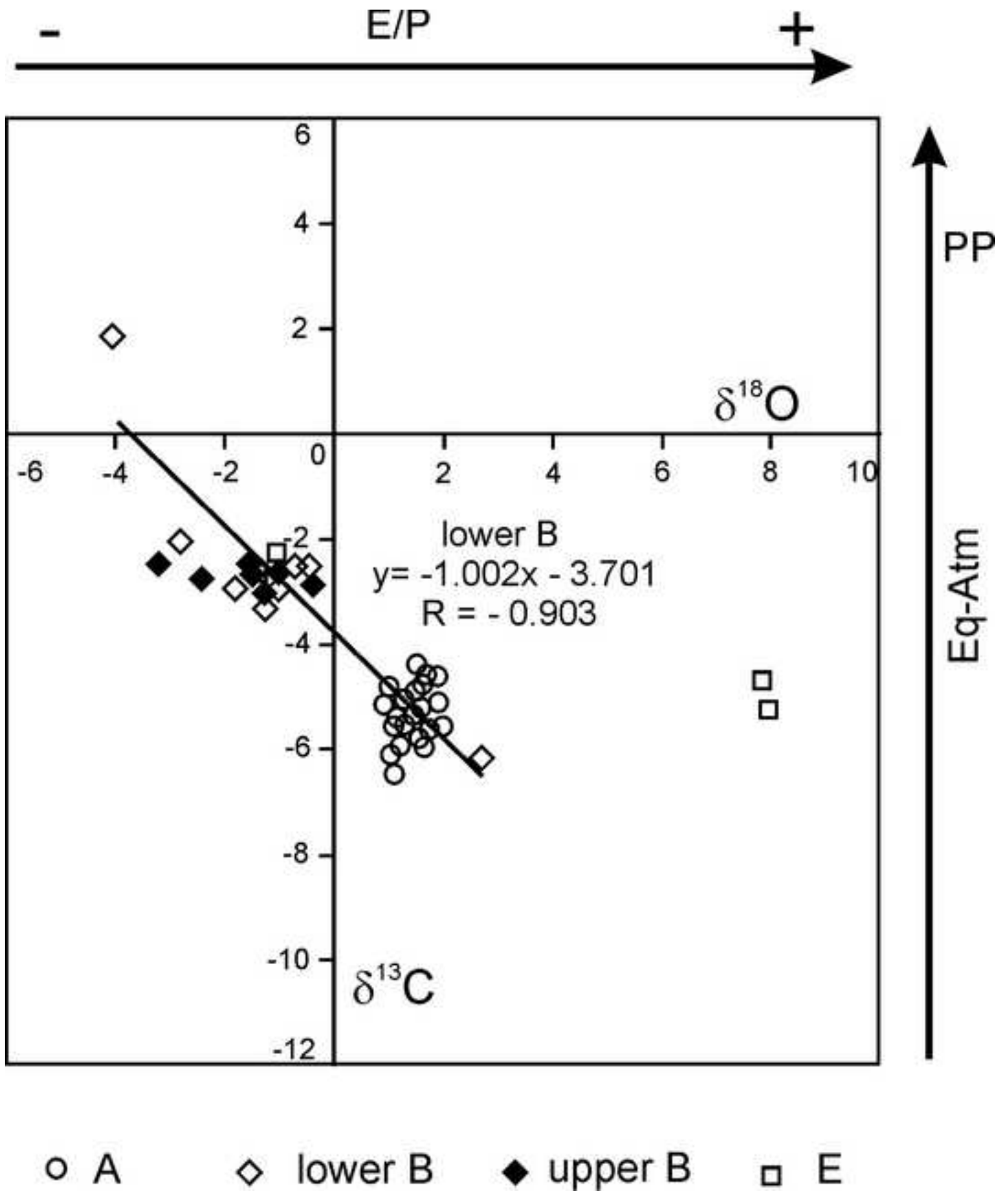
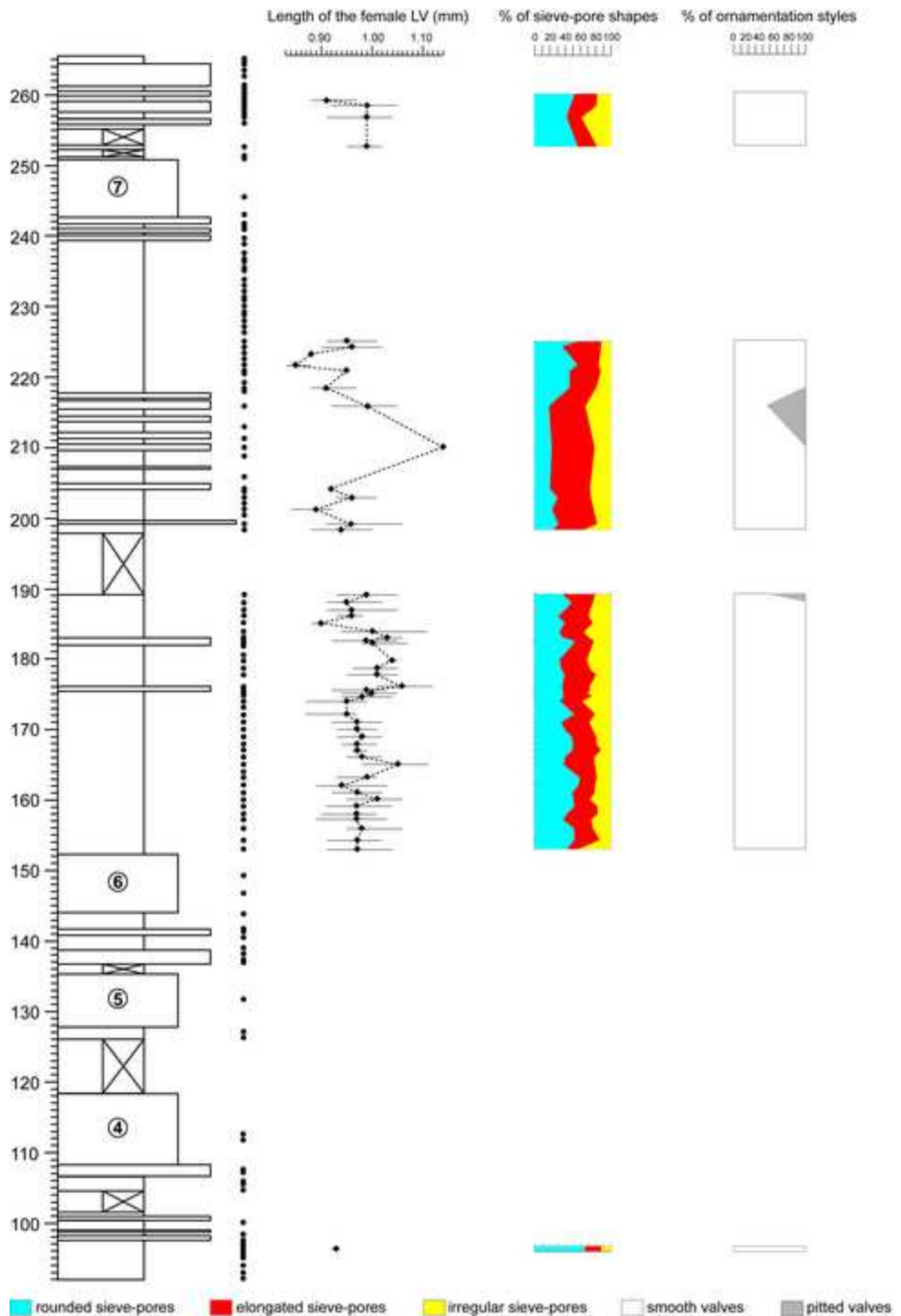


Figure 7

[Click here to download high resolution image](#)



**Figure 8**  
[Click here to download high resolution image](#)

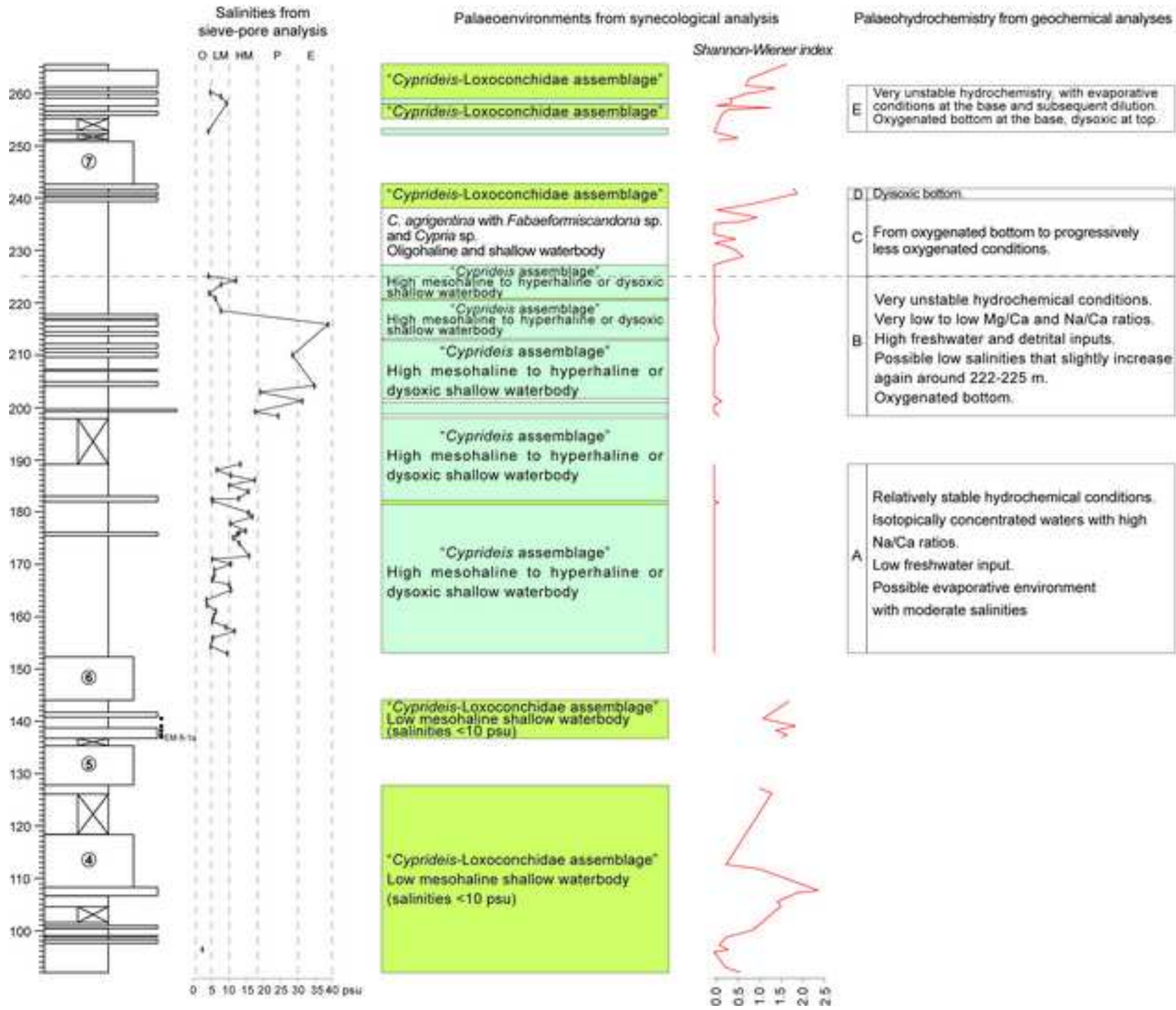


Figure 9  
[Click here to download high resolution image](#)

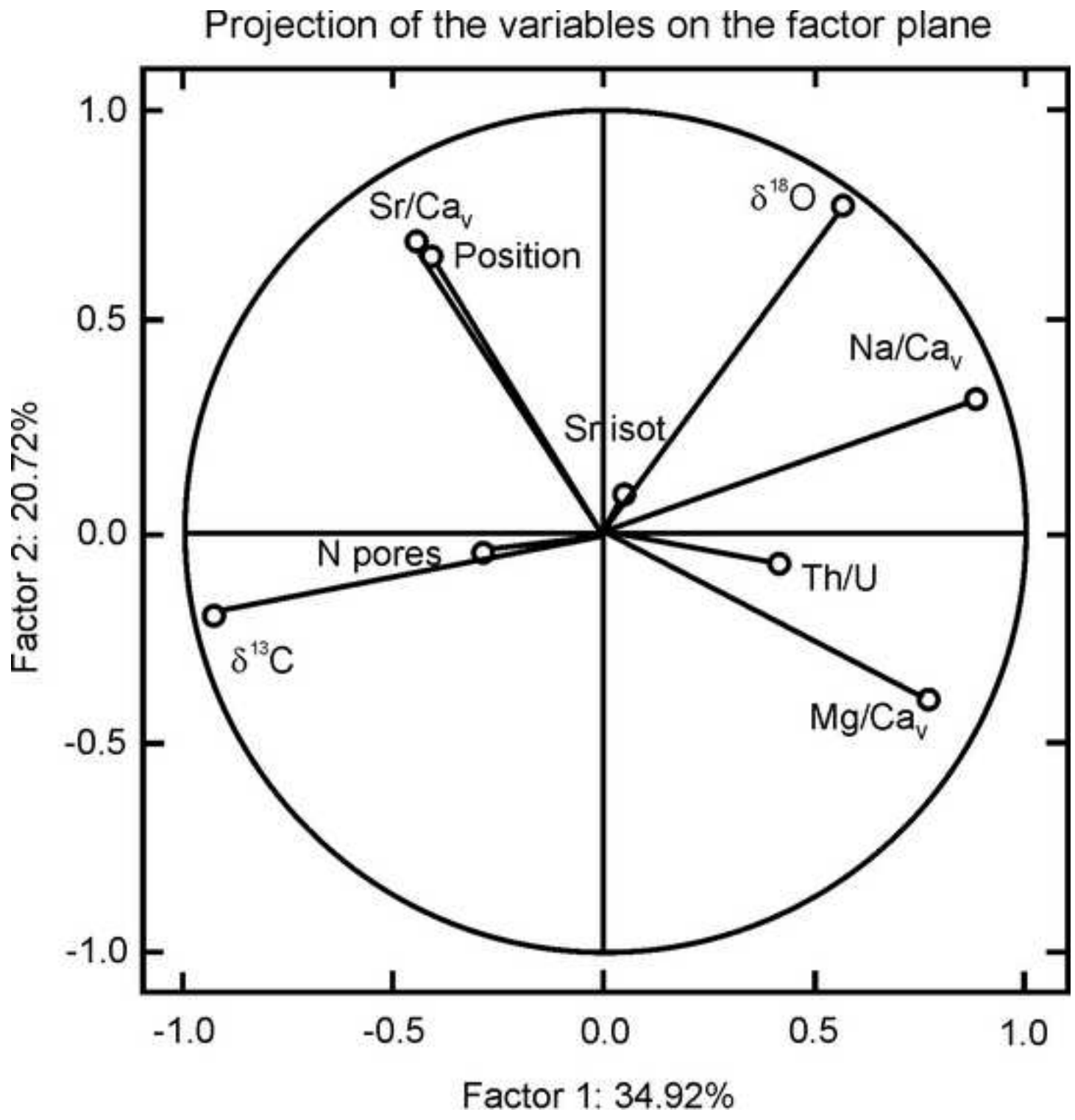


Figure 10  
[Click here to download high resolution image](#)

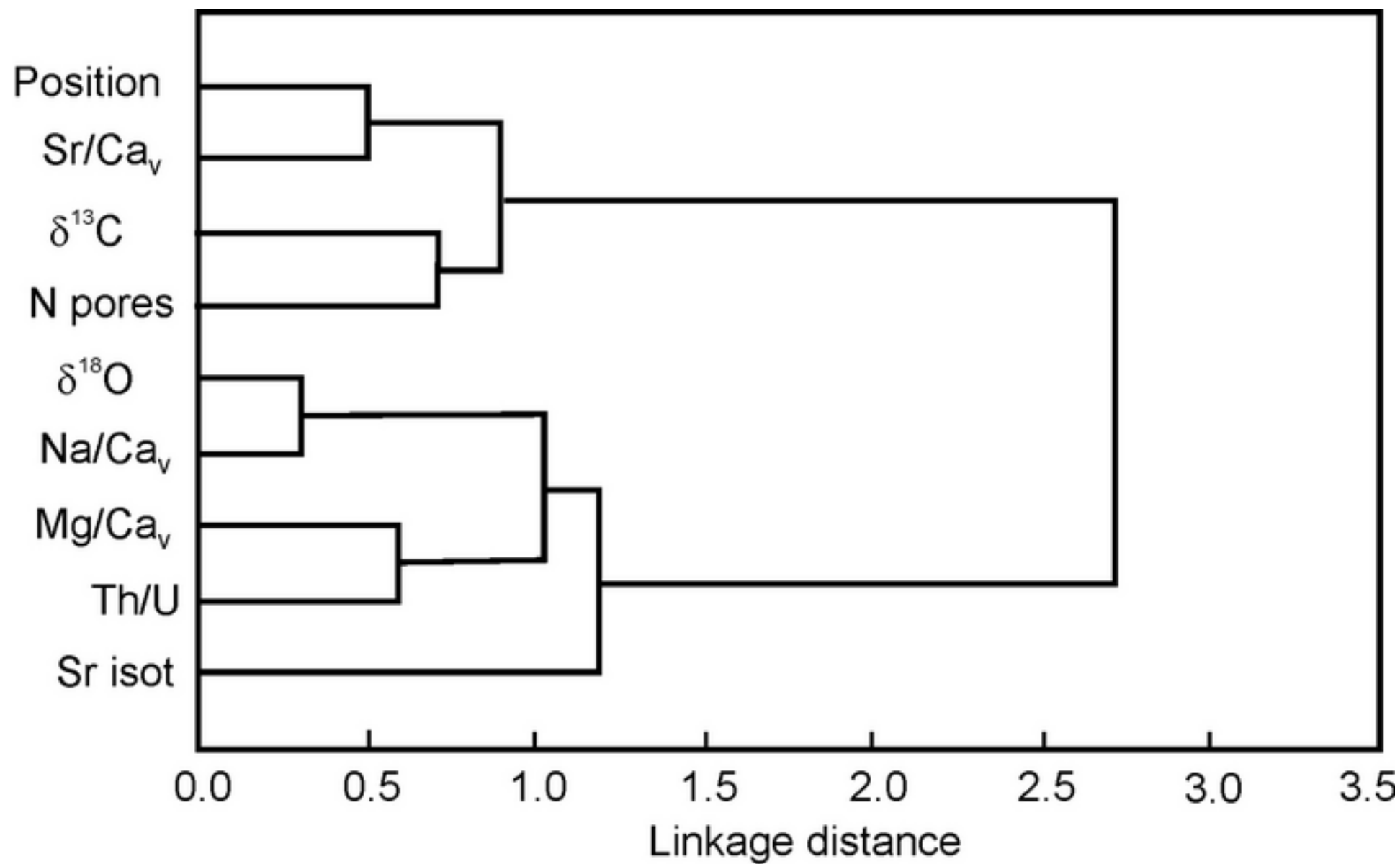


Table 1

Height (m)	Sample	Lithology	Stable Isotopes (n. of valves)	d <sup>13</sup> C (VPDB)	d <sup>18</sup> O (VPDB)	Trace elements (n. of valves)	Me/Ca molar			87Sr/86Sr ±se*
							Mg/Cav	Sr/Cav	Na/Cav	
259.1	EM 8-11	sandstone	8	-2.68	-1.37	10	0.0082	0.0025	0.0032	0.708640 ±6
258.5	EM 8-9	marl	8	-2.29	-1.02	10	0.0092	0.0025	0.0035	0.708630 ±8
257.8	EM 8-7	sandstone	8	-4.70	7.83	10	0.0060	0.0051	0.0041	0.708647 ±10
252.8	EM 8-3	marl	8	-5.24	7.95	10	0.0058	0.0051	0.0046	0.708704 ±7
225.0	EM 7-10	marl	8	-2.67	-1.44	10	0.0115	0.0034	0.0039	0.708637 ±11
224.3	EM 7-9	marl	8	-2.47	-1.52	10	0.0098	0.0035	0.0039	0.708602 ±2
223.5	EM 7-8	marl	8	-2.87	-0.37	8	0.0086	0.0040	0.0039	
220.9	EM 7-5	marl	8	-3.01	-1.27	9	0.0085	0.0039	0.0038	0.708629 ±7
219.1	EM 7-3	marl	8	-2.63	-0.98	9	0.0083	0.0040	0.0041	
218.5	EM 7-2	marl	8	-2.46	-3.20	10	0.0102	0.0042	0.0035	0.708552 ±9
218.0	EM 7-1	marl	8	-2.76	-2.40	9	0.0078	0.0042	0.0040	
216.0	EM 6"-20	sandstone	8	-2.92	-1.01	8	0.0094	0.0048	0.0035	0.708666 ±10
210.0	EM 6"-17	sandstone	8	-2.88	-1.79	7	0.0066	0.0050	0.0034	0.708510 ±7
208.9	EM 6"-16	marl	8	-2.00	-2.81	8	0.0070	0.0045	0.0036	
204.2	EM 6"-14a	marl	8	-3.27	-1.26	8	0.0100	0.0031	0.0040	0.708511 ±6
203.0	EM 6"-13	marl	8	-2.46	-0.69	8	0.0085	0.0029	0.0040	
201.1	EM 6"-11	marl	8	-2.48	-0.43	8	0.0081	0.0038	0.0038	
199.2	EM 6"-9	gravel	8	-6.14	2.72	10	0.0095	0.0030	0.0048	
198.2	EM 6"-8	marl	8	1.91	-4.08	10	0.0055	0.0054	0.0034	0.708685 ±11
189.0	EM 6"-7	marl	8	-5.53	1.99	8	0.0131	0.0029	0.0046	0.708609 ±7
188.0	EM 6"-6	marl	8	-5.08	1.93	8	0.0132	0.0030	0.0046	
187.0	EM 6"-5	marl	8	-5.20	1.46	8	0.0137	0.0029	0.0046	0.708654 ±9
186.0	EM 6"-4	marl	8	-4.56	1.69	9	0.0124	0.0030	0.0043	
185.0	EM 6"-3	marl	8	-5.88	1.65	8	0.0115	0.0029	0.0043	0.708608 ±9
183.9	EM 6"-2	marl	8	-4.57	1.90	8	0.0128	0.0027	0.0041	
183.1	EM 6"-1	marl	8	-4.35	1.52	6	0.0152	0.0028	0.0041	
182.8	EM 6'-31	sandstone	8	-4.74	1.63	8	0.0122	0.0028	0.0038	
180.0	EM 6'-27	marl	8	-4.93	1.55	9	0.0149	0.0028	0.0040	0.708663 ±7
177.8	EM 6'-25	marl	8	-5.44	1.33	10	0.0139	0.0029	0.0042	0.708729 ±10
176.0	EM 6'-24	marl	8	-4.89	1.55	8	0.0144	0.0028	0.0043	
175.5	EM 6'-23	sandstone	8	-4.82	1.58	7	0.0137	0.0028	0.0046	
175.1	EM 6'-22b	sandstone	8	-4.83	1.49	8	0.0130	0.0028	0.0039	0.708619 ±6
174.6	EM 6'-22	marl	8	-5.08	1.38	8	0.0127	0.0028	0.0039	
173.9	EM 6'-21	marl	8	-5.25	1.46	7	0.0131	0.0028	0.0046	
172.0	EM 6'-19	marl	8	-5.35	1.50	7	0.0125	0.0029	0.0045	0.708671 ±6
171.0	EM 6'-18	marl	8	-5.27	1.39	7	0.0122	0.0029	0.0042	
169.9	EM 6'-17	marl	8	-5.15	1.29	9	0.0126	0.0029	0.0044	
169.0	EM 6'-16	marl	8	-5.87	1.21	8	0.0132	0.0027	0.0044	0.708602 ±7
168.0	EM 6'-15	marl	8	-6.05	1.05	8	0.0134	0.0029	0.0046	
167.0	EM 6'-14	marl	8	-5.02	1.28	8	0.0125	0.0027	0.0043	
166.0	EM 6'-13	marl	8	-5.13	0.94	8	0.0129	0.0028	0.0044	
165.0	EM 6'-12	marl	8	-5.17	1.57	8	0.0136	0.0026	0.0041	0.708658 ±9
163.0	EM 6'-10	marl	8	-5.60	1.76	8	0.0120	0.0026	0.0043	
162.0	EM 6'-9	marl	8	-5.74	1.56	8	0.0122	0.0027	0.0044	0.708614 ±6
161.0	EM 6'-8	marl	8	-5.52	1.28	9	0.0132	0.0028	0.0043	
160.0	EM 6'-7	marl	8	-5.48	1.17	7	0.0128	0.0027	0.0043	
159.1	EM 6'-6	marl	8	-5.55	1.12	8	0.0131	0.0027	0.0045	0.708685 ±5
158.0	EM 6'-5	marl	8	-4.80	1.02	8	0.0135	0.0027	0.0042	
157.1	EM 6'-4	marl	8	-5.35	1.07	9	0.0123	0.0028	0.0041	
156.0	EM 6'-3	marl	8	-6.40	1.12	8	0.0133	0.0028	0.0046	0.708675 ±10
154.3	EM 6'-2	marl	8	-5.00	1.30	7	0.0158	0.0025	0.0044	
153.0	EM 6'-1	marl	8	-5.34	1.14	6	0.0111	0.0028	0.0044	0.708612 ±11
96.2	EM 4-7	marl	8	-1.81	-3.00	7	0.0052	0.0022	0.0032	0.708729 ±10

Table 2

[Click here to download Table: Table 2 - NRD corrected.xls](#)

Table 2

Height (m)	Sample	U (mean) (ppm)	Th		K		U <sub>aut</sub> (ppm)	U <sub>aut</sub> (%)	Th/U
			(ppm)	error (%)	%	error (%)			
260.4	EM 8-11	6.7	5.3	0.1	0.96	0.03	5.4	81	0.8
259	EM 8-9	11.7	8.7	0.1	1.76	0.03	9.5	81	0.7
257.8	EM 8-7	4.7	9.0	0.1	1.88	0.03	2.5	53	1.9
252.8	EM 8-3	4.0	9.0	0.1	1.99	0.03	1.8	45	2.3
241.8	EM 7-33	8.5	4.4	0.1	0.76	0.02	7.4	87	0.5
240.9	EM 7-31	10.1	7.8	0.1	1.56	0.03	8.2	81	0.8
239.8	EM 7-28	5.0	7.9	0.1	1.66	0.03	3.0	61	1.6
236.2	EM7-24	5.7	6.8	0.1	1.47	0.03	4.0	70	1.2
230.9	EM 7-17	4.4	9.3	0.1	1.91	0.03	2.1	48	2.1
228	EM7-13	2.8	10.1	0.1	1.90	0.03	0.3	11	3.6
225	EM 7-10	4.6	10.0	0.1	2.00	0.03	2.1	46	2.2
220.9	EM 7-5	4.7	10.3	0.1	2.11	0.04	2.1	45	2.2
218.5	EM 7-2	4.5	9.8	0.1	1.80	0.03	2.0	44	2.2
216	EM 6"-20	3.1	9.5	0.1	2.02	0.03	0.7	23	3.1
204.5	EM 6"-14a	3.4	8.8	0.1	1.83	0.03	1.2	35	2.6
199.0	EM 6"-9	2.7	5.8	0.1	0.81	0.03	1.3	48	2.1
198.5	EM 6"-8	3.1	10.2	0.1	1.93	0.03	0.6	19	3.3
189.0	EM 6"-7	4.5	8.3	0.1	1.60	0.03	2.5	56	1.8
185	EM 6"-3	3.1	9.7	0.1	1.83	0.03	0.7	22	3.1
180	EM 6"-27	2.4	8.0	0.1	1.92	0.03	0.4	17	3.3
178	EM 6"-25	3.2	8.6	0.1	2.05	0.03	1.1	34	2.7
172	EM 6"-19	3.3	9.0	0.1	1.89	0.03	1.1	33	2.7
169	EM 6"-16	3.9	9.3	0.1	2.03	0.03	1.6	41	2.4
165	EM 6"-12	2.9	9.1	0.1	2.18	0.04	0.6	22	3.1
159	EM 6"-6	2.9	9.7	0.1	2.02	0.03	0.5	17	3.4
153	EM 6"-1	3.1	9.1	0.1	1.91	0.03	0.8	26	2.9
96.5	EM 4-7	5.9	8.0	0.1	1.62	0.03	3.9	66	1.4



Table 3

[Click here to download Table: Table 3 bis last.xls](#)

	Position	$\delta^{13}\text{C}$	$\delta^{18}\text{O}$	Mg/Ca <sub>v</sub>	Sr/Ca <sub>v</sub>	Na/Ca <sub>v</sub>	N pores	Sr isot	Th/U
Position	1.000								
<i>p</i>									
$\delta^{13}\text{C}$	0.192	1.000							
<i>p</i>	p=0.418								
$\delta^{18}\text{O}$	0.238	<b>-0.690</b>	1.000						
<i>p</i>	p=0.311	<b>p=0.001</b>							
Mg/Ca <sub>v</sub>	-0.331	<b>-0.628</b>	0.039	1.000					
<i>p</i>	p=0.154	<b>p=0.003</b>	p=0.872						
Sr/Ca <sub>v</sub>	<b>0.506</b>	0.376	0.216	<b>-0.562</b>	1.000				
<i>p</i>	<b>p=0.023</b>	p=0.102	p=0.360	<b>p=0.010</b>					
Na/Ca <sub>v</sub>	-0.173	<b>-0.823</b>	<b>0.693</b>	<b>0.516</b>	-0.095	1.000			
<i>p</i>	p=0.466	<b>p=0.000</b>	<b>p=0.001</b>	<b>p=0.020</b>	p=0.692				
N pores	0.078	0.286	-0.231	-0.030	0.349	-0.188	1.000		
<i>p</i>	p=0.743	p=0.221	p=0.328	p=0.901	p=0.131	p=0.428			
Sr isot	-0.244	0.035	0.192	-0.166	0.068	-0.035	0.275	1.000	
<i>p</i>	p=0.299	p=0.882	p=0.418	p=0.484	p=0.777	p=0.884	p=0.240		
Th/U	-0.403	-0.219	0.080	0.410	0.211	0.420	0.392	0.084	1.000
<i>p</i>	p=0.079	p=0.353	p=0.738	p=0.072	p=0.372	p=0.065	p=0.087	p=0.725	